

Ecology and Development Series No. 21, 2004

Editor-in-Chief:
Paul L.G. Vlek

Editors:
Manfred Denich
Christopher Martius
Nick van de Giesen

Bart Wickel

Water and nutrient dynamics of a humid tropical
agricultural watershed in Eastern Amazonia

Cuvillier Verlag Göttingen

To Beth

ABSTRACT

Agriculture in the “zona Bragantina” in the eastern Amazon region has been based on slash-and-burn shifting cultivation for over 130 years. With the increase of pressure on this agricultural land use system, management techniques such as mulching and change of the cropping system have been proposed as alternatives. In order to make recommendations regarding the ecological effects of such changes in land use, a detailed study of water and nutrient dynamics at a watershed level was performed. The research objective of this study was to determine the main hydrological processes and their related pathways, and to quantify water and nutrient fluxes.

Field measurements were conducted from August 2000 until July 2002 at three first order catchments in the Cumaru watershed. The fields used for the 2001 cropping cycle were prepared with mechanical mulch treatment (watershed 1, WS1) and burning (watershed 2, WS2), while watershed 3 (WS3) served as the control catchment. Throughout the study period a high-resolution (temporal and spatial) database of hydrological, hydrochemical, micro-meteorological, land cover, and topographical data was assembled.

Of the 2253 mm of rainfall measured over the year 2001, 1333 mm left the catchment through evapotranspiration (ET) at WS1 and 1396 mm at WS3, with estimates based on the catchment water balance. For WS2 the data record was incomplete, but the conditions at this watershed were thought to be comparable to WS3. The estimates obtained with the chloride balance were in close agreement with this value for both watersheds. ET estimates for one year old fallow vegetation using the micrometeorological Penman-Monteith method yielded a value of 1337 mm. Fallow vegetation (4.5 year old) intercepted 13.5 % of the incoming rainfall, while riparian forest intercepted approximately 9%. At WS1 and WS3 respectively 920 mm and 857 mm left the catchment as stream flow. Of the 920 mm of total streamflow at WS1 over 2001, 905 mm was baseflow and only 15 mm stormflow. The rainfall-runoff dynamics during storm events demonstrated an extremely strong correlation between the two in this area, indicating that stormflow consists entirely of saturation overland flow generated in the riparian wetland area. This saturated valley bottom of the Igarapé accounts for only 0.7% of the total catchment area. Other forms of overland flow which could potentially lead to a quick transport of water from the surrounding area to the stream were absent.

The nutrient balance at a watershed level was close to balanced, indicating that inputs approximately equal outputs on an annual basis. No significant differences in nutrient exports were observed between the mulched watershed and the control watershed. During peak events after extended dry periods, peaks in the exports of potassium, calcium, sulphate and nitrogen originating from the canopy of the riparian forest were observed. This effect diminished as the rainy season progressed. At the main channel of the Igarapé-Cumaru elevated exports of calcium and nitrogen were observed, most likely due to sources such as chicken farms and extensive pepper plantations which were not present in the headwater catchments of this study. In contrast to the observations at a watershed level, point level estimates show significant losses of nutrients to groundwater, depending on the recent land use. The observed losses to groundwater are the lowest under the mulched and the burned plots, and the highest under plantations of perennial crops like passion fruit and pepper.

Based on the analyses of the measurements made for this study it was concluded that on an annual basis the water and nutrient balance for the study catchments were closed, meaning that all components could be accounted for. Furthermore, it was concluded that quick transports of water and nutrients from the fields in the form of overland flow or sub-surface stormflow were absent, and that the hydrological response of both the mulched watershed (WS1) and the control watershed (WS3) were comparable. No significant differences in water and nutrient dynamics at the watershed level were observed over the study period between WS1 and WS3.

KURZFASSUNG

Landwirtschaft in der „Zona Bragantina“ im östlichen Amazonasgebiet basiert seit über 130 Jahren auf Brandrodungs-Landwirtschaft (*slash-and-burn shifting cultivation*). Mit zunehmendem Druck auf dieses landwirtschaftliche Nutzungssystem wurden Managementtechniken wie Mulchen zusammen mit veränderte Anbaumethoden als Alternativen vorgeschlagen. Um Empfehlungen hinsichtlich der ökologischen Auswirkungen solcher Landnutzungsveränderungen machen zu können, wurde eine eingehende Untersuchung der Wasser- und Nährstoffdynamik in einem Wassereinzugsgebiet durchgeführt. Das Forschungsziel dieser Untersuchung war es, sowohl die wichtigsten hydrologischen Prozesse und ihre Fließbahnen zu bestimmen als auch die Wasser- und Nährstoffströme zu quantifizieren auf die Ebene von einem ganzes Wassereinzugsgebiet. Von August 2000 bis Juli 2002 wurden Feldmessungen in drei Sub-Einzugsgebieten erster Ordnung im Einzugsgebiet der Igarapé-Cumaru durchgeführt. Die Felder, die für den Anbauzyklus 2001 genutzt wurden, wurden mit einer mechanischen Mulchbehandlung (Einzugsgebiet 1, WS1) und durch Brennen (WS2) vorbereitet, während Einzugsgebiet 3 (WS3) als Kontrollgebiet diente. Im Verlauf der Untersuchungsperiode wurde eine (zeitlich und räumlich) hochauflösende Datenbank mit hydrologischen, hydrochemischen, mikro-meteorologischen, Landbedeckungs- und topographischen Daten zusammengestellt.

Von den im Jahr 2001 gemessenen 2253 mm Niederschlag gingen, nach Schätzungen auf Grundlage der Wasserbilanz des Einzugsgebietes, durch Evapotranspiration (ET) im WS1 1333 mm und im WS3 1396 mm verloren. Für WS2 war der Datenbestand unvollständig, es wird jedoch angenommen, daß die Bedingungen dieses Einzugsgebietes mit WS3 vergleichbar sind. Die Schätzwerte, die durch die Chloridbilanz erhalten wurden, stimmten gut mit diesem Wert für beide Einzugsgebiete überein. ET-Schätzungen für einjährige Brachvegetation unter Verwendung der mikrometeorologischen Penman-Monteith Methode kombiniert mit Schätzungen der Interzeption ergaben 1337 mm. In Brachvegetation (4,5 Jahre alt) betrug die Interzeption 13,5 % des gefallenen Niederschlags, verglichen mit ungefähr 9 % in Auenwäldern. Der Abfluß betrug 920 mm im WS1 und 857 mm im WS3. Von den 920 mm des gesamten Abflusses im WS1 waren 905 mm *baseflow* und nur 15 mm *stormflow*. Die Niederschlag-Abfluß-Dynamik bei Regenereignissen zeigte eine sehr starke Korrelation zwischen Niederschlag und Abfluß, was darauf hindeutet, daß *stormflow* gänzlich aus *saturation overland flow* besteht, der in den ufernahen Feuchtgebieten erzeugt wird. Dieser gesättigte Talboden des Igarapé macht lediglich 0,7 % des gesamten Einzugsgebietes aus. Andere Formen von Oberflächenabfluß, die potentiell zu einem schnellen Wassertransport aus der Umgebung zum Fluß führen könnten, waren nicht vorhanden.

Die Nährstoffbilanz auf Einzugsgebietsebene war beinahe ausgeglichen, was darauf hindeutet, daß sich Inputs und Outputs im Jahresverlauf annähernd ausgleichen. Zwischen dem gemulchten Einzugsgebiet und dem Kontrolleinzugsgebiet konnten keine signifikanten Unterschiede hinsichtlich des Nährstoffaustrages beobachtet werden. Während Spitzenereignissen nach längeren Trockenperioden wurden Austragsspitzen von Kalium, Kalzium, Sulfat und Stickstoff, die aus dem Laub der Uferwälder stammen, beobachtet. Dieser Effekt verringerte sich im Verlauf der Regenzeit. Im Hauptkanal vom Igarapé-Cumaru wurden erhöhte Output von Kalzium

und Stickstoff beobachtet, die sehr wahrscheinlich auf Quellen wie Hühnerfarmen und ausgedehnte Pfefferplantagen, die in den Quellgebieten dieser Untersuchung nicht vorhanden waren, zurückzuführen sind. Im Gegensatz zu den Beobachtungen auf Einzugsgebietsebene zeigen Schätzungen auf Standortebene signifikante Nährstoffverluste an das Grundwasser in Abhängigkeit von der Landnutzung. Die beobachteten Verluste an das Grundwasser sind am geringsten unter den gemulchten und den gebrannten Flächen und am höchsten unter Pflanzungen perennierender Kulturen wie Passionsfrucht und Pfeffer.

Auf Grundlage der Analysen der Messungen, die für diese Untersuchung durchgeführt wurden, kann gefolgert werden, daß die Wasser- und Nährstoffbilanz der untersuchten Einzugsgebiete im Jahresverlauf ausgeglichen ist. Dies bedeutet, daß alle Komponenten quantifiziert werden konnten. Des weiteren wird der Schluß gezogen, daß schnelle Wasser- und Nährstofftransporte von den Feldern in Form von Oberflächen- (*overland flow*) oder Zwischenabfluß (*sub-surface stormflow*) nicht vorkommen, und daß die hydrologische Reaktion des gemulchten Einzugsgebietes (WS1) und des Kontrolleinzugsgebietes (WS3) vergleichbar sind. Im Untersuchungszeitraum wurden zwischen WS1 und WS3 keine signifikanten Unterschiede bei Wasser- und Nährstoffdynamik auf Einzugsgebietsebene beobachtet.

RESUMO

A agricultura na “zona Bragantina”, da Amazonia Oriental baseou-se no sistema de cultivo de corte e queima ao longo dos últimos 130 anos. Com o aumento da pressão sobre esse sistema agrícola de uso do solo, técnicas de manejo como trituração e mudanças no sistema de plantio apresentam-se como alternativas. Em ordem de advertir sobre os efeitos ecológicos de tais mudanças no uso da terra, um estudo detalhado da dinâmica da água e dos nutrientes em nível de microbacia hidrográfica foi realizado. O objetivo desse estudo foi determinar os principais processos hidrológicos e seus relativos caminhos preferenciais assim como, quantificar o fluxo da água e dos nutrientes. Medidas de campo foram realizadas de agosto de 2000 a julho de 2002 em três drenagens de primeira ordem na bacia hidrográfica do igarapé Cumaru. As microbacias investigadas foram trituradas (microbacia 1, WS1) e queimadas (microbacia 2, WS2) em 2001, enquanto que a microbacia 3 (WS3) serviu como microbacia de referência. Ao longo do período de estudo, uma base de dados (temporal e espacial) hidrológica, hidroquímica, micro-meteorológica, de cobertura do terreno e topográfica de alta resolução foi coletada. As microbacias hidrográficas são caracterizadas por solos altamente permeáveis e uma topografia levemente ondulada, dissecada por canais rasos (igarapés) com terras alagadas de floresta ripariana (igapó). A cobertura do solo consiste principalmente de vegetação secundária conhecida por capoeira, terrenos agrícolas e pastagem.

Dos 2253 mm de precipitação medidos sobre o ano de 2001, 1333 mm deixaram a bacia através de evapotranspiração (ET) na WS1 e 1396 mm na WS3, com estimativas baseadas em seu balanço hídrico. Para a WS2, os dados registrados foram incompletos, mas as condições nesta microbacia foram identificadas como bastante próximas a WS3. As estimativas obtidas com o balanço do cloro encontram-se próximas aos valores para ambas microbacias. Estimativas de ET para capoeiras de um ano de idade utilizando o método meteorológico Penman-Monteith combinada com estimativas de interceptação forneceram estimativas de 1337 mm. A capoeira de 4,5 anos interceptou 13,5% da precipitação pluviométrica, enquanto que, a floresta ripariana interceptou aproximadamente 9%.

Nas microbacias WS1 e WS3, respectivamente 920 mm e 857 mm deixaram como fluxo superficial. De cerca de 920 mm do fluxo superficial na WS1 no ano de 2001, 905 mm se deu na forma de fluxo de base e apenas 15 mm como fluxo de tempestade. A dinâmica do processo precipitação-escoamento superficial durante eventos de tempestade demonstraram uma correlação extremamente forte entre ambas nas duas áreas, levando à conclusão de que o fluxo de tempestade consiste inteiramente da saturação do fluxo superficial gerado na área alagada de floresta ripariana. O fundo de vale saturado do igarapé cobre apenas 0,7% da área total da microbacia. Outras formas de fluxo superficial que poderiam potencialmente levar a um rápido transporte de água das áreas adjacentes para a drenagem não foram identificadas.

O balanço de nutrientes identificado em nível de microbacia é próximo do balanceado, significando entradas aproximadamente iguais às saídas em uma base anual. Não foram observadas diferenças significantes na exportação entre a microbacia triturada e a microbacia de controle. Durante os eventos de pico após longos períodos de seca, foram observados picos na saída de potássio, cálcio, sulfato e nitrogênio originários do dossel da floresta ripariana. Este efeito diminui com o progresso da

estação chuvosa. No canal principal, elevadas saídas de cálcio e nitrogênio foram observadas, mais comumente devido a fontes como criações de galinha e extensas plantações de pimenta do reino, que não se encontravam presentes no topo das microbacias desse estudo.

Em contraste às observações em nível de microbacia, estimativas em nível pontual mostram significantes perdas de nutrientes para as águas subterrâneas, dependendo do recente tipo de uso da terra. As perdas observadas para as águas subterrâneas são mais baixas sob as áreas trituradas e queimadas, e mais elevadas sob plantações perenes como maracujá e pimenta.

Baseado na análise das medidas realizadas para esse estudo foi possível concluir que, em uma base anual, o balanço hídrico e de nutrientes para o estudo das microbacias é próximo, significando que todos os componentes podem ser correlacionados. Além do mais, concluiu-se que o transporte rápido da água e de nutrientes dos campos na forma de fluxo superficial ou fluxo de tempestade de sub-superfície foram ausentes, e a resposta hidrológica de ambas microbacias trituradas (WS1) e da microbacia de controle (WS3) foram comparável.

TABLE OF CONTENTS

1	GENERAL INTRODUCTION	1
1.1	Introduction	1
1.2	The SHIFT project framework	1
1.3	Water and nutrient dynamics	3
1.4	Aims and outline	5
2	DESCRIPTION OF THE STUDY REGION	7
2.1	Study area	7
2.2	Climate	7
2.3	Geology	8
2.4	Soils	10
2.5	Topography	11
2.6	Land use	12
2.7	Land cover classification	15
3	STUDY SITES AND INSTRUMENTATION	18
3.1	Description of the study sites	18
3.2	Rainfall measurements	21
3.3	Throughfall measurements	23
3.4	Micrometeorological measurements	24
3.5	Runoff measurements	25
3.6	Infiltration measurements	26
3.7	Groundwater measurements	27
4	WATER BALANCE	30
4.1	Introduction	30
4.2	Rainfall	31
4.2.1	Rainfall observations	31
4.2.2	Rainfall intensity and occurrence	32
4.2.3	Seasonal variation	34
4.2.4	Water balance summary rainfall	36
4.3	Rainfall interception	37
4.3.1	Introduction	37
4.3.2	Methodology	38
4.3.3	Throughfall results	40
4.3.4	Forest structural parameters	46
4.3.5	Gash model results	48
4.3.6	Water balance summary interception	49
4.4	Evapotranspiration	51
4.4.1	Introduction	51
4.4.2	The Penman-Monteith method	51
4.4.3	Evapotranspiration results	54
4.4.4	Water balance summary evapotranspiration	58

4.5	Runoff.....	61
4.5.1	Introduction.....	61
4.5.2	Hydrograph separation.....	62
4.5.3	Runoff observations.....	64
4.5.4	Stormflow	64
4.5.5	Infiltration	68
4.5.6	Rainfall interception estimation from stormflow measurements.....	70
4.5.7	Water balance summary runoff.....	73
4.6	Groundwater	75
4.6.1	Introduction.....	75
4.6.2	Observations and analysis.....	75
4.6.3	Storativity.....	79
4.6.4	Finite Element Model	79
4.7	Catchment water balance.....	81
5	NUTRIENT BALANCE.....	83
5.1	Introduction	83
5.2	Field and laboratory procedures	83
5.3	Rainfall chemistry	84
5.3.1	Introduction.....	84
5.3.2	Methodology	85
5.3.3	Rainwater composition	85
5.3.4	Nutrient inputs from rainwater.....	87
5.4	Groundwater chemistry	88
5.4.1	Introduction.....	88
5.4.2	Groundwater composition.....	88
5.4.3	Nutrient output to groundwater.....	90
5.5	Streamwater chemistry	92
5.5.1	Introduction.....	92
5.5.2	Methodology	93
5.5.3	Baseflow composition.....	94
5.5.4	Stormflow composition.....	98
5.5.5	Downstream changes	102
5.5.6	Nutrient exports with streamflow	103
5.6	Catchment nutrient balance	103
6	CONCLUSIONS.....	107
7	REFERENCES.....	110
	ACKNOWLEDGEMENTS	121

TABLE OF ABBREVIATIONS

SHIFT	Studies of Human Impacts on Forests and Floodplains in the Tropics
EMBRAPA	Empresa Brasileira de Pesquisa Agropecuária
ZEF	Zentrum für Entwicklungsforschung
BmBF	Bundesministerium für Bildung und Forschung
CNPq	Conselho Nacional de Desenvolvimento Científico e Tecnológico
PPG-7	Programa Piloto para a Proteção das Florestas Tropicais do Brasil
IBGE	Instituto Brasileiro de Geografia e Estatística

1 GENERAL INTRODUCTION

1.1 Introduction

Long before European colonization indigenous groups practiced shifting cultivation, also known as slash-and-burn agriculture, on small plots throughout the Amazon region (Vosti et al., 2002). The eastern Amazon was the first region to be settled by ‘outsiders’, mainly from the Brazilian northeast and Europe. These settlers used an intensified form of slash-and burn agriculture in a crop rotation scheme, which has been practiced for several generations in this region since. Within this agricultural system, a plot of secondary (or primary depending on the stage of invasion) forest is slashed and after a short drying period burned, to provide the nutrients for a one to two year cropping cycle. Subsequently, the land is left for the fallow vegetation to grow back for a varying number of years, and accumulate the nutrients needed for a next agricultural cycle (Nye and Greenland, 1960; Whitmore, 1998). The strong population growth in Brazil since the 1960’s resulted in an increase in pressure on the agricultural land and accelerated the deforestation of primary forest (Fearnside, 1987; Nepstad et al., 1999). The intensification of land use led to shorter fallow periods and the extension of cropping cycles, leaving soils depleted of nutrients and ultimately resulting in the inability of the fallow vegetation to accumulate the nutrients needed for the next cropping cycle (Sanchez, 1976; Uhl, 1987; Uhl and Jordan, 1984). In addition to negative local effects of burning, such as soil fertility depletion and deterioration of soil physical properties, slash and burn agriculture affects global warming by the emissions of greenhouse gasses (Fearnside, 1996; Fearnside, 2000). In an effort to reduce the practice of burning, mulching (chopping and dispersion of the biomass) in combination with zero tillage has been suggested as a sustainable alternative (Denich et al., 2004; Lal, 1981; Thurston, 1997). Mulching is generally thought to have positive effects dry season soil moisture conditions, increase infiltration, reduce erosion, reduce soil temperatures, increase soil organic matter and soil nutrients, and increase crop yields over time (Lal, 1975; Thurston, 1997).

1.2 The SHIFT project framework

The German-Brazilian SHIFT program (Studies of Human Impacts on Forests and Floodplains in the Tropics) financed by the BmBf, CNPq and PPG-7 started in 1989

with the aim to increase the knowledge regarding the structure and key functions of the tropical ecosystem, to develop concise concepts for sustainable land use by recuperation of degraded and abandoned areas, and to improve the scientific assessment of human actions with respect to environmental risks. Under the umbrella of the SHIFT project in Brazil, numerous studies throughout Eastern and Central Amazonia, the Atlantic forests, and the floodplains of the Paraguay River have been developed over the past decade and a half. The common factors connecting all the project areas of research, are nutrient and water flux studies, ecosystem functioning, and socio-economic parameterization of the local population, and the potential uses for management systems. The Eastern Amazonian leg of the program was focused on the functioning and management of secondary forests and fallow vegetation (SHIFT-Capoeira; project code ENV 25).

Within the SHIFT-Capoeira project, various studies on the functioning of the fallow vegetation ecosystem were conducted. Studies of the floristic composition and function of fallow vegetation in the region were performed by Denich (1989), Baar (1997) and Schuster (2001). Fallow regeneration and root zone dynamics were studied by Wiesenmüller (1999), while nitrogen fixation by fallow vegetation and the potentials for natural fallow enrichment were studied by Thielen-Klinge (1997), Paparcikova (1998) and Brienza (1999). Soil biological and physical characteristics were studied by Diekmann (1997) and Maklouf Carvalho et al. (1997). Mackensen et al. (1996) studied the nutrient losses to the atmosphere of the traditional slash and burn system, while Hölscher (1995) and Klinge (1997) studied nutrient transfers to the soils. Social studies of small holding farmer communities were made by Souza-Filho (2004), Hurtiene (1998) and others.



Figure 1.1 a) Traditional slash and burn agriculture and b) mulching in action

Based on these and other studies, mulch technology was proposed as a sustainable agricultural management tool (Denich, 1996). However, mulching in comparison to traditional burning on crop productivity resulted decline in productivity (Kato et al., 1999; Kato, 1998), which revealed the need for a more integrated optimization approach with changes in the cropping calendar, and enrichment of fallow vegetation (Brienza Jr., 1999). The actual technical implementation of mulch technology was studied by Block (2004), whereas the social and economical feasibility was studied by Hedden-Dunkhorst et al. (2003). Micrometeorology was an integral part of the studies of Klinge (1998), Hölscher (1995), Sommer (2000), Giambelluca et al. (1997; 2000; 2003) and Sá et al. (1996; 1999). A water and nutrient cycling study examining the differences between mulching and burning at a point and plot scale was performed by Sommer (2000).

1.3 Water and nutrient dynamics

Under humid tropical conditions, the pathways and fluxes of nutrients are intimately connected with the pathways and fluxes of water through the (catchment) ecosystem (Bruijnzeel, 1983; Likens and Bormann, 1977). In order to assess the effects of changes in land use on water and nutrient dynamics, a sound understanding of the processes that determine these pathways and fluxes is required (Bonell and Balek, 1993; Bonell and Fritsch, 1997; Bruijnzeel, 1989b; Bruijnzeel, 1991). The various pathways of water through a vegetated hill slope are shown in Figure 1.2. Proctor (1987) summarized the major sources, sinks and pathways of nutrients in water solution in a forested ecosystem with the sketch given in Figure 1.3. For the agroecosystem under study in our experiment, several additions to this sketch were be made. The traditional land preparation gives both a quick release of nutrients from burned vegetation to the soil as well as massive nutrient losses to the atmosphere, whereas mulching and the required use of fertilizers give extra nutrient inputs to the soil (Denich et al., 2004; Lal, 1981; Thurston, 1997).

The studies by Hölscher (1995) and Mackensen (1996) demonstrated that nutrient losses to the atmosphere were several orders of magnitude greater than losses by leaching to drainage water. The anticipated increase in nutrient losses when the vegetation is mulched instead of burned was shown to be minimal due to

immobilization of nutrients by microorganisms and plant uptake (Sommer, 2000). The deep root system of the fallow vegetation was shown to attenuate leaching losses and improve soil fertility.

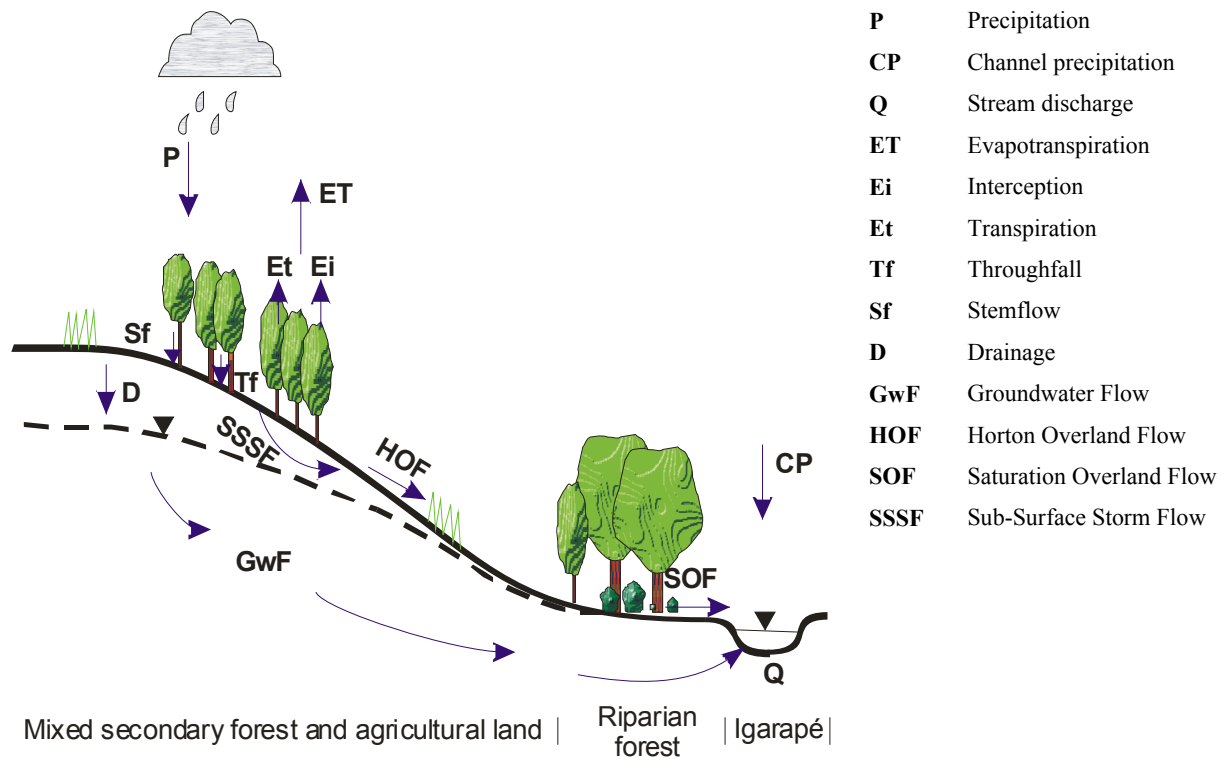


Figure 1.2 Hydrological cycle of a vegetated hill slope (adapted from Waterloo, 1994)

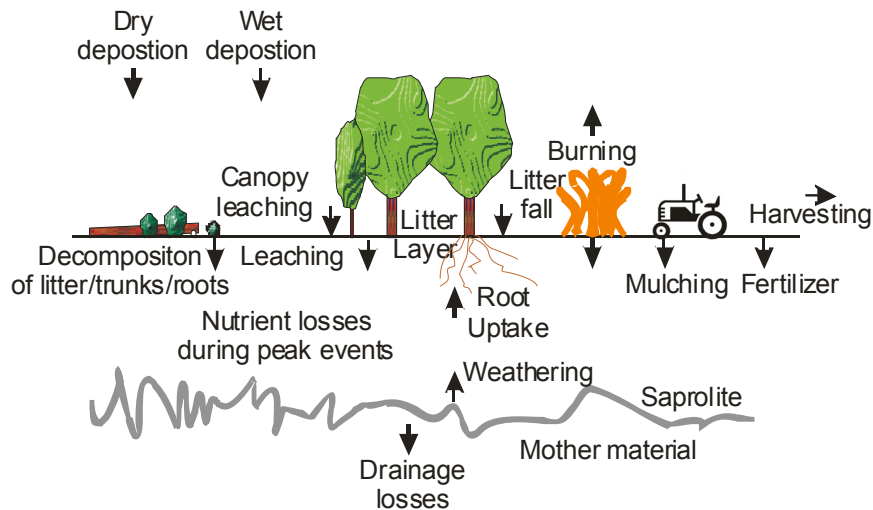


Figure 1.3 Nutrient cycles in an agricultural ecosystem under land preparation with and without burning (modified from Proctor (1987))

To examine the water and nutrient cycle in this study, the small watershed approach (Likens and Bormann, 1977) was followed. This method allows an accurate estimate of the water and nutrient cycle if the watershed conforms to the assumption that the watershed is underlain by an impermeable base, and that the only outflow occurs as streamflow (Bruijnzeel, 1990, Lesack, 1993b).

Following this assumption, the only inputs would be atmospheric and biological (including agriculture), and the only losses atmospheric, biological and geological (Likens and Borman, 1977). Most studies reviewed by Bruijnzeel (1991) and Brinkmann (1983), and more recent studies within our study region (Hölscher, 1995; Sommer 2000; Klinge, 1998) based their ecosystem nutrient loss estimates on shallow to intermediate depth, point to plot-scale measurements of soil water nutrient concentrations. For a complete understanding of the system, incorporation of measurements of groundwater and streamflow under base and peakflow conditions is essential. This study provides a look at the water and nutrient dynamics at a watershed scale in an agricultural ecosystem in the Eastern Amazon region.

1.4 Aims and outline

Based on the knowledge of the previous project phases, the current study is aimed at the integration of this knowledge and at providing an overview of the hydrological and biogeochemical functioning of the smallholder agricultural system in Eastern Amazonia. By analyzing the processes governing water and nutrient movement at the landscape and watershed level, reliable predictions can be made about the physical suitability of fallow management practices in and around the project area. In order to arrive at the overall aim, the specific research objectives were:

- To obtain a closed water balance for a set of experimental watersheds with different fallow clearing techniques by measuring rainfall, actual evapotranspiration, and stream flow
- To obtain a nutrient balance for these watersheds
- To measure and model the main water and nutrient flowpaths in order to reliably establish the extrapolation domain of the obtained results

The general components of the field measurements and the structure of their results are illustrated in Figure 1.4. After the general introduction to the study area in chapter 2,

and a description of the instrumentation in chapter 3, chapter 4 is dedicated to the main components of the water balance. The hydrological processes are followed from the point of entry of water into the system as rainfall, through the evaporation and interception process until it arrives at the ground surface, after which the rainfall-runoff processes and the groundwater dynamics are discussed. The contribution to the water balance of each component is given at the end of each section. Chapter 5 discusses the chemistry of rain, groundwater and runoff, as well as the changes in water chemistry between entrance and exit from the system, and gives the nutrient balance for the three first order watersheds and the entire Cumaru watershed. Chapter 6 closes with a general conclusion.

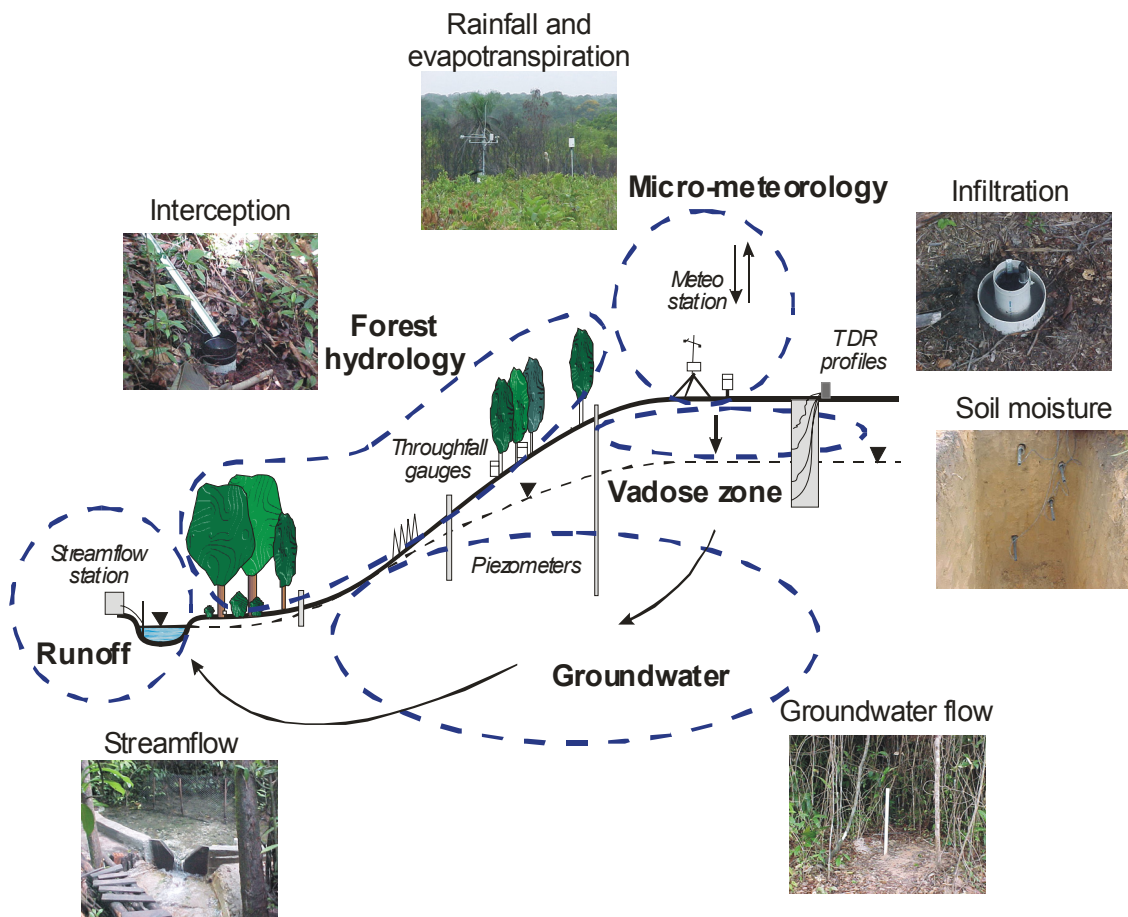


Figure 1.4 The main hydrological pathways and their subdivision in hydrological monitoring units

2 DESCRIPTION OF THE STUDY REGION

2.1 Study area

The study area is located 110 km northeast of the city Belém in the ‘zona-Bragantina’, eastern Amazonia, Brazil (Figure 2.1). The study area comprises three first-order catchments of the Cumaru watershed situated at 1°11' S, 47°34' W, situated 30 to 70 m above sea level. The landscape is characterized by a rolling topography covered with a heterogeneous patchwork of agricultural fields, fallow areas and pasture, and is dissected by streams fringed with a strip of riparian wetland forest.

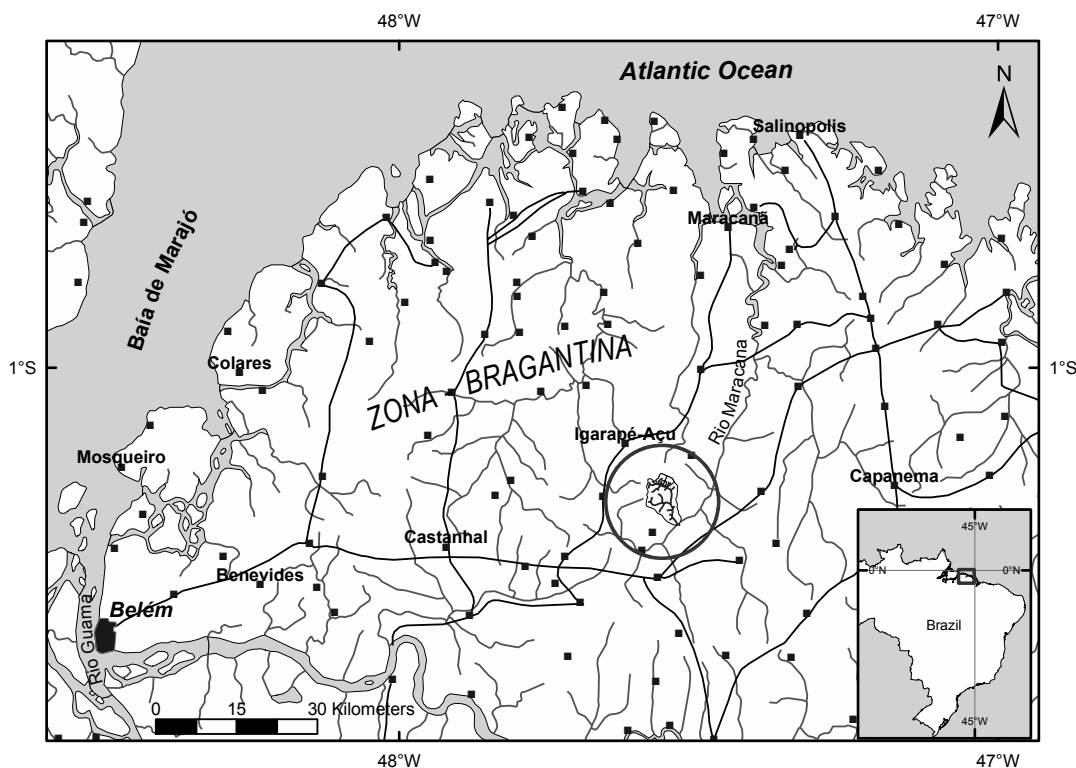


Figure 2.1 Location of the Cumaru watershed

2.2 Climate

The climate of the region is humid tropical with an average temperature of 26°C and a dry season with less than 60 mm of rainfall during the driest month (Am, following the classification of (Köppen, 1936). The northeasterly to easterly winds from the South Atlantic and Azorean anticyclones bring moisture-laden air from the Atlantic Ocean throughout most of the year. Disturbances may originate from temperate systems traveling along the east coast, squall (instability) lines instigated by the convergence of

sea breeze and small-scale convective storms (Griesinger and Gladwell, 1993; Molion, 1993; Nimer, 1972). Small-scale convective storms cause the typical afternoon showers which form during the morning hours and precipitate around 1400 to 1600 hours local time (Molion, 1993; Nimer, 1972; Nimer, 1991). The average annual rainfall amounts to about 2500 mm \pm 10% (Figure 2.2), of which typically 60% falls during the wet season between January and April (Bastos and Pacheco, 1999; EMBRAPA, 1977-2002).

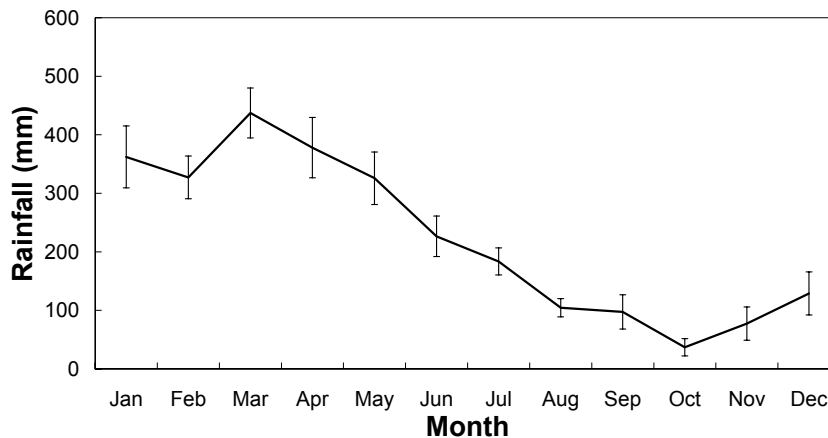


Figure 2.2 Average monthly rainfall totals for the period 1994-2002 for the meteorological station of EMBRAPA, located approximately 5 km from the Cumaru watershed (for location see Figure 3.1)

2.3 Geology

The study region is situated on the ‘Bragança platform’, which makes part of a horst-graben rift system that extends from Marajó in the west to São Luis in the east. The area went through various phases of complex tectonic activity since the Miocene period (Rego Bezera, 2001; Rossetti, 2001; Rossetti, 2003). Two sets of features characterize the area: northeast dipping normal faults which developed during the Late Tertiary and northeast-southwest and east-west strike-slip faults (Costa et al., 2001).

The stratigraphy of the study region (Figure 2.3) is dominated by the Barreiras formation, which is underlain by the Pirabas formation. The Barreiras formation, which at some locations reaches a thickness of 120 m, was deposited from late Tertiary (Pliocene) to Early Quaternary (Pleistocene) in an alternating fluvio-lacustrine and marine environment. This resulted in a complex variation of clays, siltstones and sandstones.



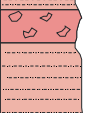
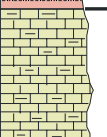
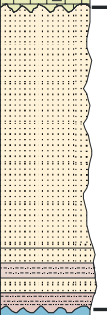
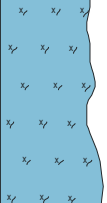
ERA	UNIT			LITHOLOGY	THICKNESS (m)	LITHOLOGICAL DESCRIPTION
	Chronostratigraphic		Lithostr.			
	System	Series	Formation			
CENOZOIC	QUATERNARY	HOLOCENE	POS-BARREIRAS		±5	Unconsolidated sediments, composed by clays, silts and sands.
		PLEISTOCENE	BARREIRAS		±120	Kaolinic clays, sandy-silty and clayey-sandy sediments of yellowish to reddish colours. Levels of ferruginous sandstones are common in irregular and single blocks ("grés do Pará") and sandy interleaving showing cross-bedding and local disconformities.
	TERTIARY	PLIOCENE		PIRABAS		
		MIOCENE			±5	Fossiliferous limestone interbedded with clay and calcareous sandstones.
EOPALEOZOIC					±26	Light colored sandstones, partially silicified with medium to coarse granulometry. Intercalations of silty-clayey layers with worm tubes and prints with partially silicified sandstones showing cross-stratification.
PRECAMBRIAN	ARCHAEOZOIC					Gneissic Complex (with predominance of biotite-gneisses)

Figure 2.3 Stratigraphic column of the 'zona Bragantina' (Rossetti, 2001; Schultz Jr., 2000)

The Pirabas formation consists of fossiliferous limestone (Rossetti, 2001; Schultz Jr., 2000). The Barreiras formation is topped with a Quaternary series of variable thickness, of sands and clays called the 'Post-Barreiras' formation (Rossetti, 2001). This formation consists of unconsolidated, sandy sediments with fine and coarse quartz grains with clayey layers of varying colors. The Barreiras and Post-Barreiras formations are generally separated by a lateritic crust of varying thickness.

Soil samples obtained from bore holes drilled for the installation of the groundwater wells demonstrated that the material to a depth of 10 meters has the same

lithological characteristics as Pós-Barreiras sediments (Reis de Melo Jr. et al., 2002). The weathered products of the Barreiras formation were found to a depth of 32 meters.

2.4 Soils

The soils in the region are predominantly ‘terra firme’ soils which are typically found in upland areas throughout the Amazon region, and were formed in the heavily weathered fluvio-lacustrine sediments of the ‘Barreiras’ and Post-Barreiras formations. Vieira et al. (1967) classified the dominant soil types in the ‘zona Bragantina’ as Ultisols, Oxisols and Entisols according to the US soil taxonomy system (table 3.1). Rego et al. (1993) classified the predominant soil type in the municipality of Igarapé Açu as Yellow Latosol (‘Latossolo Amarelo’) according the Brazilian soil classification system (EMBRAPA, 1999). Following the US Soil Taxonomy, Rego et al. classified the soils as Typic Kandiudult, which is a type of Ultisol. In a large-scale mapping of soils in the Amazon region, Moraes et al. (1995) set the Yellow Latosol equal to the North American class of Oxisols. Teixeira (2001) compared the Yellow Latosol to the Xantic Hapludox (Soil Survey Staff, 1997) or a Xantic Ferralsol according to the FAO system (FAO, 1990). Ultisols are generally less weathered and exhibit slightly higher fertility levels than Oxisols (Bruijnzeel, 1990).

Table 2.1 Names of the soils according to the US soil taxonomy encountered in the study region and their Brazilian soil classification equivalent

US soil taxonomy	Brazilian soil classification system
Ultisols	Podzólico Amarelo
Oxisols	Latossolo Amarelo
Entisols	Areia Quartzosa

(EMBRAPA, 1999; USDA, 1999; Vieira et al., 1967)

The strong weathering leaves the soils poor in nutrients, concentrates aluminum hydroxide and promotes the formation of kaolinite. In general, terra-firme soils are poor in nutrients and typically lack easily weatherable minerals (Sombroek, 1966; Sombroek, 1984) and have a low cation exchange capacity and low C, N and P concentrations (Hölscher, 1995; Sommer, 1990). The hydraulic conductivity of the soils in the study area is typically high. The soils consist typically of yellow and reddish loamy sands with fine gravel beds, clay lenses and iron concretions. The profile is strongly

dependent on topographical position. Lateric layers of several centimeters to decimeters at variable depths are present throughout the profiles. Thicker kaolinic clay banks are usually found at greater depth.

For soils under fallow vegetation at a plot nearby the current study area, Hölscher (1995) reported a texture gradient from 84% sand and 11% clay near the surface to 67% sand and 26% clay at a greater depth with an average bulk density of 1.4 g cm^{-3} . Sommer (2000) reported a very similar gradient (Table 2.2) for a plot adjacent to the current study area. Teixeira (2001) demonstrated for plots in Central Amazonia that soil structural parameters such as bulk density and pore size distribution under secondary forest did not differ significantly from the parameters observed under primary forest.

Table 2.2 Summary of soil physical properties over a 6m profile

Depth (cm)	2.5	70	200	400	600
pH	5.4 - 5.8	5.00	4.80	4.80	5.20
CEC	1.6 – 4.1	1.14	0.73	0.44	0.26
Bulk density (g cm^{-3})	1.21	1.56	1.65	1.73	1.80
Sand (%)	80	65	65	68	72
Silt (%)	10	8	10	8	8
Clay (%)	10	27	25	24	22

From Sommer (2000)

2.5 Topography

Given the paucity of detailed topographical information for this region, a digital elevation model (DEM) from the Shuttle Radar Topography Mission (SRTM; Rabus et al., 2003) was used to generate a topographical map shown in Figure 2.4. SRTM data has a resolution of 90 meters, which is sufficient for a regional topographical map but too coarse to capture the topographical variations in the study area. Overall, the elevations obtained from the SRTM data correspond very well with the ground measurements made with a differential global positioning system (D-GPS). The D-GPS system consisted of one stationary receiver at the base station and one mobile receiver for the point measurements. From these point measurements a more detailed DEM was generated resulting in a detailed topographical map of the study area, which is shown in Figure 2.5. The slopes in the Cumaru watershed are generally very low, ranging between 0 and 8° in the higher parts. Along the valleys, however, steep drop-offs of up to 80° occur.

2.6 Land use

Deforestation of the primary forest in the region around Igarapé-Açu began after the colonization of the zona Bragantina by settlers from the Brazilian northeast, as well as European immigrants. This deforestation accelerated following the construction of a railroad between Belém and Bragança in 1883 (Cruz, 1955; Penteado, 1967). At the beginning of the 20th century, Japanese farmers migrated to the region and settled around the towns Tomé-Açu and Igarapé-Açu.

Nowadays, agriculture in this region is dominated by small holding farms of typically less than 50 ha in size (IBGE, 1997). These farms typically consist of a patchwork of secondary / fallow vegetation and small agricultural fields planted with ‘traditional’ crops such as cassava, corn, beans, rice, pepper and passion fruit. Land is usually prepared using a slash-and-burn crop rotation system. The crops are typically grown over a period of 2 years in a sequence of corn, cowpea or rice and cassava (locally known as mandioca) after which the fields are abandoned and fallow vegetation is allowed to for a period of 3 to 10 years. Over the past decades smallholder farms have begun the practice of planting ‘cash’ crops such as passion fruit and pepper next to the traditional crops. For these cash crop plantations the fields are tilled, which severely changes the regenerative capacity of secondary vegetation after the plantations are abandoned in 4 to 8 years. Large-scale agriculture in the region consists of pepper and oil palm plantations, chicken farms and extensive cattle ranching. The only areas not suitable for farming are the riparian wetlands because they are continuously waterlogged. A steep drop off of several meters typically marks the transition to the wetland. The wetlands are clearly visible in the landscape by the presence of riparian gallery forest.

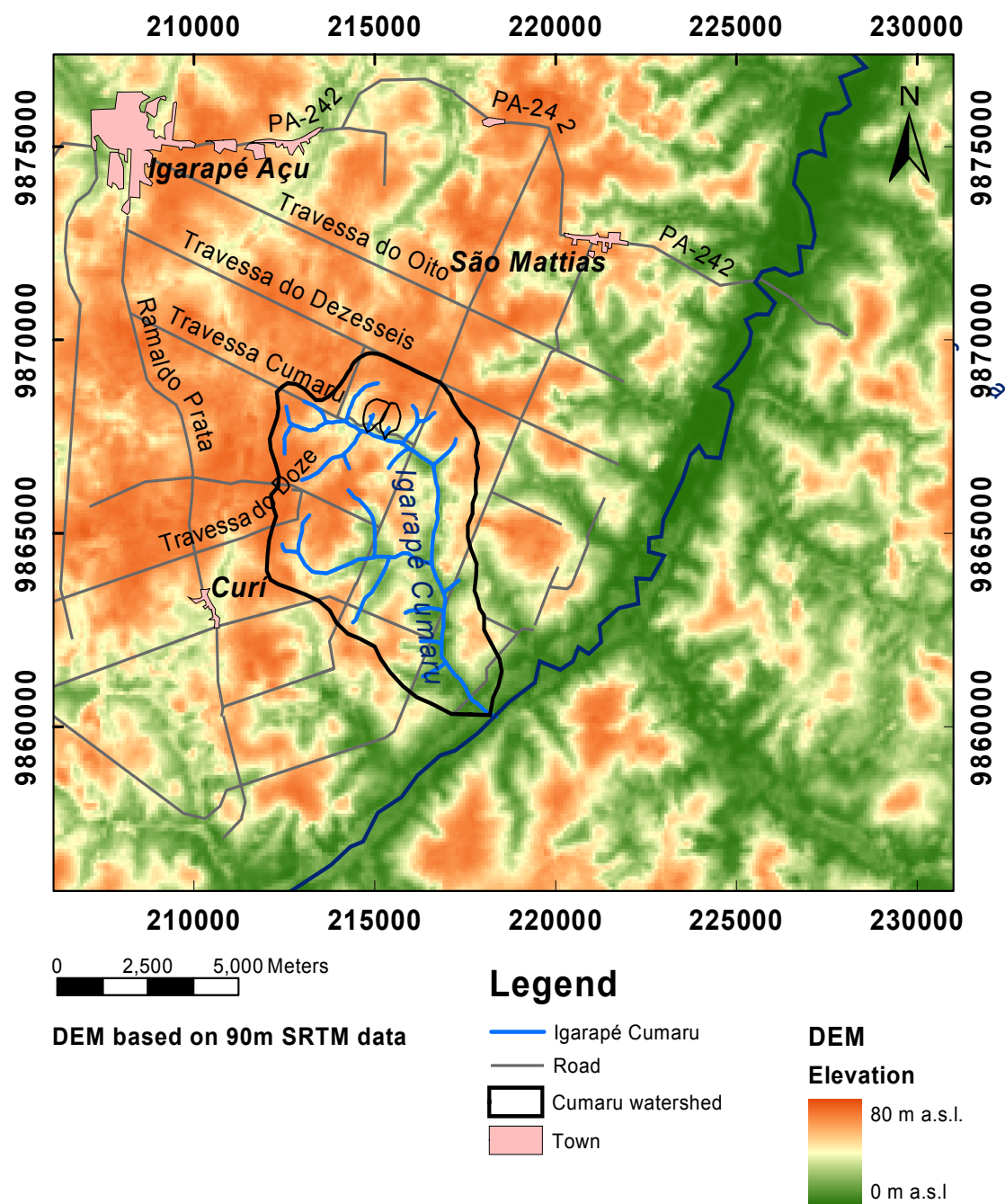


Figure 2.4 Regional digital elevation model based on 90m SRTM data

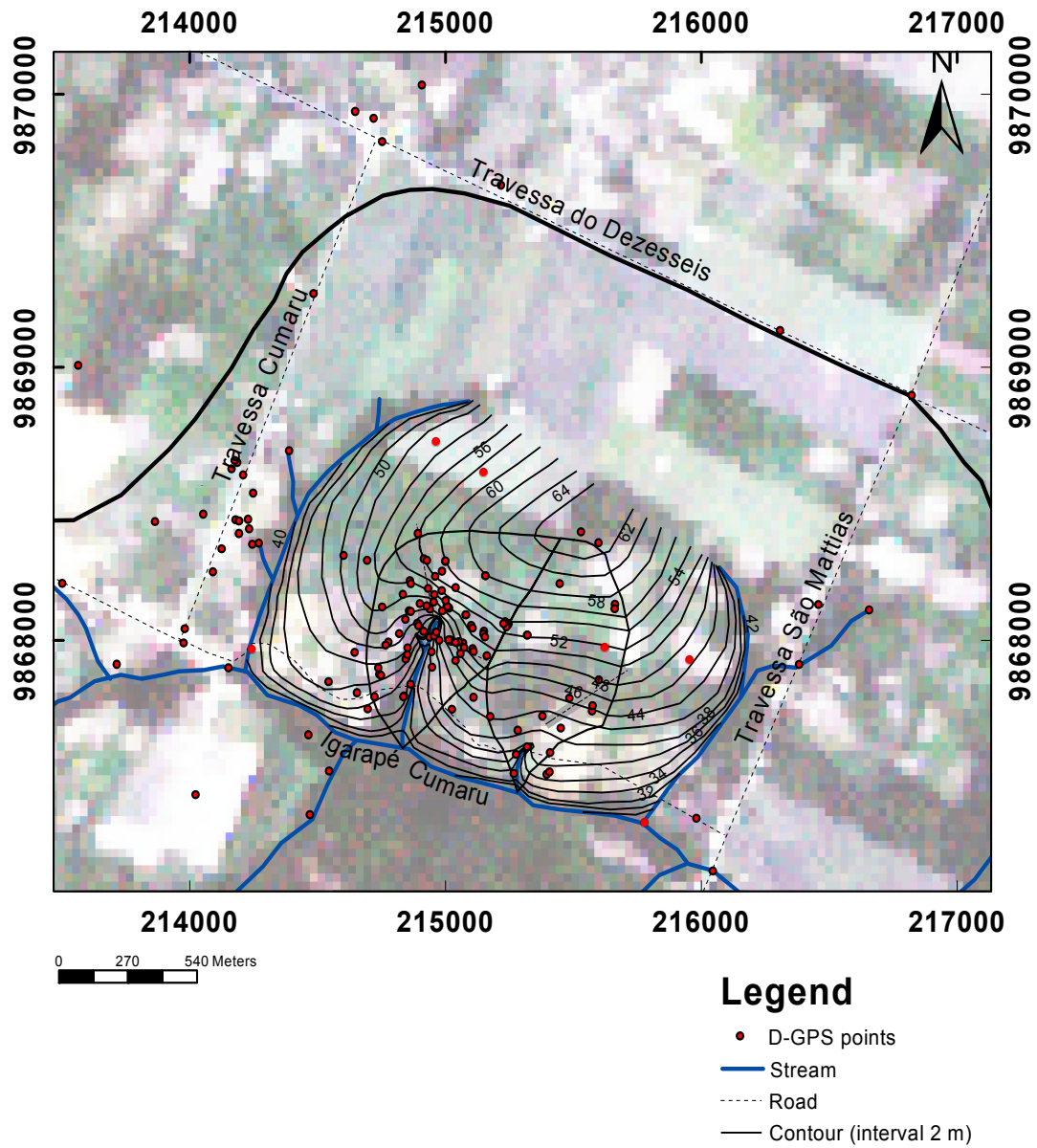


Figure 2.5 Detailed topographical map superimposed on a Landsat7 ETM+ image (July 2002). The red dots indicate D-GPS measurement points

2.7 Land cover classification

As part of the current study, a land cover classification was performed on a Landsat 7 ETM+ satellite image taken on the 3rd of August 2001. The image was classified by using a supervised maximum likelihood classification of the region surrounding the Cumaru watershed based on 12 ground truth training sites. The main problem with the classification of land use in this region is the heterogeneity of the landscape and of the smallholder farms in particular. These farmers plant on fields typically 1 ha or less in size, while one pixel of a Landsat image covers approximately 1 ha. This obviously leads to an underestimation of the area used for agriculture. Also, the young secondary vegetation seems to have a very similar spectral response to that of cassava and corn, making it difficult to distinguish between them. To study the effect of the spatial heterogeneity land cover classification a study with high resolution (1 m) IKONOS data is in progress (Puig, 2003).

The results of the classification with the Landsat ETM+ image are summarized in Table 2.3. The majority of the land cover consists of trees (59%), of which 45% is estimated to represent secondary / fallow vegetation. The riparian forest could be easily classified and only 13% of the region is thought to consist of this land cover class. In total 33% of the land cover is estimated to be used for agriculture. Although previous studies used a slightly larger area for the classification the current results compare fairly well. The land cover of greatest interest to the farmers and therefore to the ecological studies performed within the SHIFT project is secondary (fallow) vegetation.

Watrin (1994) performed a land cover classification of a Landsat 5 image from 1991, and estimated the percentage of woody secondary vegetation at approximately 55% of vegetative land cover in the municipality Igarapé-Açu. This value seems rather high in comparison with the current study and values reported in the IBGE census of 1995, and the classification by Metzger (1997). Given his low estimate for riparian forest, it seems that Watrin may have classified some of this forest type as secondary vegetation. The studies of 1995, 1996, and 2001 also show agreement on the percentage of agricultural area, suggesting that although the land undergoes rotational cropping, the total amount of land used for agriculture in this region is relatively constant.

Description of the study region

Table 2.3 Landcover classification of the study region based on Landsat 5 and 7 images of 1991, 1996 and 2001, and as reported in the census of 1995

Year of classification		1991	1995	1996	2001
Size of classification area					
Method / type of imagery		Landsat 5	Census IBGE	Landsat 5	Landsat 7 ETM+
Land use class		Area (%)			
Woody vegetation	Fallow vegetation < 4 yr	-	7	-	8.5
	Fallow vegetation 4-10 yr	-	36	-	21.7
	Secondary forest (Fallow > 10y)	-	-	-	14.6
	Total fallow vegetation	55	43	46	45
	Riparian forest	5	15	10	13
	Forest plantation	1	0.2	-	-
Total trees		61.0	58.2	56.0	59.0
Agricultural	Perennial crops (Maracuja / Pepper)	-	7	-	7.6
	Rotational crops	-	8	-	-
	Planted pasture	14	12	-	15.7
	Natural pasture / degraded grassland	2	4	-	9.8
Total agricultural		16.0	31.0	31.0	33.1
Other	Urban / bare soil	-	-	-	4.9
	Other	-	6	-	3.0

¹Watrin (1994), 2IBGE (1997), 3Metzger (1997), 4Wickel (2003)

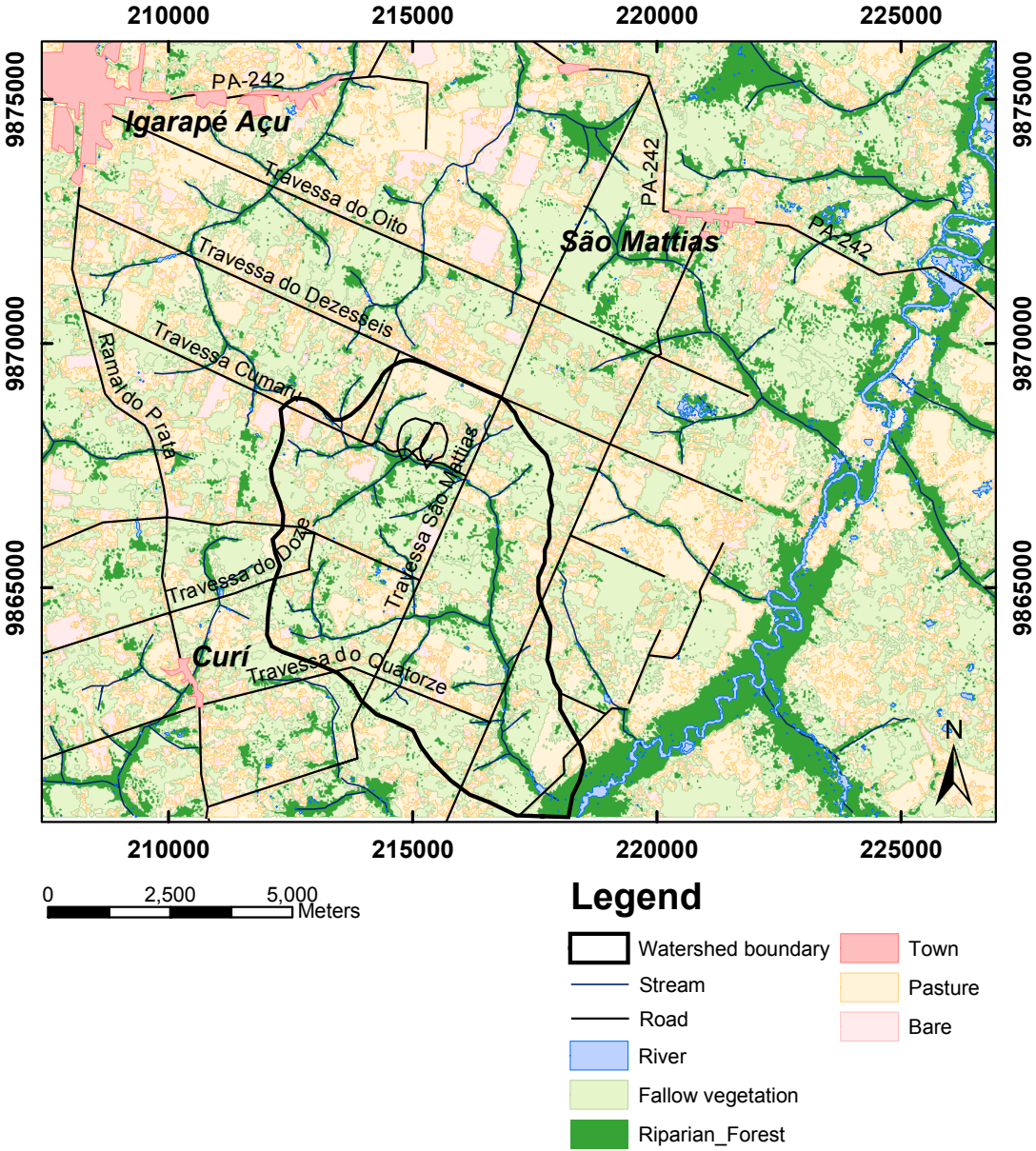


Figure 2.6 Land cover classification map generated from a supervised classification of a Landsat7 ETM+ image of the 3rd of August, 2001

3 STUDY SITES AND INSTRUMENTATION

3.1 Description of the study sites

To measure the large set of parameters required for the water and nutrient balance study, a wide variety of instruments were installed at three first order catchments. The catchments were located in the Cumaru watershed (Figure 3.1 and Figure 3.2). The field topographical mapping and installation of the equipment with data loggers took place between July and December 2000. For the current study mainly the data collected between the 1st of January 2001 and the 18th of June 2002 were used. Most instruments were located in watershed 1 (Figure 3.2).

Watershed 1 (WS1) covered approximately 35.79 ha of which 25.5 ha was estimated to contribute to weir W1. Watershed 2 (WS2) was measured at 34.6 ha, 28.6 ha of which were estimated to contribute to weir W2. Watershed 3 (WS3) was much smaller at only 12.2 ha, 9.6 ha of which were estimated to contribute to weir W3. At the beginning of this study approximately 60% of WS1 and WS2, and 30% of WS3 were covered with fallow vegetation, with the remaining area being used for smallholder agriculture. The agriculture at all watersheds consisted of small patches planted with traditional crops and small plots (<1ha) of passion fruit and pepper. The IKONOS image (Figure 3.1) gives a good indication of the heterogeneity of the landscape and the distribution of forested areas (red) and agricultural areas (blue-green).

For the 2000-2001 growing season land at all watersheds prepared with the traditional slash-and-burn method. For the growing season of 2001-2002 two plots of 3.0 and 1.1 ha in size and directly adjacent to the riparian forest of WS1 were prepared with the mulch machine. At WS2, two fields of 2.5 ha and 1 ha in size adjacent to the riparian forest were prepared with the traditional slash-and-burn method. WS3 served as a 'control' catchment where the normal agricultural system continued with burning of fields at a greater distance from the source.

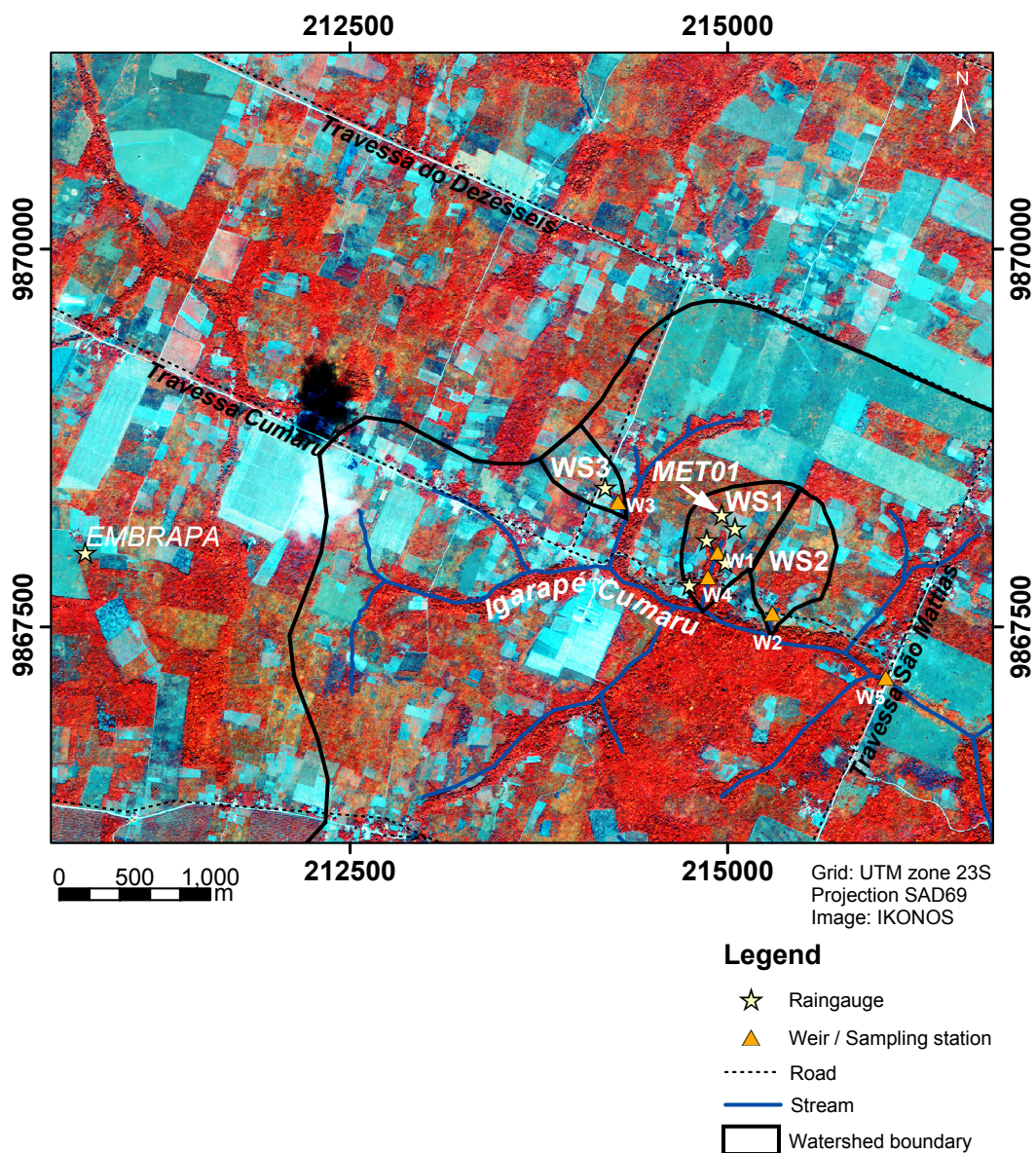


Figure 3.1 Location of the first order watersheds, the weirs and the rain gauges (IKONOS image from J. Puig, in preparation)

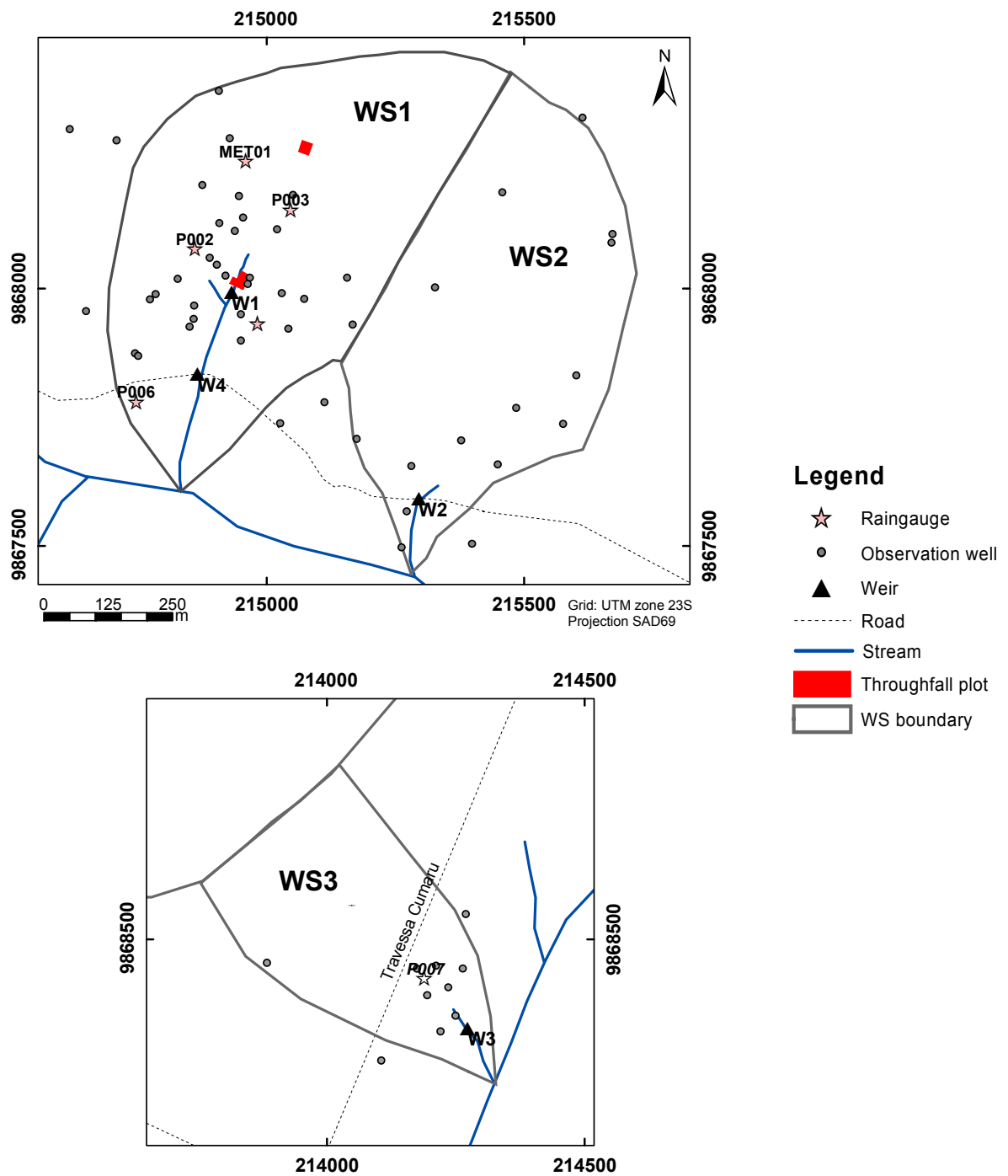


Figure 3.2 Location of various types of instruments distributed through the watersheds

3.2 Rainfall measurements

Gross rainfall (P) at WS1 was measured using a tipping bucket rain gauge (Young 52203; 0.1 mm per tip), and recorded at 5 minute intervals by a Campbell Scientific automatic weather station (MET01). A second tipping bucket rain gauge (Onset RG2-M; calibrated at 0.3 mm per tip) was located at a 50 m distance from MET01. This rain gauge was used from the 5th of March 2002 until the end of the fieldwork period because the MET01 rain gauge stalled. Five totalizing rain gauges were distributed throughout in open fields in WS1, WS2 and WS3 in order to determine spatial variation in the rainfall distribution. The totalizing gauges with a funnel diameter of 10 cm were emptied after every major rainfall event. Events were defined by periods of rain separated by minimally 3 hours of no rainfall.

The accuracy of the tipping bucket rain gauge of MET01 was verified by cross calibrating rainfall event totals with the amounts measured by a HOBO rain gauge (located 50m east of MET01), the totalizing rain gauges distributed over WS1, WS2 and WS3 and monthly rainfall totals from a meteorological station operated by EMBRAPA (located approximately 5 km west of MET01; Figure 3.1).

Figure 3.3a shows the linear regression plot of the rain catch of 53 events measured at the MET01 rain gauge versus the HOBO rain gauge total. The slight difference between the two is most likely due to the slightly lower accuracy of the HOBO gauge. Based on this calibration, the HOBO gauge was deemed reliable for extrapolating the rainfall record from the 5th of March 2002 until the end of the fieldwork period. Figure 3.3b indicates a strong correlation between the rainfall measured at MET01 and three selected totalizing gauges. The scattering of the points is thought to be caused mainly by spatial variability of rain distribution. Figure 3.3c shows the monthly totals measured at MET01 as compared with the values measured at the EMBRAPA station. The EMBRAPA station recorded a slightly higher annual rainfall over the year 2001 which is likely due to differences in exposure and location.

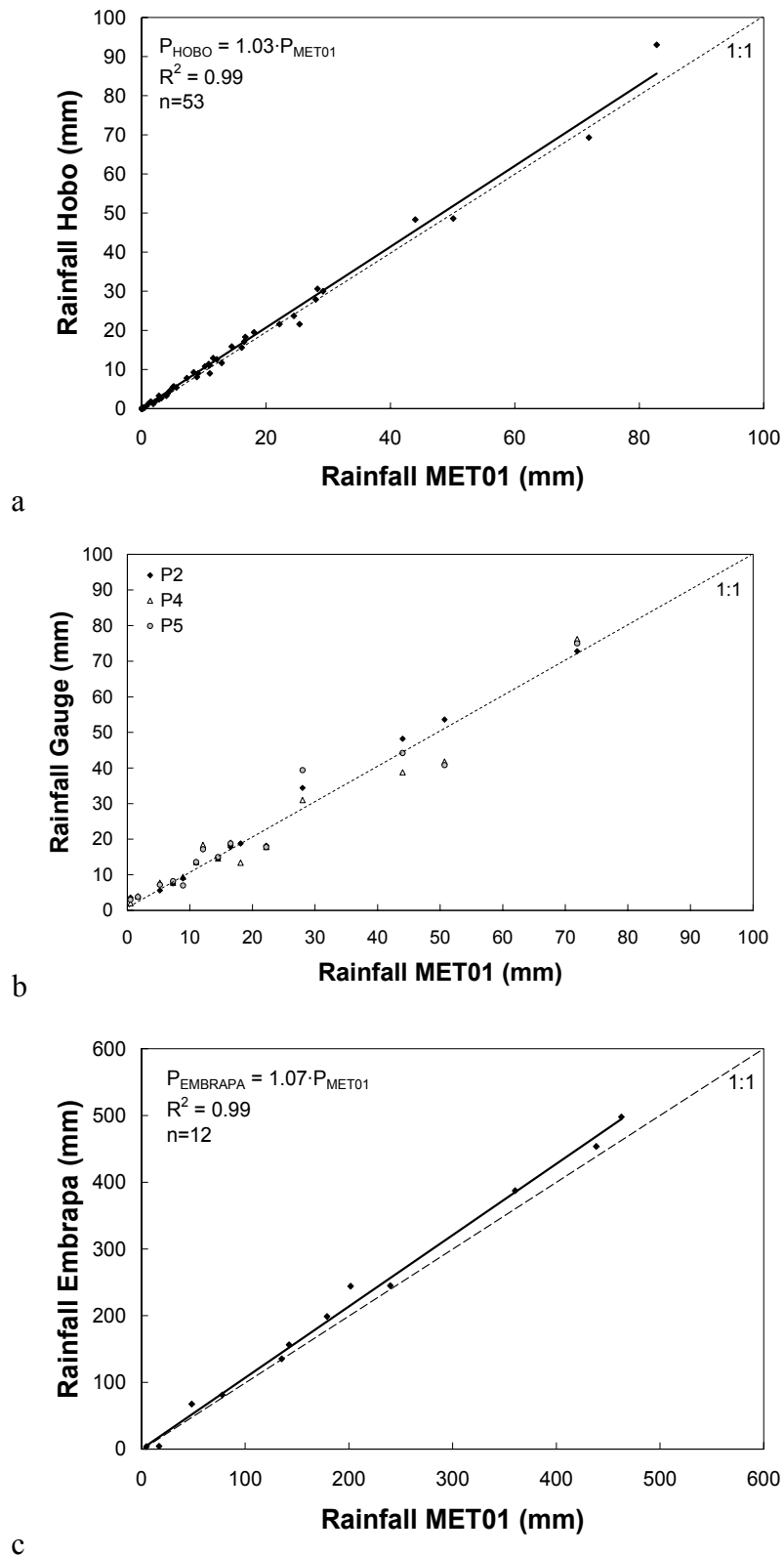


Figure 3.3 Correlation between the rainfall measured by MET01 and a) the automatic HOBO rain gauge at 50 m distance, b) the totalizing rain gauges and c) 2001 monthly rainfall totals at the EMBRAPA station

3.3 Throughfall measurements

Throughfall (*Tf*) was measured at two plots (15 by 15 m) following the method of Lloyd and Marques (1988) using 15 randomly distributed totalizing collectors of the same type as the totalizing rain gauges for each plot (Figure 3.7c). The first plot was located in a stand of approximately 4.5 year old fallow vegetation (Figure 3.4a), and the second in the riparian forest (Figure 3.4b). Measurements were made between the 7th of January and the 30th of April 2002. The *Tf* collectors were emptied and randomly relocated after each major storm.

In addition to the gauge measurements in the riparian forest plot, continuous *Tf* measurements were conducted using two sharp-rimmed 2 m long gutters (Figure 3.7d) each equipped with a tipping bucket event recorder (Onset RG2-M; 0.2 mm per tip) between the 1st of February and 23rd of April 2002. The tipping bucket gauge was covered with a lid, so that only water from the trough was measured. This lid was removed for the photo (Figure 3.7d).



Figure 3.4 a) Mulched area with riparian forest in the background; b) Mulched surface with approximately 5 year old fallow vegetation in the background

The strong correlation between the measured daily totals by the two gutters is shown in Figure 3.5a. For the period that both gauge and trough data were available, the cumulative throughfall is plotted in Figure 3.5b. The strong correlation between both the trough and gauge measurements indicates that the measurements contain only a small error of estimate.

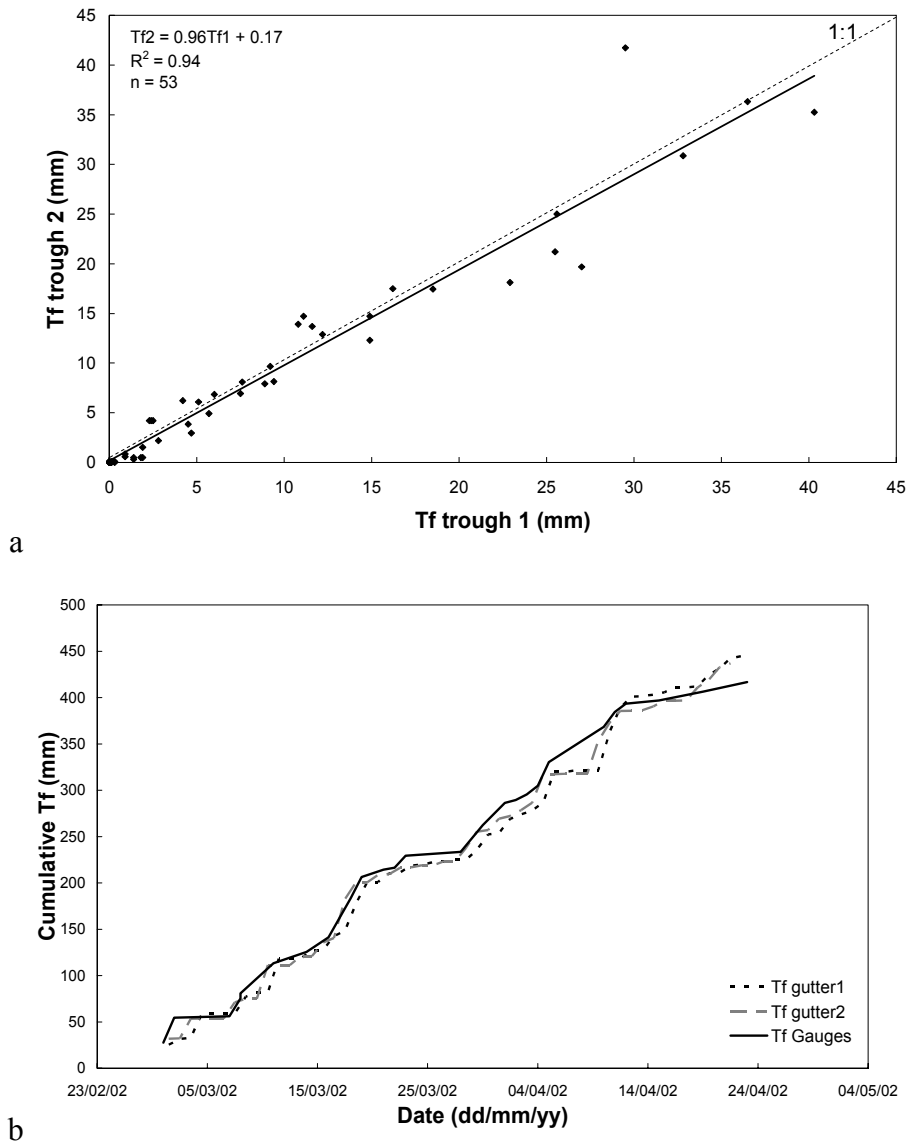


Figure 3.5 a) correlation between throughfall measured with the two troughs in the riparian forest; b) cumulative throughfall of the two throughfall gutters and throughfall gauges

3.4 Micrometerological measurements

Micrometeorological observations required for the calculation of evapotranspiration were made using an automatic weather station based on a Campbell Scientific CR23X data logger. The weather station was situated in the center of a 0.7 ha plot of 1 to 2.5 year old fallow vegetation (Figure 3.7a and b). Wind speed and direction at 2.5 m above the ground surface were measured using a Vector instruments anemometer and wind vane (A100R and W200P). Air temperature, relative humidity and net radiation were

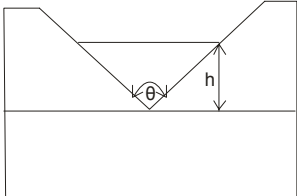
measured with a Rotronic MP100A probe. The net short and long wave energy balance (0 to 100 μm) were measured with a Kipp en Zonen NR-Lite radiometer. Incoming shortwave radiation (350-1100 nm) was measured with a Skye SP1100 pyranometer. The soil volumetric water content over the top 20 cm was measured with a Campbell Scientific CS615 water content reflectometer. Soil heat flux measurements were made using a Hukseflux Heat Flux Plate (HFP01) at 10 cm below the soil surface, and soil temperature at 5, 10, 25, and 50 cm depth respectively with CS107 thermistor probes. All climatic data were stored at 5 minute intervals in a CR23X data logger.

3.5 Runoff measurements

Runoff measurements at WS1 were made using a V-notch weir (W1; Figure 3.7e) situated 100m from the source of the stream, and a culvert weir 200 m downstream and close to the catchment outlet. The V-notch weir was equipped with an ISCO 6700C automatic water sampler with a water level sensor and an YSI multi-parameter sensor (Figure 3.7j) which measured pH, conductivity and temperature at 5 minute intervals. Runoff measurements at the culvert (W003) were made with a TD-DIVER pressure sensor (Van Essen Instruments) which recorded water level and temperature. Runoff measurements at WS2 and WS3 were performed with a 90° V-notch weir (W2; Figure 3.7f, and W3) equipped with a TD-DIVER. The DIVERS logged water level and temperature at a 5 minute interval and were corrected for changes in the air pressure with a barometric pressure logging at the same interval. A weir station at the outlet of the Cumaru watershed (Figure 3.7h) was originally projected, but due to theft of equipment it was unfortunately never constructed. This point, indicated as W5 (Figure 3.1), was only used for streamflow sampling during baseflow conditions.

The relation between water level and discharge for a 90° V-notch weir is given by (Bos, 1976; Kindsvater and Carter, 1957):

$$(3.1) \quad Q = C_e \frac{8}{15} \sqrt{2g} \tan \frac{\theta}{2} h_e^{2.5}$$



Q = discharge (m^3/s)

C_e = Coefficient of discharge (-)

g = gravity (m/s^2)

θ = angle of weir

h_e = effective head

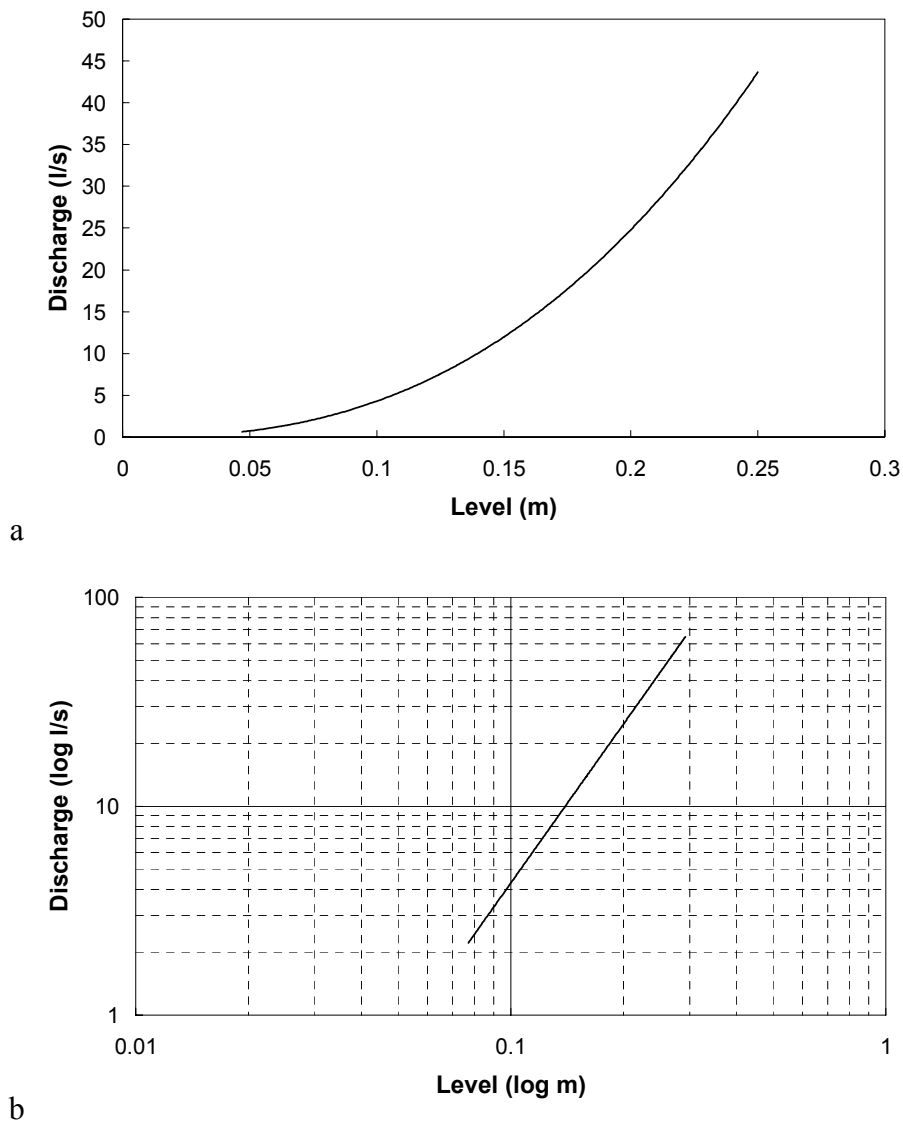


Figure 3.6 Relationship between water level and runoff for a 90° V-notch weir a) normal plot, b) log-log plot

3.6 Infiltration measurements

The infiltration rate of the soil is approximately equal to the saturated conductivity under a unit hydraulic gradient in the soil. Numerous methods for the estimation of the infiltration rate are available. The infiltration capacity of the soil was determined with infiltration measurements using the double ring infiltrometer at 14 distributed points throughout WS1. First the soil inside and surrounding the ring was saturated, and the center ring of the infiltrometer was filled with water. The outer ring was maintained full

of water. An automatic pressure sensor logged the water level every 30 seconds until the water level receded to approximately 5 cm above the soil surface.

A blue dye tracer experiment was performed at three locations to evaluate the flowpaths of infiltrating water. A mixture of water with Brilliant Blue FCF dye was infiltrated through a metal ring with a diameter of 25 cm, which was driven 20 cm into the soil. After 20 liters were infiltrated the wetting front was dug out and its depth was measured and photos of the profile were made.

3.7 Groundwater measurements

Throughout the study period a network of 67 monitoring wells was distributed over WS1, WS2 and WS3 (Figure 3.2). The wells consisted of high density polyethylene (HDPE) tubes (\varnothing 5 cm) with a one meter slotted filter. A filter ‘sock’ covered the filter to prevent sand from entering the tube. For the first 4 months of the 18 month study period, daily observations of the water levels were made between 6:00 and 9:00 in the morning with an electronic tape gauge. For the remaining 14 months the observations were made every other day because short term changes were minimal. In four selected wells a water level and temperature logger (TD-DIVER) was installed, recording initially at a 5 minute interval, and later reduced to a 30 minute interval. The DIVER measurements were corrected for changes in the air pressure with a barometric pressure logging at the same interval.

Study sites and instrumentation





Figure 3.7

a) Meteorological station situated in one year old fallow vegetation; b) close-up of the instruments; c) totalizing throughfall gauge; d) throughfall gutter with tipping bucket rain gauge; V-notch weirs at e) W1 and f) W2; g) double-ring infiltrometer; h) main channel of Igarapé Cumarú at W5; i) overview of the mulched field planted with corn, j) automatic water sampler; k) soil pit in 'Latosolo Amarelo'; l) setting the depth record / 30 m deep observation well; m) weir construction crew; n) drilling crew

4 WATER BALANCE

4.1 Introduction

The main components of the water budget of a vegetated surface in a humid tropical environment (Figure 1.2) are rainfall (P), total evapotranspiration (ET), runoff (Q) deep drainage (D) and groundwater storage (ΔS) (Eq. 4.2). ET is made up of rainfall interception (Ei or Ew ; evaporation from a wet canopy or interception), transpiration (Et ; evaporation from a dry canopy) and evaporation from the soil/litter (Es). The stream runoff consists of baseflow (Q_b) and stormflow (Q_s).

$$(4.1) \quad P = Et + Ei + Es + HOF + SOF + SSSF + GwF + D \pm \Delta S$$

$$(4.2) \quad P = ET + Q_s + Q_b + D \pm \Delta S$$

P	Precipitation	D	Deep drainage
Q	Runoff	GwF	Groundwater Flow
Qb	Baseflow	HOF	Horton Overland Flow
Qs	Stormflow	SOF	Saturation Overland Flow
ET	Evapotranspiration	SSSF	Sub-Surface Storm Flow
Ei	Interception		
Et	Transpiration		

Over an entire year, changes in groundwater storage of a balanced system are minimal. While P and Q are measured with fairly straightforward techniques, the calculation of ET often yields larger uncertainties. ET can be estimated using various methods, of which the water balance method and micro-meteorological methods are the most commonly used (Bruijnzeel, 1990).

The micrometeorological methods require detailed measurement of a wide variety of atmospheric and vegetation parameters (Shuttleworth, 1988; Shuttleworth, 1989), which is usually a costly affair. The water balance methods involve measurements of rainfall and streamflow or drainage, changes in soil moisture and changes in groundwater (Bruijnzeel, 1990). These methods are based on the assumption that an area is water tight and all water flow is gauged as streamflow ($D \approx 0$), or that subterranean fluxes are known. Otherwise, this method can lead to severe underestimation of ET (Bruijnzeel, 1990; Dingman, 1994; Ward and Robinson, 2000).

In this chapter the annual water balance for two small first order watersheds is solved by quantifying each component. Rainfall (P) and rainfall processes are discussed in section 4.2, and the rainfall interception process is quantified in section 4.3. Based on a micrometeorological method, ET is estimated in section 4.4. An estimate of ET based on the water balance method is incorporated in the conclusion (section 4.7). The rainfall-runoff dynamics are discussed in section 4.5 evaluating the occurrence of overland flow and quantifying the base and stormflow contributions to Q . In section 4.6 groundwater level variation (ΔS) and regional groundwater flow are evaluated, followed by the water balance summary in section 4.7.

4.2 Rainfall

4.2.1 Rainfall observations

The hourly rainfall record over the 18-month study period is shown in Figure 4.1. Between the 1st of January and the 31st of December 2001, the total rainfall yielded approximately 2253 mm. Due to short interruptions in the first month of operation, this figure may represent a slight underestimation of the total annual rainfall. Measurements were interrupted between the 20th and the 22nd of August to resolve some calibration issues with other sensors. However, the nearby totalizing rain gauges did not record any rainfall over this period. Between the 1st of January 2002 and the end of the current study on the 18th of June 2002, the total recorded rainfall was 1798 mm.

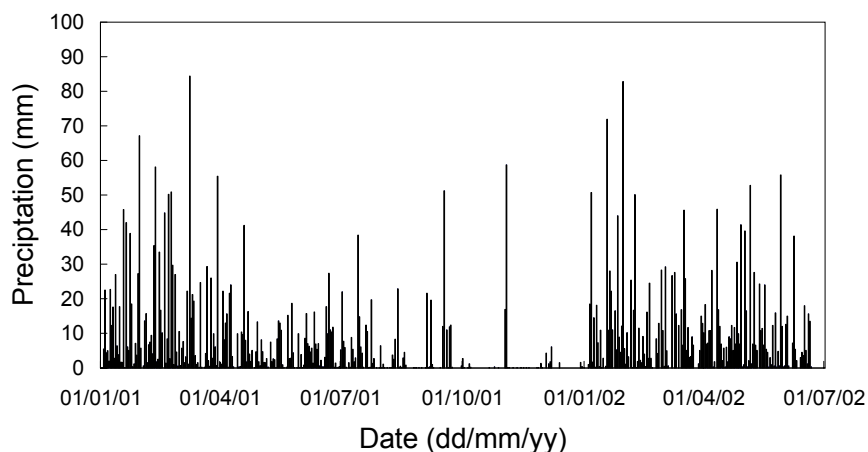


Figure 4.1 Daily rainfall record at the Cumaru meteo station (MET01) between the 3rd of January 2001 and the 18th of June 2002

The total annual rainfall for the region typically ranges between 1700 and 2700 mm, with a long- term average around 2400 mm (EMBRAPA, 1977-2002). The record of monthly rainfall totals for the fieldwork period as compared with the 8-year record of the EMBRAPA station is represented in Figure 4.2.

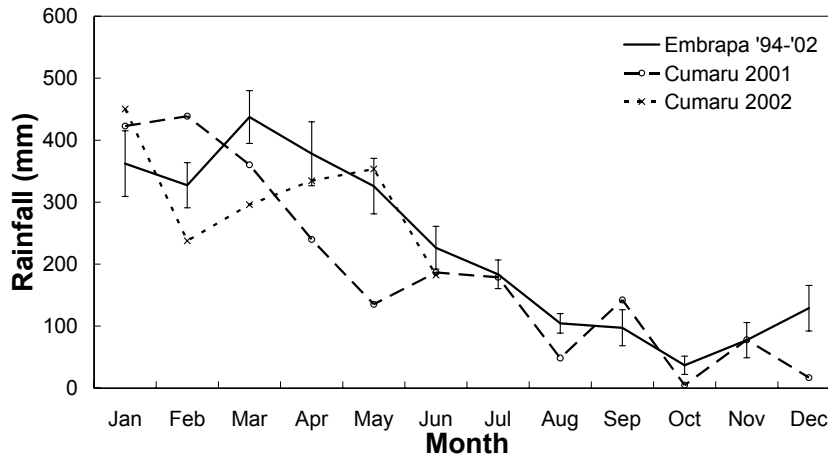


Figure 4.2 Comparison of the total monthly rainfall values of the year 2001 and the first six months of 2002 at the Cumaru meteorological station (MET01), with the 1994-2001 rainfall recorded at the EMBRAPA station

4.2.2 Rainfall intensity and occurrence

Rain in this region typically falls in high intensity events of short duration, which predominantly occur between 12:00 and 18:00. Over the period between the 3rd of January and the 31st of December 2001, 263 separate events were recorded. An event is defined by a 5-minute rainfall total greater than 0.1 mm, and is separated from a subsequent event by a minimum period of 3 hours without rainfall. Of all storms over the measured period, 73 % totaled less than 10 mm of rainfall (figure 4.3a), and 91 % were of duration shorter than 3 hours. No storms lasting longer than 11 hours were recorded (Figure 4.3b). Interestingly, the 32 events that yielded more than 20 mm of rainfall accounted for 53 % of the total annual rainfall amount (figure 4.3a). The largest rainfall event of 2001 yielded 84.8 mm in 565 minutes on the 11th of February. Some 52% of all rainfall occurred between 12:00 and 18:00 yielding 60% of total annual rainfall (Figure 4.4). The highest hourly rainfall intensity over the experiment period was 43.3 mm hr⁻¹ for 2001, measured on the 17th of September, and 52.5 mm hr⁻¹ for the first half 2002 on the 4th of May. The average rate of rainfall over 2001 was 6.7 mm hr⁻¹, with an average storm size of 7.7 mm, and an average duration of only 69 minutes.

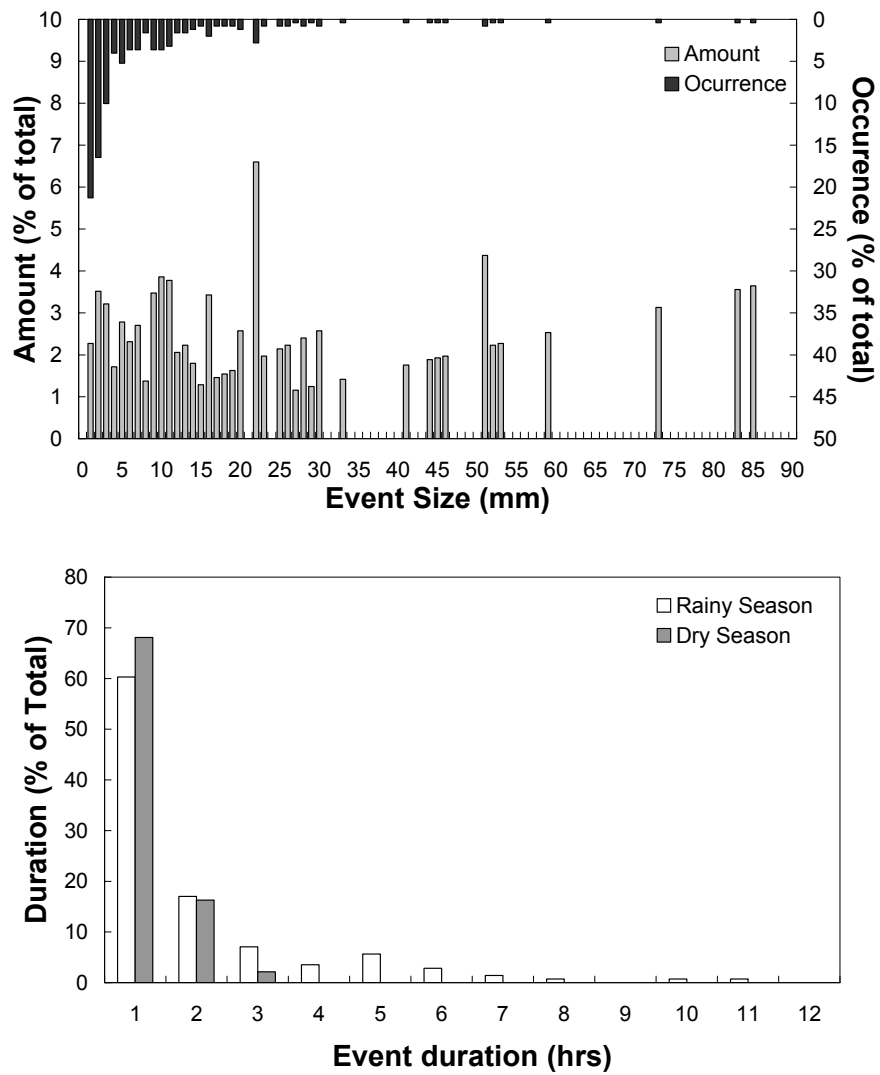


Figure 4.3 a) Distribution of occurrence and relative contribution to total annual rainfall by differently sized storm events; b) Storm duration distribution in the dry and the wet season

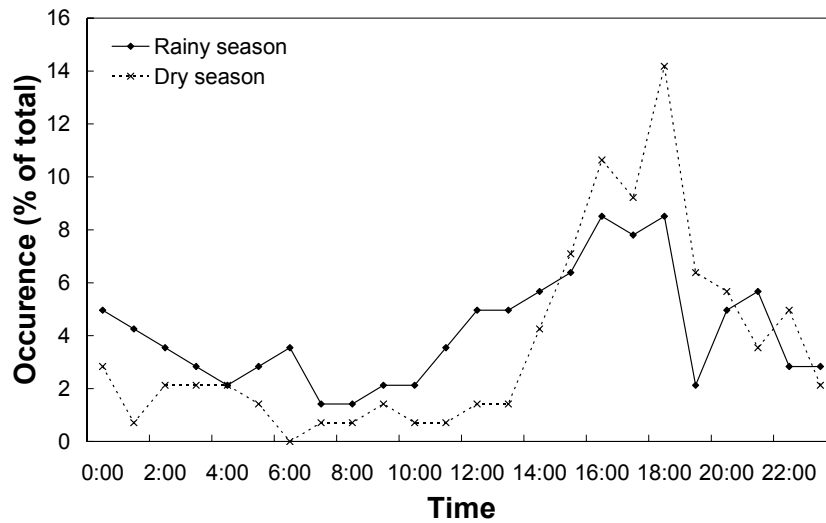


Figure 4.4 Diurnal distribution of occurrence and relative amounts of rainfall over the year

4.2.3 Seasonal variation

Given the rainfall characteristics summarized in Table 4.1, it becomes clear that the wet and the dry season rainfall events differ markedly in intensity and duration. During the wet season (January-April) rain comes in longer duration events with lower intensity than in the dry season. Figure 4.5 shows the diurnal patterns of rainfall occurrence for two selected months. In the month February (Figure 4.5b) rain is mainly generated by two storm types. The first type originates from large-scale disturbances traveling along the coast independent of diurnal influences. The second storm type originates from small-scale convective storms which form during the morning hours and precipitate around 14:00 to 16:00 hours local time. In the months May and June a transition to the dry season is observed with more convective storms. In November, precipitation comes (with a few exceptions) from intense convective afternoon showers (Figure 4.5b).

Table 4.1 Summary of the rainfall characteristics over the study period

	Events (no.)	Total (mm)	Mean (mm)	Median (mm)	St Dev (mm)	Intensity (mm/hr)	Duration (min)
Wet season 2001	141	1426	10.1	3.0	15.7	5.7	94
Dry season 2001	122	793	6.5	2.9	8.9	8.4	46
Entire year 2001	263	2253	8.4	3.0	6.7	6.7	69
Wet season 2002	148	1285	7.3	1.5	13.6	6.4	53

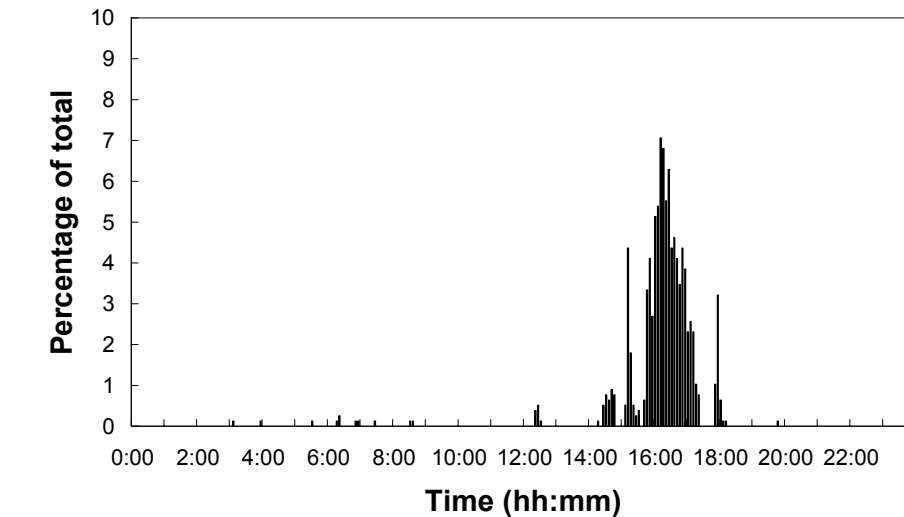
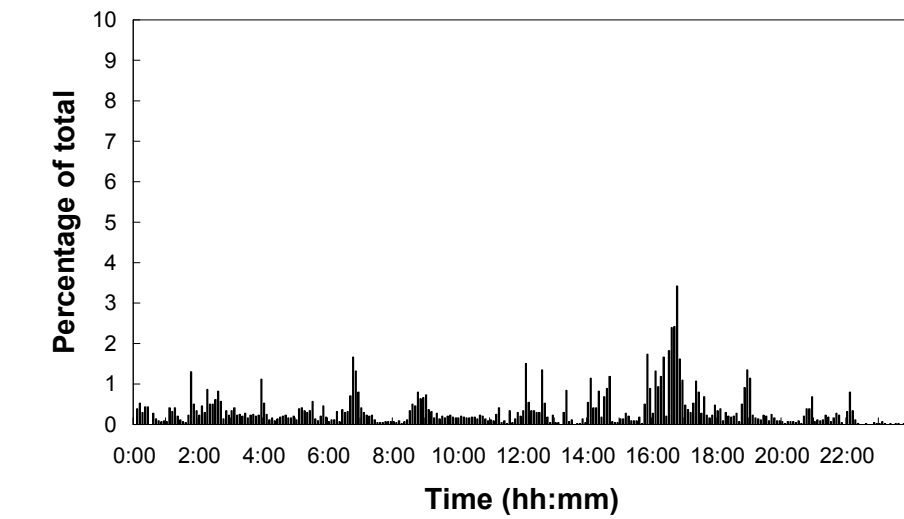


Figure 4.5 Diurnal distribution of the occurrence of rain events for a) February 2001 and b) November 2001

4.2.4 Water balance summary rainfall

The total rainfall measured over the year 2001 at WS1 (2253 mm) was close to the long term regional average of 2400 mm (EMBRAPA, 1977-2002). In the first half of 2002, 1854 mm of rain was measured versus 1784 mm for the same period in 2001. This indicates that the first half of 2002 did not deviate from the normal pattern. Spatial variation over the studied watersheds was shown to be minimal (section 3.2), and therefore it was concluded that the value measured at WS1 could be used for all watersheds. The patterns observed in the current study match very well with the climatologic description given in various review works of the Amazon region (Molion, 1993; Nimer, 1972; Nimer, 1991).

Table 4.2 Observed monthly rainfall totals at the Cumaru watershed between January 2001 and June 2002

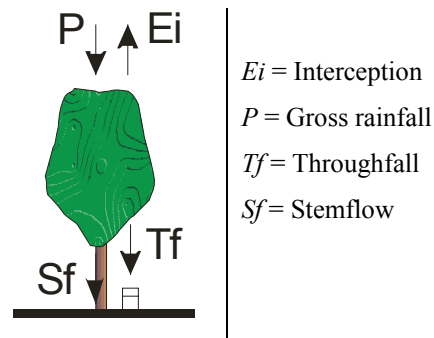
	2001 P (mm)	2002 P (mm)
January	423	450
February	439	238
March	360	296
April	239	335
May	135	353
June	187	182
July	179	
August	49	
September	142	
October	5	
November	78	
December	17	
Subtotal Jan.-Jun.	1784	1854
Total	2253	

4.3 Rainfall interception

4.3.1 Introduction

For humid tropical fallow vegetation as present in the research area the only input into the hydrological system is rainfall. Outputs from the canopy include wet and dry canopy evaporation. When the rainfall reaches the canopy it is partitioned into throughfall (Tf), stem flow (Sf), and interception (Ei). Throughfall is defined as the proportion of rainfall that reaches the forest floor, directly or indirectly through the forest canopy, and stem flow by flow along branches and tree trunks. The interception loss can therefore be determined by subtracting the measured throughfall and stem flow from the rainfall:

$$(4.3) \quad Ei = P - (Tf + Sf)$$



Rainfall interception (Ei) depends on spatially variable parameters like rainfall and vegetation characteristics, which make it a complex process (Jackson, 1975; Zinke, 1967). Important factors controlling the interception process are micro-meteorological factors such as rainfall rate and duration, available energy, temperature, humidity and wind speed, as well as vegetation characteristics such as structure, density and surface properties (Clegg, 1963; Leonard, 1967; Pearce et al., 1980). Under similar climatic conditions, the increase in foliar biomass with forest age should result in an increase of rainfall interception. After canopy closure is completed the fraction of intercepted rainfall by the canopy should be fairly constant (Waterloo, 1994). Reported estimates of Ei of tropical vegetation vary considerably, ranging between 4.5 (Jordan and Heuvelink, 1981) to 22 % (Franken et al., 1992) of gross rainfall for tropical lowland forests. Reported stemflow (Sf) percentages for these types of forests are typically in the order of 1 to 2 %. Secondary or fallow vegetation tends to display a similar range of estimates for Ei ranging from 3.1 % (Schroth et al., 1999) to 24 % (Hölscher et al., 1998). The estimates of Ei reported by these fallow vegetation studies coincide with very high estimates for Sf of 20.3 % and 38 % respectively. No references to rainfall

interception studies of riparian forests were found in literature, although in general this vegetation seems to resemble lowland forest in its structure.

4.3.2 Methodology

Forest structural parameters

The hydrological characteristics of the canopy are typically expressed with the following parameters: the canopy storage capacity (S), the free throughfall coefficient (p) the trunk storage capacity (St) and the proportion of rain diverted to the trunk (pt). S is the amount of water stored on the saturated canopy after rainfall and TF have ceased (Gash, 1979).

Various methods for determining S were given by Reynolds and Leyton (1963), Gash and Morton (1978), Rowe (1983), and Jackson (1975). In an evaluation of these methods for tropical forest sites on Puerto Rico by Wickel (1997) and Schellekens (1999) and on Jamaica by De Jeu (1996), the methods of Leyton et al. (1967) and Jackson (1975) were found to give the most accurate estimate of S . Both methods are based on the assumption that evaporation during storm events is negligible.

Using the method of Leyton et al. (1967) S is determined by drawing a line of unit slope ($1-pt$) passing through the upper points of events greater than 1.5 mm rainfall. It is assumed that these points represent conditions with minimal evaporation. S is determined by the negative intercept with the y-axis (Leyton et al., 1967; Gash and Morton, 1978). The method of Jackson (1975) is somewhat similar, but separates storms large enough to saturate the canopy and smaller storms by identifying the ‘inflection point’ in the plot of P versus Tf where the graph gets steeper.

$$(4.4) \quad S = P_{inflection} - Tf_{inflection}$$

S = Canopy saturation value
 $P_{inflection}$ = Rainfall at infl. point
 $Tf_{inflection}$ = Throughfall at infl. point

The line of near unit slope is drawn through the upper points of events greater than the inflection point. The slope of the linear regression for storm smaller the inflection point yields an estimate of the free throughfall coefficient (p). Since the method of Jackson (1975) requires observations of small events of rainfall an automatic station is required.

Since only the riparian forest plot was equipped with *Tf* troughs this method could only be used for that plot.

The Gash analytical model

The Gash analytical model (Gash, 1979) is based on the Rutter model (Rutter et al., 1971) has been used with reasonable to good results for various different forests, especially under tropical conditions (Bruijnzeel and Wiersum, 1987; Gash et al., 1995; Lloyd et al., 1988; Schellekens et al., 1999; Van Dijk, 2002; Waterloo, 1994; Wickel, 1997). The Gash model combines the simple features of the empirical regression approach (Jackson, 1975; Leonard, 1967; Zinke, 1967) with the conceptual basis of the Rutter model (Rutter et al., 1971). The model is based upon the assumption that the actual rainfall pattern can be represented by a series of discrete (daily) storms, separated by periods during which the canopy dries completely. A modification was suggested by Gash et al. (1995) for sparse canopy and certain meteorological conditions. For the current study these modifications were not required.

The Gash model requires storm based or daily records of gross rainfall (P_g), mean rainfall rate (\bar{R}) mean evaporation rate from wet canopy (\bar{E}_w), and the following canopy trunk parameters: Canopy storage capacity (S) the free throughfall coefficient p , the trunk storage capacity (S_t), and the proportion of rain diverted to the trunk (p_t).

Gash (1979) defined that the interception loss can be is given by:

$$(4.5) \quad E_i = aP_g + b$$

E_i = Interception
 P_g = Gross rainfall
 b = constant

where the regression slope a is given by:

$$(4.6) \quad a = \frac{\bar{E}_w}{\bar{R}}$$

\bar{E}_w = Mean evaporation rate from wet canopy
 \bar{R} = Mean rainfall rate

It should be noted that a and \bar{E}_w , and therefore \bar{R} are considered to be constant. The precipitation needed to fill the entire canopy storage (P') is calculated from (Gash, 1979):

$$(4.7) \quad P' = \frac{-\bar{R}S}{\bar{E}_w} \ln \left[1 - \frac{\bar{E}_w}{\bar{R}} \left(\frac{1}{1-p-pt} \right) \right]$$

$P' =$ rain needed to fill canopy storage

$S =$ canopy saturation value

$p =$ free throughfall coefficient

$pt =$ fraction of P diverted to trunks

The analytical formulations of the components that make up the total interception loss according to Gash (1979) are listed in Table 4.3.

Table 4.3 Analytical formulation of the components of interception loss (after Gash, 1979)

Component of interception loss	Formulation
For m small storms ($Pg < Pg'$)	$(1-p-p_t) \sum_{j=1}^m P_{gj}$
Wetting up of the canopy in n large storms ($Pg \geq Pg'$)	$n(1-p-p_t)P'_g - nS$
Evaporation from the saturated canopy during rainfall	$\frac{\bar{E}}{\bar{R}} \sum_{j=1}^n P_{gj} - P'_g$
Evaporation after rainfall ceases for n large storms	nS
Evaporation from trunks in q storms that fill the trunk storage	qS_t
Evaporation from trunks in $(m+n-q)$ storms that do not fill the trunk storage	$p_t \sum_{j=1}^{m+n-q} P_{g,j}$

The model efficiency is determined with the goodness of fit based on the error variance (Nash and Sutcliffe, 1970):

$$(4.8) \quad E = \left[1 - \frac{\sigma_\varepsilon^2}{\sigma_o^2} \right]$$

$E =$ modeling efficiency

$\sigma_\varepsilon^2 =$ error variance

$\sigma_o^2 =$ variance of the observations

where the error of variance is defined as

$$(4.9) \quad \sigma_\varepsilon^2 = \frac{1}{T-1} \sum_{t=1}^T (\hat{y}_t - y_t)^2$$

$\sigma_\varepsilon^2 =$ error variance

$\hat{y}_t =$ predicted value of variable y

at time step $t = 1, 2, \dots, T$

4.3.3 Throughfall results

The cumulative gross rainfall above the canopy (Pg) over the four month period presented here yielded 1108 mm in 64 events, and the cumulative throughfall (Tf) measured with the gauges yielded 974 mm (88 %) for the riparian forest plot and 845 mm (76 %) for the 4.5 year old fallow vegetation plot (Figure 4.6). Measurements

between the 28th of February and the 23rd of April 2002 with the gutters in the riparian forest plot yielded 460 mm of *Tf* with 511 mm from rainfall input (90 %). Interestingly, the *Tf* amount measured at the riparian forest (Figure 3.4a; ± 20 m high trees) plot is higher than the amount measured at the much younger fallow vegetation plot (Figure 3.4b ± 4 m high bushes). This is contrary to the general perception that with increasing forest age the amount of *Tf* decreases.

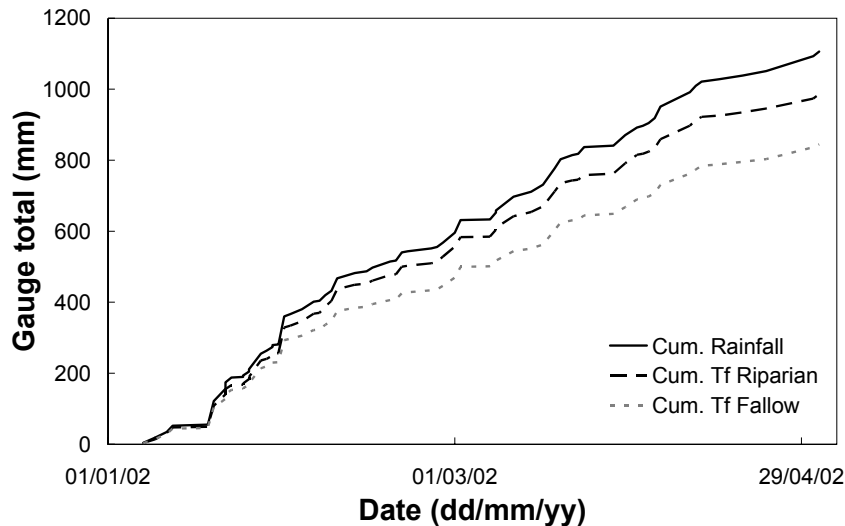


Figure 4.6 Cumulative *Pg*, and *Tf* for the riparian forest and fallow vegetation plots

On average the standard deviation is higher for *Tf* measured at the riparian forest plot (Figure 4.7). This indicates the higher heterogeneity in the structure of the riparian forest. A frequency analysis of *Tf* as a percentage of total rainfall for the 64 rain events shows a distinct difference between the two plots (Figure 4.8). The *Tf* measured with gauges in the riparian forest plot ranged from 0 to 580 %, with a maximum around 80 % of the total incident rainfall (Figure 4.8). The maximum single recorded ‘over-catch’ in the riparian forest was 71 mm of *Tf* resulting from only 12 mm of rainfall (*Tf* exceeded *Pg* by 578%). For the fallow plot the range was 0 to 360 % of the incident rainfall, with a maximum around 60% (Figure 4.8). In the riparian plot the *Tf* of a single gauge exceeded gross rainfall in 30 % of the events, versus 12 % under the fallow vegetation. The ‘over-catch’ by single gauges is caused by the funneling of rainwater towards concentration points on the leaves (‘drip-points’). The main cause of the differences in *Tf* characteristics of the two plots are the result of differences in species composition and therewith in vegetation density and canopy structure. This leads to the conclusion

that the throughfall distribution for the two cases described here can be seen as an indicator for canopy heterogeneity.

Hölscher et al. (1998) demonstrated for two stands of fallow vegetation (± 2.5 and 10 years old), that the *Ei* amounts were strongly determined by floristic composition of the plot, and in particular by the presence of *P. Guyannense*, a banana-like non-woody species. Banana like species are notorious in tropical vegetation for partitioning the rainfall into large amounts of stemflow (*Sf*). Schuster (2001) determined an abundance of 4 % of *P. Guyannense* in an extensive inventory of 8 plots of 3 year old fallow vegetation in the study area. Two of these plots were adjacent to the 4.5 year old fallow vegetation plot of the current study. Schroth et al. (1999) reported high *Sf* volumes (23.2 %) for palm species in fallow vegetation in Central Amazonia.

A comparison with other studies on the canopy water budget of fallow vegetation and other forest types in Brazil is given in Table 4.4. The reported values for *Ei* of fallow vegetation in Eastern Amazonia are within reasonable agreement varying from 6.8 % (Sommer et al., 2003) for 2-3 year old fallow vegetation to 13.5 % (this study). An increasing trend of *Ei* with the age of the fallow vegetation was reported by Sommer et al. (2003). The rainfall partitioning percentages of the riparian forest resemble the values reported for older secondary forest in Eastern Amazonia (Jipp et al.; cited from Sommer 2003) and ‘Terra Firme’ forests in central Amazonia (Lloyd et al., 1988; Ubarana, 1996).

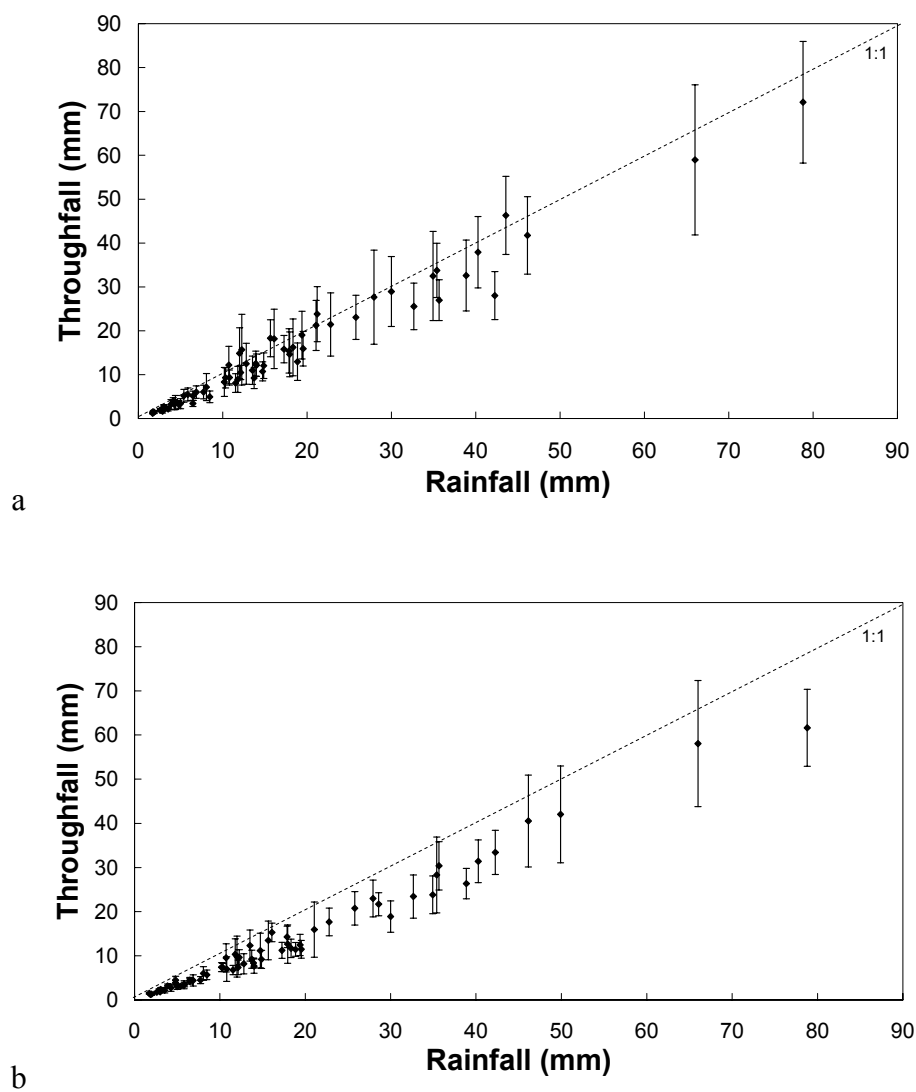


Figure 4.7 Scatter plot of event rainfall versus the resulting throughfall for a) riparian forest and b) 4-5 year old fallow vegetation. The bars indicate the standard deviation

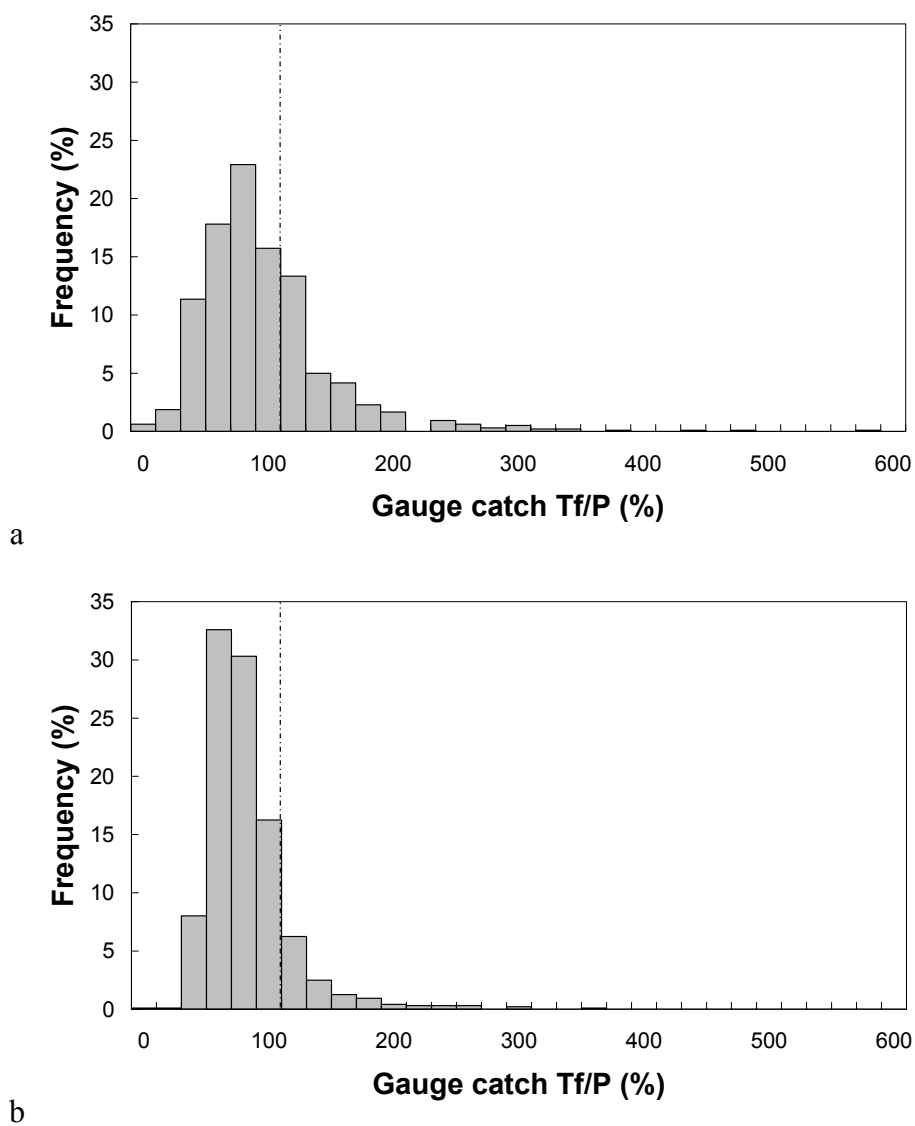


Figure 4.8 Frequency distribution of individual throughfall gauge yield as a percentage of total rainfall for a) riparian forest and b) 4-5 year old fallow vegetation

Table 4.4 Comparison of results of rainfall partitioning studies throughout the Amazon and other locations in Brazil

Forest type, Location	P (mm)	Gauges ³	Obs. ⁴	Tf %	Sf %	Ei %	Reference
Eastern Amazonia, Igarapé Açu							
Riparian forest	1091 ¹	15 R	64 E	88	1	9	This study
Fallow 4.5 yr,	1091 ¹	15 R	64 E	76.5	10	13.5	This study
Fallow 2-3 yr	1956 ¹	15 R	78 W	65	23	12	(Hölscher et al., 1998)
Fallow 10 yr	1956 ¹	15 R	78 W	38	38	24	(Hölscher et al., 1998)
Fallow 3.5 yr	2104 ¹	50 R	BW	77.4	15.8	6.8	(Sommer et al., 2003)
Fallow 4.5 yr	2545 ¹	50 R	BW	71.5	20.5	8.0	(Sommer et al., 2003)
Sec. Forest 17 yr	-			88.8	1.7	9.5	(Jipp et al., in review)
Eastern Amazonia, Other loc.							
Terra firme forest, Peixe Boi	-			83	0.5	16.5	(Jipp et al., in review)
Terra firme forest, Belem	2669 ¹	33 F	-	84.6	0.4	15	(Klinge, 1998)
Terra firme forest Paragominas	492 ¹	24 F	37 E	79.1	-	20.9	(Schuler, 2003)
Terra firme forest, Marabá	1650 ¹	30 R	39 E	86.2	0.8	12.9	(Ubarana, 1996)
Central Amazonia							
Fallow vegetation,	2352 ¹	6 R	107 E	76.9	20.3	3.1	(Schroth et al., 1999)
Terra firme forest, Reserva Ducke	2721 ¹	36 R	47 W	91	1.8	7.2	(Lloyd et al., 1988)
Terra firme forest, Reserva Ducke	3094 ¹	20 F	-	77.7	0.3	22	(Franken et al., 1992)
Terra firme forest, Reserva Ducke	2570 ¹	20 F	49 W	80.2	-	19.8	(Franken et al., 1992)
Western Amazonia							
Rain forest, Caqueta, Colombia	3400 ¹	20 R	-	82- 87	0.9- 1.5	12- 17	(Tobón Marin et al., 2000)
Other locations Brazil							
Mata Atlântica, Reserva Cunha, SP	2319 ²	16 F	67 E	81.8	-	18.2	(Fujieda et al., 1997)
Primary forest, Reserva Jaru, RO	3564 ¹	30 R	78 E	86.2	0.8	12.9	(Ubarana, 1996)

¹measured amount over study period; ²mean annual precipitation

³R = randomly relocated, F = fixed position; ⁴E = events, W = weeks, BW = bi-weekly

4.3.4 Forest structural parameters

The results obtained for determining the canopy storage capacity (S) for both plots using the method of Leyton et al. are given in Table 4.5. The values of S derived with this method were 0.39 mm for riparian forest and 0.65 mm for the fallow vegetation plot. The method of Jackson (1975) gave a lower estimated value for S of 0.43 mm and p of 0.18 for the riparian plot (Figure 4.9). The estimated values for S for riparian forest are rather low in comparison with values reported for other tropical vegetation types (Table 4.5). The strong spatial variability in throughfall under this forest type and the occurrence of drip points (see previous section) may lead to an underestimation of S . Estimation of S using Tf gutter data resulted in a higher estimate, but still is at the low end of the reported values. Doubts about the validity of the determination of S are expressed by Vrugt et al. (2003). However, given the absence of better straightforward field methods for the determination of S , the canopy water balance methods provide at least an estimate. Sampling networks with higher densities and automated gauge systems are thought to result in more accurate estimates.

Table 4.5 Forest structural parameters (section 4.3.2) for various studies

Forest type, Location	S (mm)	p	pt	St	Reference
Riparian Forest, Igarapé Açu	0.39 ¹ , 0.43 ²	0.18 ¹	-	-	This study
Fallow 4.5 yr, Igarapé Açu	0.65 ¹	-	-	-	This study
Sec. forest 17 yr, Peixe Boi	1.1				(Jipp et al., in review)
Primary forest, Rondônia	1.03 ¹	0.031 ²	0.010	0.09	(Ubarana, 1996)
Terra firme forest, Marabá	1.25 ¹	0.044 ²	0.023	0.1	(Ubarana, 1996)
Terra firme rainforest, Manaus	0.74 ¹	0.08			(Shuttleworth, 1988)
Terra firme forest, W-Amaonia	1.3 ⁵	0.32			(Elsenbeer et al., 1994)
Acacia plantation, Java	0.5-0.6 ¹	0.34-	0.07-	0.037-	(Bruijnzeel and Wiersum, 1987)
		0.38	0.08	0.087	
Primary forest, Ivory coast	0.61 ¹	0.03	-	-	(Hutjes et al., 1990)
Agroforestry system, Kenya	0.71-0.93 ¹	-	0.026	0.185	(Jackson, 2000)
Primary forest, Malaysia	1.3 ¹	0.1	0.001	0.01	(Asdak et al., 1998)
Lowland tropical forest, Brunei	0.93 ¹				
	1.14 ²	0.1	-	-	(Dykes, 1997)
	1.07 ³				

Method used for the determination of S: ¹Leyton et al. (1967); ²Jackson (1975); ³Rowe (1983);

⁴(Gash and Morton, 1978); ⁵Bringfelt and Hårsmar, 1974; Method used for the determination of p: ¹Jackson (1975); ²Anascope readings

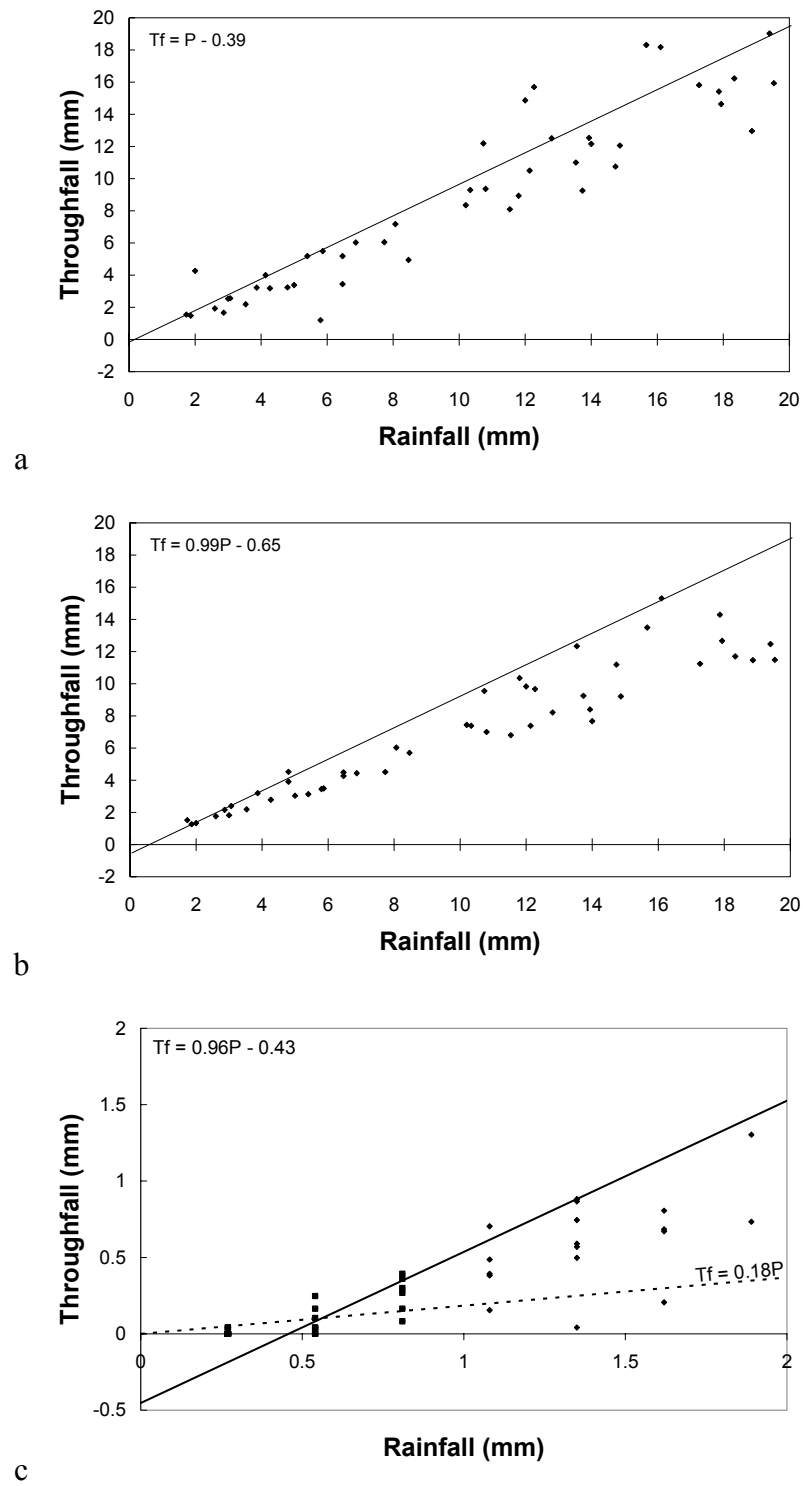
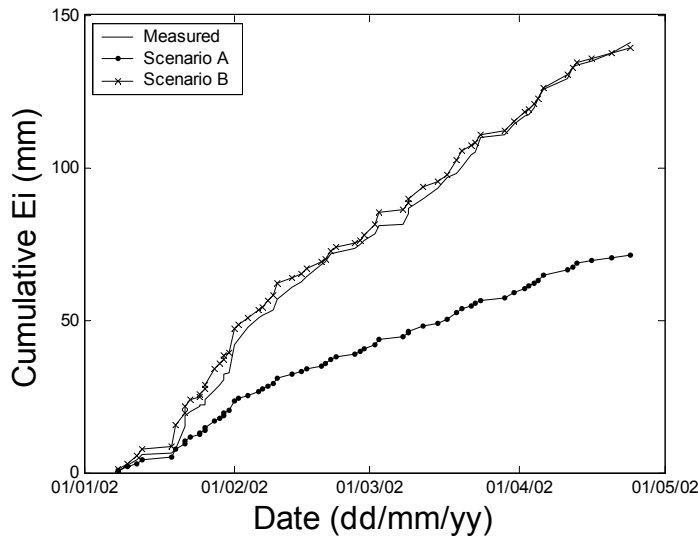


Figure 4.9 Estimation of S (0.39) using the method of Leyton et al. (1967) for a) riparian forest and b) fallow vegetation (0.65); c) Estimation of S (0.43) and p (0.18) using the method of Jackson (1975) for riparian forest

4.3.5 Gash model results

The measured and predicted cumulative totals of Ei are presented in Figure 4.10 for fallow vegetation and Figure 4.11 for riparian vegetation. The model was first run on an event basis for both plots using the forest structural parameters as determined in the previous section and with \bar{E}_w and \bar{R} as determined in section 4.4.3 and 4.2.2 respectively (scenario A). With scenario A for both riparian and secondary vegetation the Gash model severely underestimated the interception losses (Figure 4.10 and Figure 4.11). A good fit for the fallow vegetation plot ($E = 0.83$) was obtained by optimizing using the values of scenario B. For scenario B an optimized value of 0.12 for \bar{E}_w / \bar{R} derived from the linear regression of interception loss versus gross precipitation (Gash, 1979) was used.

For the riparian forest, the optimized value of \bar{E}_w / \bar{R} was determined at 0.09. This model scenario does not have a very high efficiency ($E = 0.37$), mainly because of the greater error introduced by drip points. The importance of the \bar{E}_w / \bar{R} factor is illustrated by the sensitivity analysis given in Table 4.6. A 10% change in \bar{E}_w / \bar{R} results in an 8.3 % increase in predicted interception loss over the fallow vegetation plot.



	Scenario	
	A	B
P (-)	0.18	0.18
S (mm)	0.65	0.65
pt (-)	0.1	0.05
S_r (mm)	0.05	0.05
\bar{E}_w (mm hr ⁻¹)	0.19	0.62
\bar{R} (mm hr ⁻¹)	6.4	6.4
\bar{E}_w / \bar{R} (-)	0.04	0.12
P' (mm)	0.92	0.97
E (-)	0.07	0.83

Figure 4.10 Observed and predicted cumulative interception according to the Gash model for two scenarios A and B for fallow vegetation

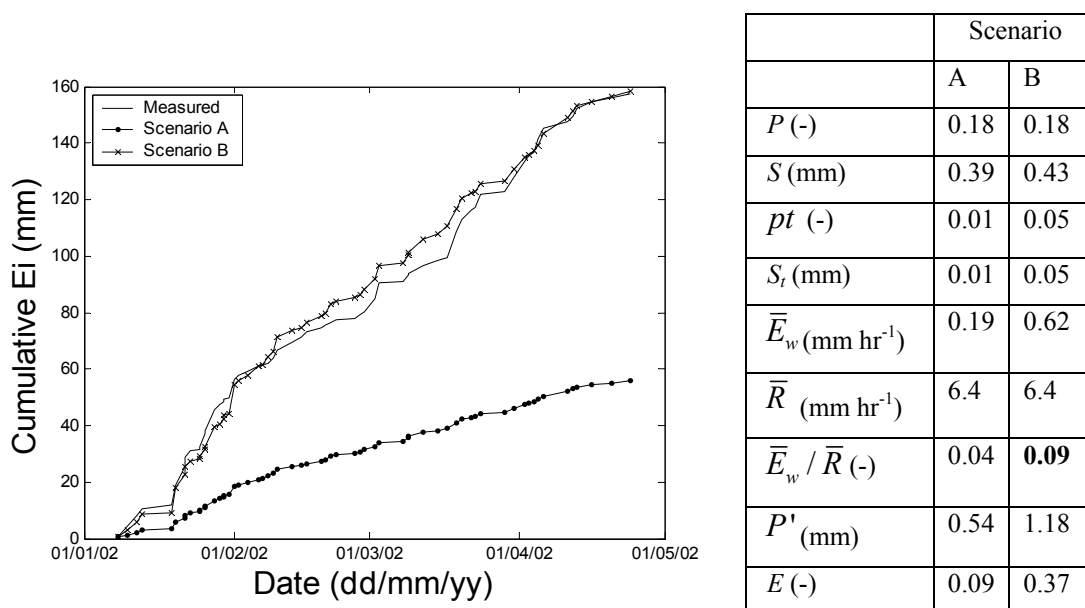


Figure 4.11 Observed and predicted cumulative interception according to the Gash model for two scenarios A and B for riparian forest

Table 4.6 Sensitivity analysis of various parameters in the model B scenario of the Gash analytical model, showing the change in predicted Ei after increasing or decreasing a parameter by 10%

Parameter (initial value)	% change model result	
	10% increase	10% decrease
p (0.18)	-0.09	0.08
S (0.43)	2.9	-2.4
pt (0.05)	-0.02	0.02
S_t (0.1)	0.41	-0.37
\bar{E} / \bar{R} (0.09)	8.3	-8.4

4.3.6 Water balance summary interception

Based on interception measurements over a 4 month period in the rainy season of 2002, monthly interception for the entire areas of WS1 and WS2 were estimated. If the entire watersheds were covered with fallow vegetation, approximately 13.5 % (304 mm) of all water would be intercepted. For the secondary vegetation in the area, which typically has an age of one to eight years, the results of the 4.5 year old fallow vegetation were thought to be representative as a spatial average. In order to come to a monthly

interception value for the watershed, the interception fraction of total monthly rainfall was multiplied with the percentage of area of each type of land. For this calculation three main land use types were respectively defined for the watersheds (WS1 and WS3), these being fallow vegetation (60% and 30%), riparian forest (6% and 3%) and agricultural land (34% and 67%). For the agricultural land, interception was set to zero although some interception takes place. The results are given in Table 4.7. The amount of rainfall interception over the first six months of 2002 was slightly higher in comparison to the preceding year due to the higher amount of rainfall over these months.

Table 4.7 Calculated rainfall interception totals for WS1 and WS3 between January 2001 and June 2002

	P (mm)	Ei (mm)		P (mm)	Ei (mm)	
		WS1	WS3		WS1	WS3
January	423	39	24	450	42	25
February	439	41	25	238	22	13
March	360	34	20	296	28	17
April	239	22	14	335	31	19
May	135	13	8	353	33	20
June	187	17	11	182	17	10
July	179	17	10			
August	49	5	3			
September	142	13	8			
October	5	0	0			
November	78	7	4			
December	17	2	1			
Subtotal Jan.-Jun.	1784	166	101	1854	173	105
Total	2253	212				

4.4 Evapotranspiration

4.4.1 Introduction

The total evapotranspiration (ET) consists of rainfall interception (E_i , see previous section), transpiration (E_t , evaporation from a dry canopy) and evaporation from the soil/litter (E_s). Given the fact that only a small percentage of the area (<1%) consists of bare soil surface and that E_s is very small for forested surfaces, it was neglected in the current study. A general distinction in methods for the determination of ET can be made between water balance methods and micrometeorological techniques (Bruijnzeel, 1990). The water balance methods involve measurements of rainfall and streamflow or drainage, changes in soil moisture and changes in groundwater (Bruijnzeel, 1990). These methods are based, as was mentioned in the introduction to this chapter, on the assumption that an area is water tight or that subterranean fluxes are known. The micrometeorological methods require detailed and costly measurement of a wide variety of atmospheric and vegetation (Shuttleworth, 1988; Shuttleworth, 1989) parameters. The numerous studies in the Amazon region show a wide range of apparent annual ET estimates, ranging from 1120 mm to 1675 mm despite similar climatic and geologic conditions. From a review of numerous humid tropical studies Bruijnzeel (1990) estimated a common average for humid tropical environments of 1400 mm yr⁻¹, and demonstrated that annual ET tends to correlate with annual rainfall as a result of increased rainfall interception.

4.4.2 The Penman-Monteith method

The energy balance for a simple soil surface where photosynthesis and advection are neglected is given by:

$$(4.10) \quad \lambda ET = Rn - H - G$$

where:

λET = latent heat flux

Rn = net radiation

H = sensible heat

G = soil heat flux

The energy used in the production of biomass through photosynthesis is neglected since it only constitutes a small fraction of the daily net radiation. Therefore Eq. 4.10 can only be applied to extensive surfaces of homogeneous vegetation.

The latent heat flux representing the evapotranspiration (ET) fraction can be derived from the energy balance equation if all other terms are known. Net radiation and soil heat fluxes can be measured, but the sensible heat flux is difficult to determine, as it requires detailed measurement of temperature gradients above the surface.

The Penman-Monteith equation includes all parameters that govern the energy exchange and the corresponding latent heat flux from uniform surfaces of vegetation, and allows calculation of the actual evapotranspiration (E_t) from relatively simple above canopy measurements of a set of micro-meteorological parameters (Monteith, 1965). For wet canopy conditions, the surface (or canopy) resistance (r_s) reduces to zero, simplifying Eq. 4.11 to Eq. 4.12 (Brutsaert, 1982; Thom, 1975).

$$(4.11) \quad \lambda E_t = \frac{\Delta \cdot (Rn - G) + \rho_a c_p \frac{VPD}{r_a}}{\Delta + \gamma \left(1 + \frac{r_s}{r_a} \right)}$$

$$(4.12) \quad \lambda E_w = \frac{\Delta \cdot (Rn - G) + \rho_a c_p \frac{VPD}{r_a}}{\Delta + \gamma}$$

where:

λE_t = latent heat flux

Rn = net radiation

H = sensible heat

G = soil heat flux

ρ_a = mean air density at constant pressure

c_p = specific heat of air [$\text{MJkg}^{-1} \text{ } ^\circ\text{C}^{-1}$]

VPD = saturation vapor pressure deficit
[kPa]

r_a = aerodynamic resistance [s m^{-1}]

r_s = bulk surface resistance [s m^{-1}]

Δ = slope of the saturation vapor deficit

γ = psychrometric constant [$\text{kPa } ^\circ\text{C}^{-1}$]

The aerodynamic resistance (r_a) was calculated from wind speed observations above the 1.5 m high fallow vegetation, assuming a logarithmic wind profile and neutral stability conditions (Thom, 1975):

$$(4.13) \quad r_a = \frac{\left(\ln \frac{z-d}{z_o} \right)^2}{k^2 \cdot u_z}$$

r_a = aerodynamic resistance [s m⁻¹]
 z = height measurements [m]
 d = zero plane displacement length [m]
 z_o = roughness length [m]
 k = von Karman's constant, 0.41 [-]
 u_z = wind speed at height z [m s⁻¹]

The ratio of the roughness length (z_o) to the vegetation height (h_v) ranges from 0.02 to 0.2 and is commonly taken to be $0.1 h_v$ (Thom, 1975). The ratio of the displacement length (d) to h_v ranges between $0.55 h_v$ to $0.83 h_v$ for agricultural crop and forest canopies. (Brutsaert, 1982; Thom, 1975). For the current study z_o was set to $0.13 h_v$ and d was set to $0.63 h_v$ (Sommer et al., 2002).

The surface resistance (r_s in s m⁻¹) of a vegetation type is inversely related to the average canopy conductance (g_c in mm s⁻¹) of all leaves of a vegetation stand. The r_s of the vegetation depends on various environmental factors such as available energy (Rn), the vapor pressure deficit (VPD), leaf physiology and soil moisture conditions (Brutsaert, 1982; Thom, 1975). Diurnal and seasonal variations of r_s of tropical fallow vegetation and primary forest have been reported, ranging from 0 s m⁻¹ at sunrise (due to dew effects) to more than 1000 s m⁻¹ in the late afternoon (Roberts et al., 1990; Sá et al., 1996; Shuttleworth, 1989; Sommer et al., 2002).

Using various methods, the stomatal conductance (g_c) of fallow vegetation of different ages in the study region near Igarapé-Açu was determined in previous studies (Sá et al., 1996; Sá et al., 1995a; Sá et al., 1995b; Sommer, 2000; Sommer et al., 2002). Sommer et al. (2002) provided a set of equations to predict canopy conductance as a function of Rn , the VPD and temperature (e.g Dolman et al. 1991; Schellekens, 2000). They considered a multiple linear regression (Eq. 4.14; $r^2 = 0.812$, $n = 2100$) with daily mean VPD , Rn , and T most suitable for the prediction of r_s on an hourly basis yielding similar results to 'Jarvis-type' model described by Wright (1995). The function was obtained by calculating multiple linear regression equations for the estimation of the canopy conductance, by solving Eq. 4.11 for hours where λET was determined with

the Bowen ratio energy balance. Soil moisture was not included in this function which may lead to an overestimate of ET in the dry season. However, moisture stress in fallow vegetation however was not observed in the dry season porometer measurements of 2001 (L. Guild. pers communication). The diurnal trends of the main parameters which determine Et (net radiation, soil heat flux, temperature, humidity and wind speed) were measured above the canopy of the fallow vegetation, and are shown in Figure 4.12.

$$(4.14) \quad g_c = e^{(1.596+0.00226 Rn-0.783 VPD+0.03692 T)}$$

where:

g_c = bulk stomatal conductance [mm s^{-1}]

Rn = net radiation

VPD = saturation vapor pressure deficit
[kPa]

T = air temperature [$^{\circ}\text{C}$]

This function was used for daytime ($Rn > 50 \text{ W/m}^2$) periods with dry canopy conditions.

4.4.3 Evapotranspiration results

Before Et could be estimated with the Penman-Monteith equation, both r_a and r_s needed to be calculated. The diurnal variation of the aerodynamic resistance (r_a) and surface resistance (r_s), derived with Eq. 4.13 and Eq. 4.14 respectively, is shown in Figure 4.13. The seasonal variation predicted for r_a and r_s , is given in Figure 4.14. The calculated r_a shows a seasonal variation due to slightly higher average hourly wind speeds in the dry season in comparison to the wet season. The predicted r_s rises markedly in the dry season due to the increase in mean hourly VPD , Rn and T .

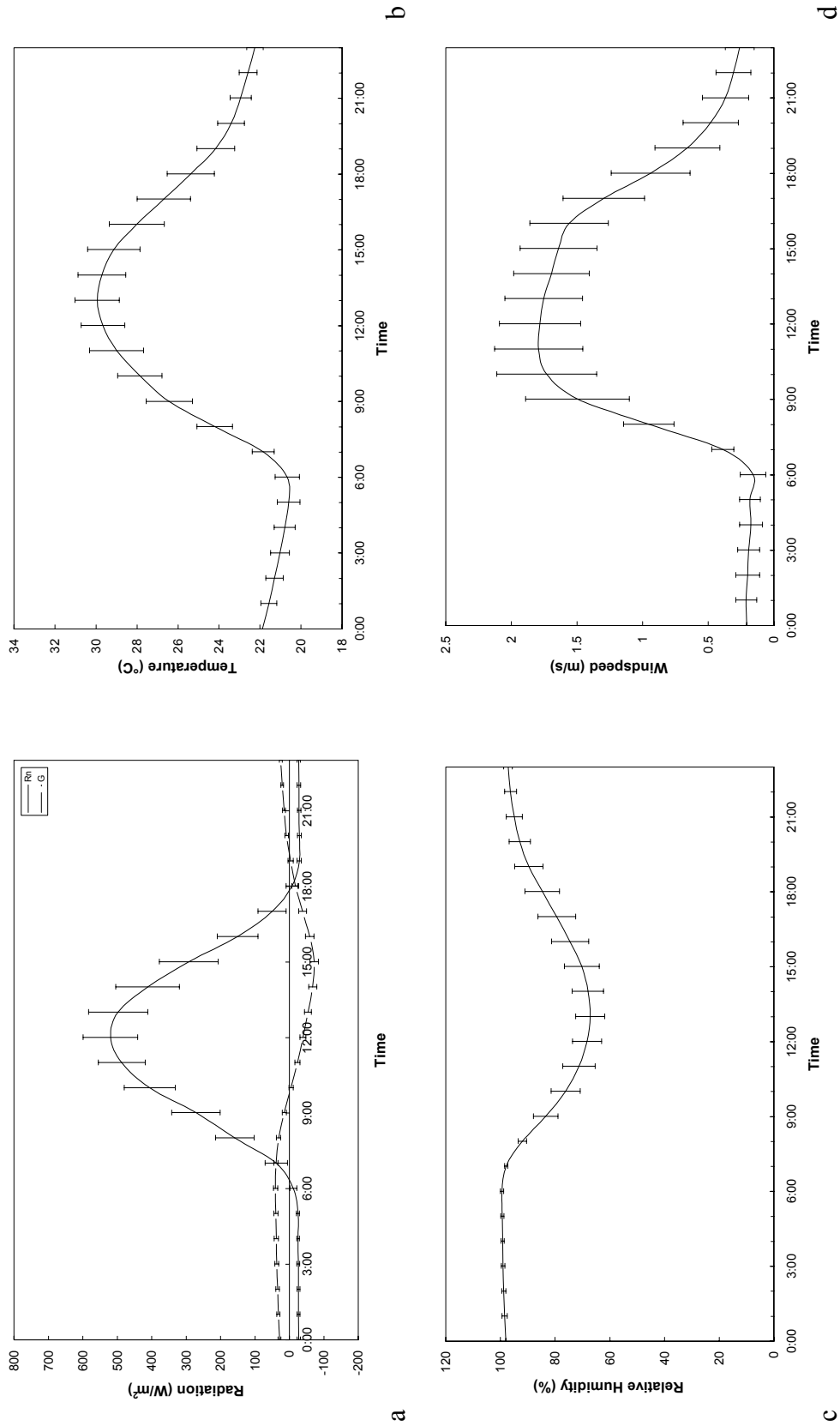


Figure 4.12 Hourly averages of a) Net radiation and soil heat flux, b) temperature, c) relative humidity and d) wind speed over the study period from January 2001-June 2002. The vertical bars indicate the standard deviation

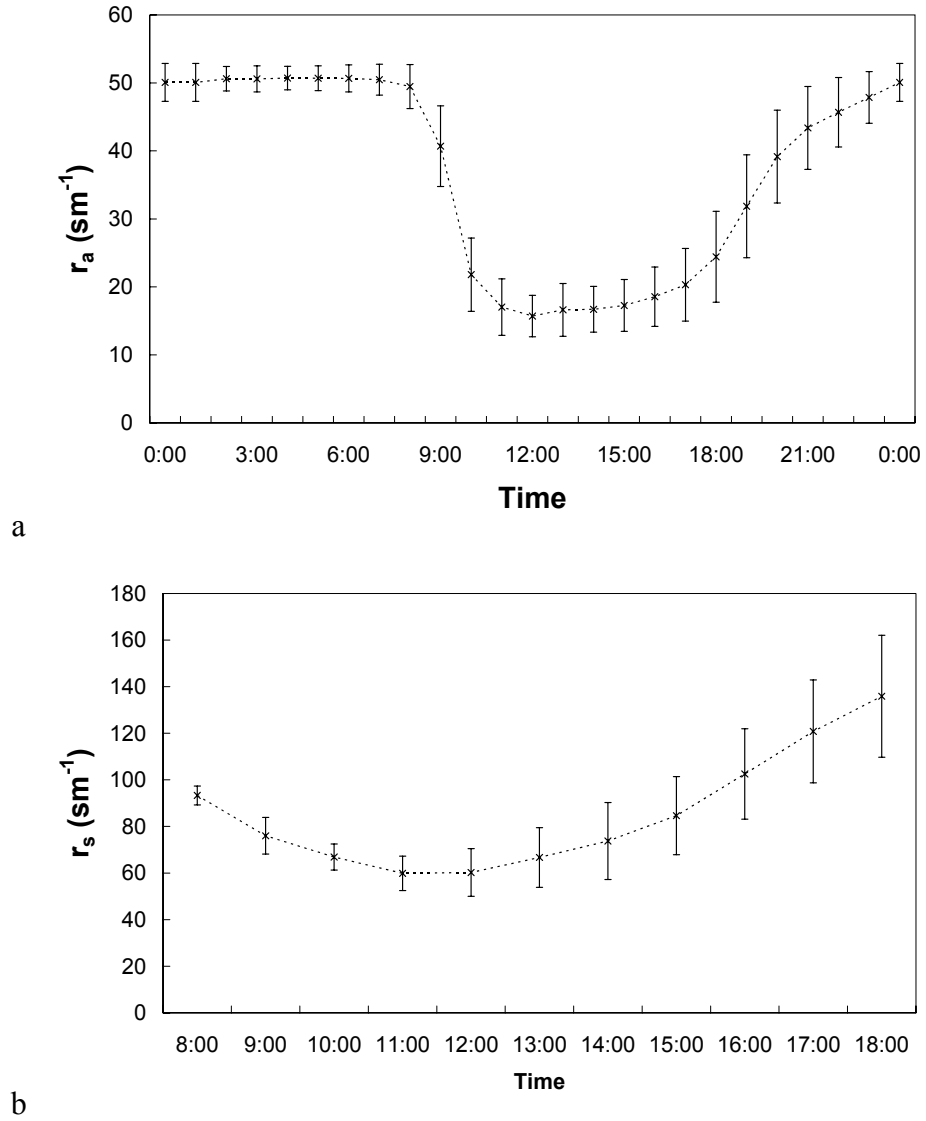


Figure 4.13 Average diurnal course of a) the aerodynamic resistance r_a and b) the calculated aerodynamic resistance r_s over the entire study period. The vertical bars indicate the standard deviation

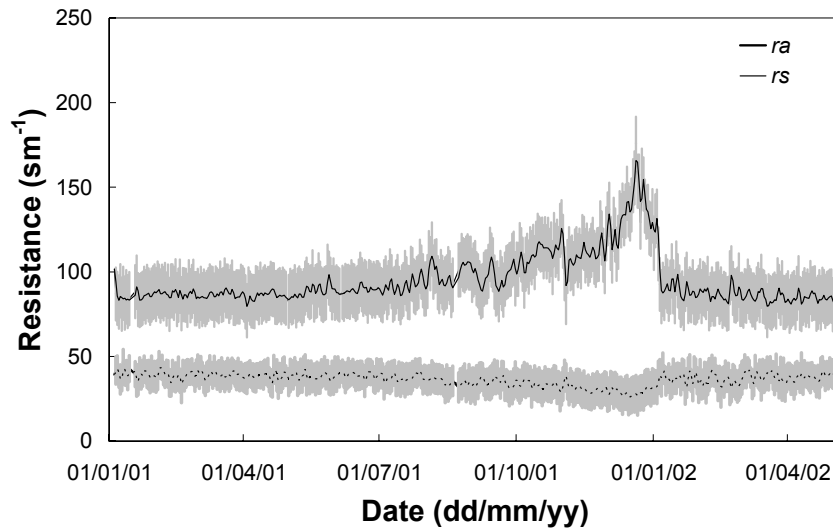


Figure 4.14 Seasonal variation in r_a and r_s over 1.5-2 year old fallow vegetation over the study period. The areas in grey indicate the standard deviation from the mean

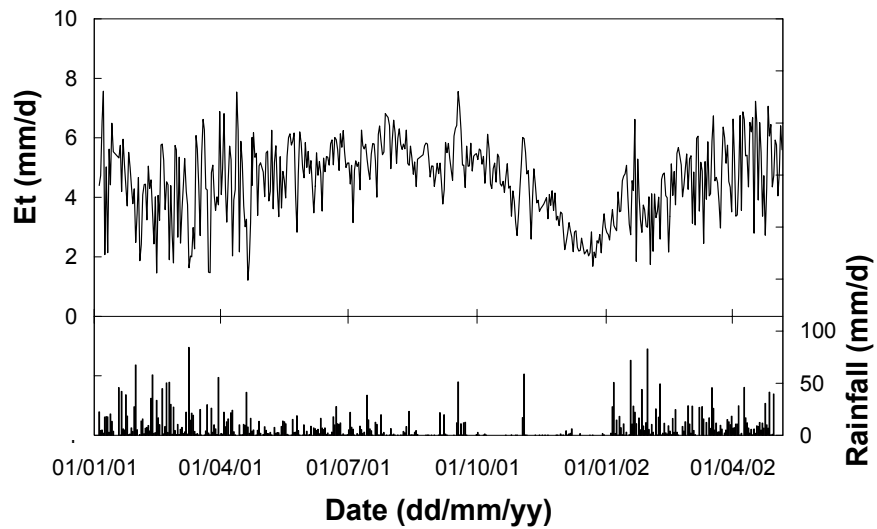


Figure 4.15 Daily value of E_t over the study period calculated with the Penman-Monteith method with a regression function estimate of r_s .

The daily Et over the study period based on hourly calculation with Eq. 4.11 and hourly calculation of r_s with the regression function of Sommer et al. (2002) is shown in Figure 4.15. The strong depression in Et throughout the dry season is predominantly caused by the increase in calculated r_s for that period. The total daytime transpiration (Et) for the year 2001 amounted to 1218 mm, and 538 mm, for the first half of 2002. Hourly rates of wet canopy evaporation (E_w ; $r_s = 0$) were computed with Eq. 3.14 and summed, resulting in a total of 116 mm for 2001 and 134 mm for the first half of 2002. The total Penman-Monteith based estimates of ET yielded 1334 mm yr⁻¹ (3.7 mm d⁻¹).

The estimated values for ET found in the current study for the 1 to 2.5 year old secondary vegetation plot are very close to the values reported in previous studies with the Bowen ratio method (1364 mm Hölscher, 1995; 1421 mm Sommer, 2000) for similar vegetation. Klinge et al. (2001) reported an estimated ET value of 1350 mm per year applying a soil water model in a stand of primary forest near Belém. Values of yearly ET reported for primary forest sites throughout the Amazon range between 1120 mm yr⁻¹ (Lesack, 1993b) and 1675 mm yr⁻¹ (Leopoldo, 1983).

4.4.4 Water balance summary evapotranspiration

Table 4.8 gives a summary of the dry canopy transpiration (Et), wet canopy evaporation (E_w), interception (Ei) and the total evapotranspiration based on the modified Penman-Monteith method ($ET1$) and a combined method including interception. The calculated Et for the first halves of 2001 and 2002 was almost the same, whereas the calculated E_w for the first six months of 2002 was substantially higher, just as was observed in the rainfall interception summary (section 4.3.6). From the summary it also becomes clear that the calculation of evaporation during wet hours (E_w) with the Penman-Monteith equation yields much lower results than the interception values calculated Ei . This is mainly caused by the exclusion of canopy storage effects which are not accounted for in the Penman-Monteith calculation.

In a comparison with other studies throughout the tropics, Schellekens (2000) demonstrated that the contribution of rainfall interception to total evapotranspiration tends to increase with increasing rainfall amounts, and typically makes up 20-25 % of the total evaporation (Table 4.9). The results of the current study in a continental edge setting are slightly lower (17%), and match with the ratio for the site of Hölscher

(1995). Above a suggested threshold value of 2500-2700 mm yr⁻¹, the rainfall interception seems to become more important (Schellekens, 2000).

Table 4.8 Summary of the monthly totals (in mm) of dry (*Et*), wet (*Ew*) and total evapotranspiration (*ET*), interception (*Ei*) and a total ET estimate based on combination of *Et* and *Ew* calculated with Penman-Monteith (*ETpm*) and *Et* and *Ei* (*ETcomb*) for one year old fallow vegetation

2001	P	Et	Ew	Ei	ETpm	ETcomb
January	423	75	25	39	100	114
February	439	66	28	41	94	107
March	360	80	14	34	94	114
April	239	91	14	23	105	114
May	135	110	8	13	118	123
June	187	113	10	18	123	131
July	179	125	7	17	132	142
August	49	124	2	5	126	129
September	142	122	2	13	124	135
October	5	123	0	1	123	124
November	78	106	2	7	108	113
December	17	85	5	2	90	87
Total 2001	2253	1220	117	212	1337	1432
2002						
January	450	76	20	43	96	119
February	238	76	18	22	94	98
March	296	87	25	28	111	115
April	335	105	17	32	122	136
May	353	99	28	33	127	132
June	182	96	25	17	121	112
Jan-Jun '02	1784	538	134	174	671	712
Jan-Jun '01	1854	535	98	168	632	634

Table 4.9 Evaporation components (in mm) for selected tropical and a temperate forest types: 1: Coastal and island sites, tropics; 2: Continental edge, equatorial; 3: Continental, equatorial; 4: Temperate coastal. Modified from Schellekens (2000)

	Type	<i>P</i>	<i>ET</i>	<i>Ei</i>	<i>Et</i>	<i>Ei/Et</i>
Queensland, Australia (Gilmour, 1975)	1	4035	1430	1010	420	2.40
Puerto Rico (Schellekens, 2000)	1	3480	2180	1365	815	1.67
Fiji (Waterloo, 1994)	1	2015	1740	365	1375	0.30
French Guyana (Roche, 1982)	2	3725	1440	560	880	0.64
Eastern Amazonia (this study, 2001)	2	2253	1429	212	1218	0.17
Eastern Amazonia (Hölscher, 1995)	2	1819	1365	220	1145	0.19
Central Amazonia (Leopoldo et al., 1995)	3	2209	1493	249	1243	0.20
Central Amazonia (Shuttleworth, 1998)	3	2390	1225	245	980	0.25
Westen Amazonia (Elsenbeer et al., 1994)	3	3065	1535	470	1065	0.44
Plynlimon, UK (Calder, 1990)	4	2035	865	530	335	1.58

4.5 Runoff

4.5.1 Introduction

The generation of runoff or stream flow is the result of a series of interactions between the land surface and the water entering the system. The volume of water appearing as stormflow in the hydrograph of a stream is often only a very small fraction of the total runoff. The remainder of the rainwater input leaves the watershed as evapotranspiration, baseflow or deep groundwater outflow (Dingman, 1994; Ward and Robinson, 2000).

Horton (1933) proposed that the soil surface partitions rain into ‘excess’ overland flow and groundwater flow based on its infiltration capacity. No overland flow will occur if the rainfall intensity is lower than the infiltration capacity. The infiltration that takes place will first fill the soil water reservoir until its moisture capacity is reached after which further infiltration through the ground surface will percolate to the groundwater (Dunne, 1978; Ward and Robinson, 2000). This seems to be a rather simple representation of reality, since Hortonian overland flow (HOF) rarely occurs. Hewlett (Hewlett and Hibbert, 1967; Hewlett and Nutter, 1970) suggested that actually only a small part of a catchment area contributes directly to storm flow, and that typically only the lower, near saturated valley slopes adjacent to the stream channel actively generate ‘saturation’ overland flow. They also suggested that with increasing rain depth these areas tend to expand, the so-called variable source area concept. Kirkby (1978) suggested that in the presence of vegetation and litter cover little overland flow may be expected to occur over much of the drainage basin, except in the most extreme storms. Kirkby and Chorley (1967) (Quoted from Chorley, 1978) noted that contributing areas of overland flow occur generally at the slope base, at concavities where surface flow lines converge and in areas of thin soil cover. Beven et al. (1988) indicated the importance of the role of catchment geomorphology on the hydrological response.

Based on a review of numerous field experiments, Bruijnzeel (1990) stated that forested and agricultural areas throughout the tropics demonstrate a wide spectrum of responses under similar rainfall conditions. At one end of the spectrum are substrates sufficiently permeable to prevent any type of overland flow from occurring more than occasionally on the hillside (Bruijnzeel, 1983; Coelho-Netto, 1987; Lesack, 1993b; Nortcliff and Thornes, 1981; Nortcliff and Thornes, 1984; Walsh, 1980). At the other

extreme are soils with a sudden decrease in permeability at shallow depths where widespread saturation overland flow occurs, often in conjunction with pipe flow (Bonell et al., 1981; Elsenbeer, 2001; Elsenbeer and Lack, 1996; Elsenbeer et al., 1999; Schellekens, 2000).

For the understanding of runoff processes at a watershed level it is essential to know at what side of the spectrum the watershed is situated. In this section the watershed hydrological characteristics and the implications for the rainfall-runoff dynamics are discussed.

4.5.2 Hydrograph separation

In order to identify what fraction of the hydrograph is stormflow or baseflow various methods have been developed (Chapman, 1999; Ward and Robinson, 2000). Traditionally these methods separate ‘old’ water (baseflow) from ‘new’ water (stormflow) by drawing a horizontal line, a line of constant slope to the inflection point, or a composite line (Chapman, 1999; Ward and Robinson, 2000).

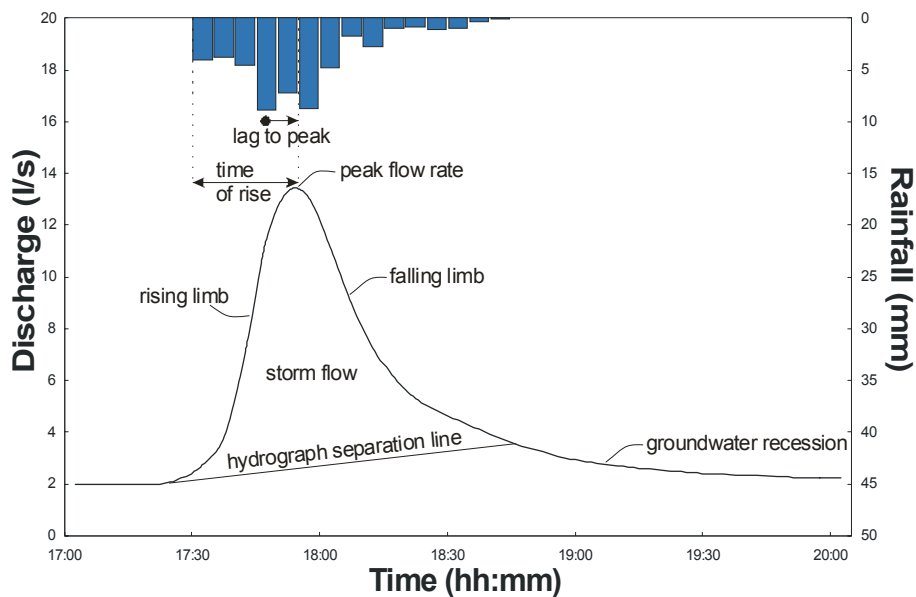


Figure 4.16 The components of a storm hydrograph (adapted from Hewlett (1982))

The start point of the runoff event is given by the time when flow starts to increase (Figure 4.16). The endpoint is commonly taken as the time when a plot of $\log Q$ against time becomes a straight line. For the current study, the straight-line method (Hewlett

and Hibbert, 1967) was thought to give a reliable estimate for the separation of stormflow and baseflow volumes.

Using the method of Hewlett and Hibbert (1967) stream discharge can be separated into two components:

$$(4.15) \quad Q = Q_B + Q_P$$

$Q = \text{Total discharge (l s}^{-1}\text{)}$
 $Q_B = \text{Baseflow (l s}^{-1}\text{)}$
 $Q_P = \text{Stormflow (l s}^{-1}\text{)}$

During dry periods Q is equal to Q_B , but during storm events baseflow is assumed to increase at the rate

$$(4.16) \quad dQ_B / dt = r$$

$Q_i = \text{flow at the start of the storm}$

The slope r is considered to be a hydrologic characteristic of the particular study site. Hewlett and Hibbert (1967) suggested a slope of $0.0472 \text{ mm hr}^{-1} \text{ d}^{-1}$ for small forested watersheds in humid regions with a high storage capacity. For the watersheds of the current study this slope was considered to be much too steep and thus a $0.0015 \text{ l s}^{-1} \text{ min}^{-1}$ ($0.0044 \text{ mm hr}^{-1} \text{ d}^{-1}$) was used. This value was obtained iteratively and follows the value used by Lesack (1993b) for a similar watershed in central Amazonia. The resulting baseflow component as a function of time during the course of a storm can then be calculated as

$$(4.17) \quad Q_B(t) = Q_i + rt$$

$r = \text{slope of the separation line}$

The end of the storm is defined as when $Q_B(t)$ is again equal to $Q(t)$. The total volume of water contributed by baseflow in a given storm is

$$(4.18) \quad V_B = \int_{t_i}^{t_f} Q_B(t) dt$$

$V_B = \text{baseflow volume}$

and the volume contributed by stormflow

$$(4.19) \quad V_P = \int_{t_i}^{t_f} Q(t) dt - V_B$$

$V_P = \text{stormflow volume}$

4.5.3 Runoff observations

The hourly rainfall-runoff record over the period between the 1st of January 2001 and the 17th of June 2002 at W1 is shown in Figure 4.17. The slow annual rise and fall of the baseflow and the rapid response of stormflow draw immediate attention. The total annual rainfall of 2251 mm resulted in 905 mm of baseflow in 2001. The total volume of stormflow was only 14.8 mm, which is only 1.6% of the total annual amount of stream flow. Over the entire study period from January 2001 to June 2002, a total stream flow of 1233 mm and a total stormflow of 21.5 mm (1.7%) were recorded.

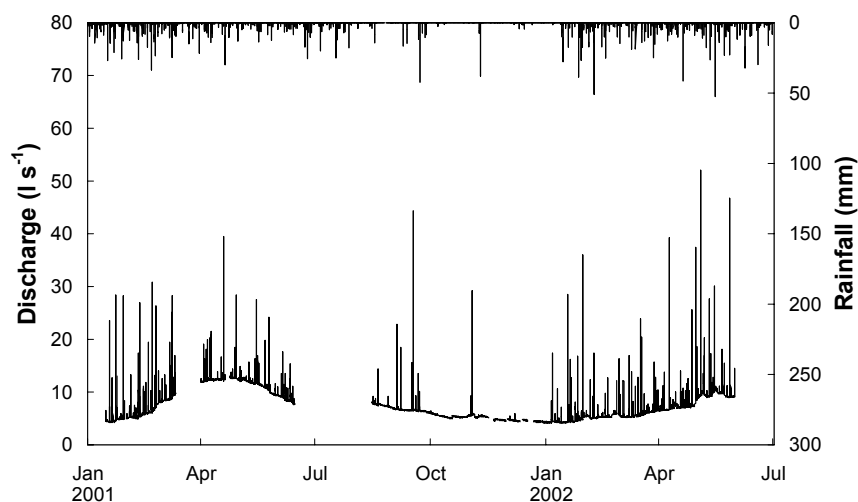


Figure 4.17 Rainfall and runoff record at W1 for the study period January 2001 through June 2002

4.5.4 Stormflow

Figure 4.18 shows the stream discharge at weir 1 (W1) and weir 3 (W3) resulting from a 84 mm rainfall event on the 9th of March 2001 and 51 mm on the 17th of September 2001. This figure illustrates the typical response of the streams in the area to rain. Directly following the onset of rain the stream exhibits a response and reaches peakflow within 5 to 10 minutes after the highest rainfall intensity ('lag-to-peak' Figure 4.16). The recession to the antecedent baseflow level is rapid (< 3 hours).

Over the 18 month study period 245 rainfall-runoff events were observed. For each event, baseflow was separated from stormflow with the linear separation technique described in section 4.5.2. The linear regression shown in Figure 4.20 reveals a remarkably strong correlation between event rain and runoff volume. The first seven

storms of the 2002 wet season are sequentially indicated in the plot (Figure 4.27a). The deviation of the first storms of the year from the regression line is thought to be caused by the filling of the upstream valley bottom reservoir. After this storage (approximately 22 mm) is filled it remains so until it is gradually depleted during the dry season. The stronger scattering of the points in Figure 4.20b is thought to be mainly caused by errors in the extrapolation of the rainfall total, since the rainfall record of WS1 was used, but the weir W3 was approximately one km away.

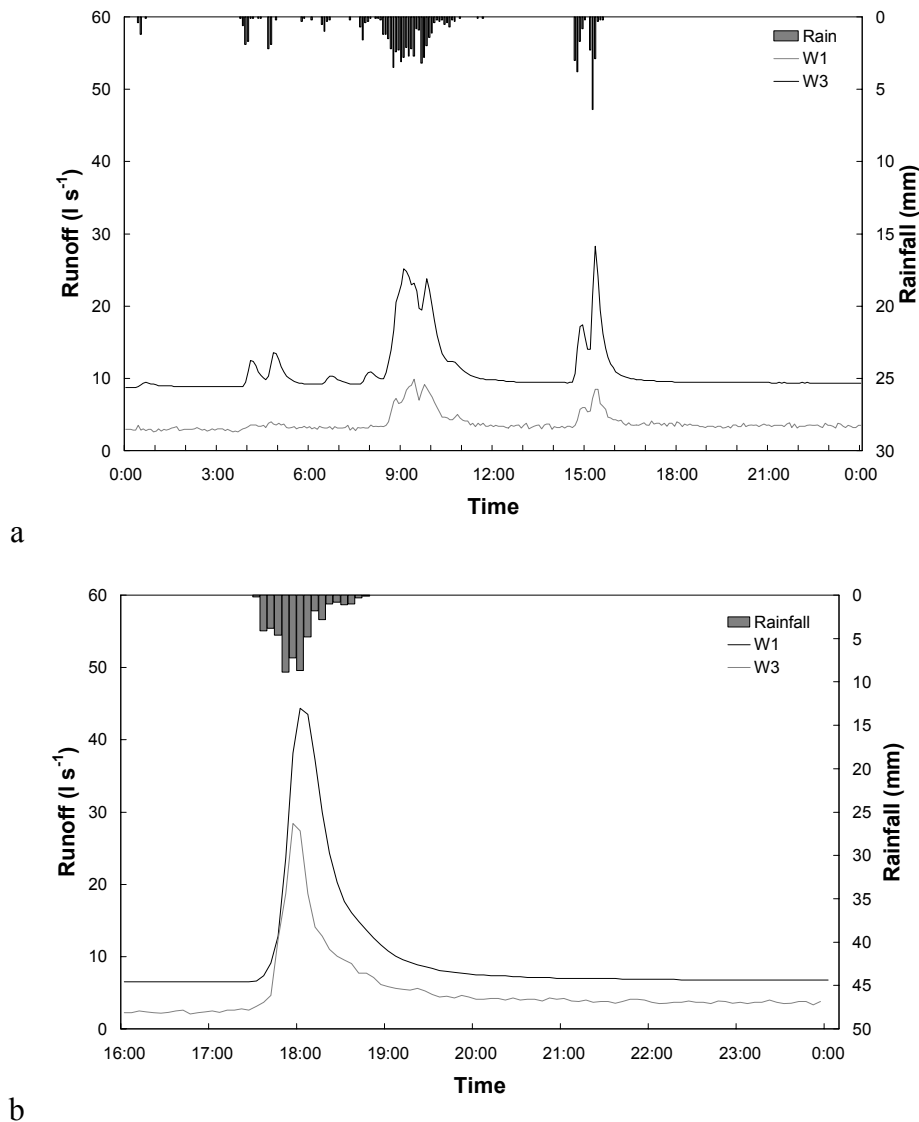


Figure 4.18 Runoff resulting at W1 and W3 from a) 84 mm of rainfall on the 9th of March 2001 and b) 51 mm on the 17th of September 2001

The slope of the linear regression provides an estimate of the maximum area contributing to the generation of event flow (Dickinson and Whiteley, 1970). In the case of W1 this is approximately 1650 m² (Figure 4.20a), and for W3 about 620 m². It should be noted that rainfall interception (approximately 10% for riparian forest; see section 4.4) is not subtracted here (see section 4.5.5 on interception estimates from stormflow), and hence the minimum contributing area tends to be underestimated. The surface area of the upstream section of the valley wetland as calculated from the DEM by delineating the valley bottom, is approximately 1650 m² for W1 (Figure 4.19) and 690 m² for W3. It is thus safe to conclude from these analyses that the stormflow is completely generated by this area, and that the stormflow is generated in the form of saturation overland flow (SOF) from the riparian wetland area. The areas contributing to W1 and W3 are approximately 25.5 ha, and 11 ha respectively in size, which means that only 0.6 % of both watersheds contributes to the generation of stormflow, and the rest of the water infiltrates.

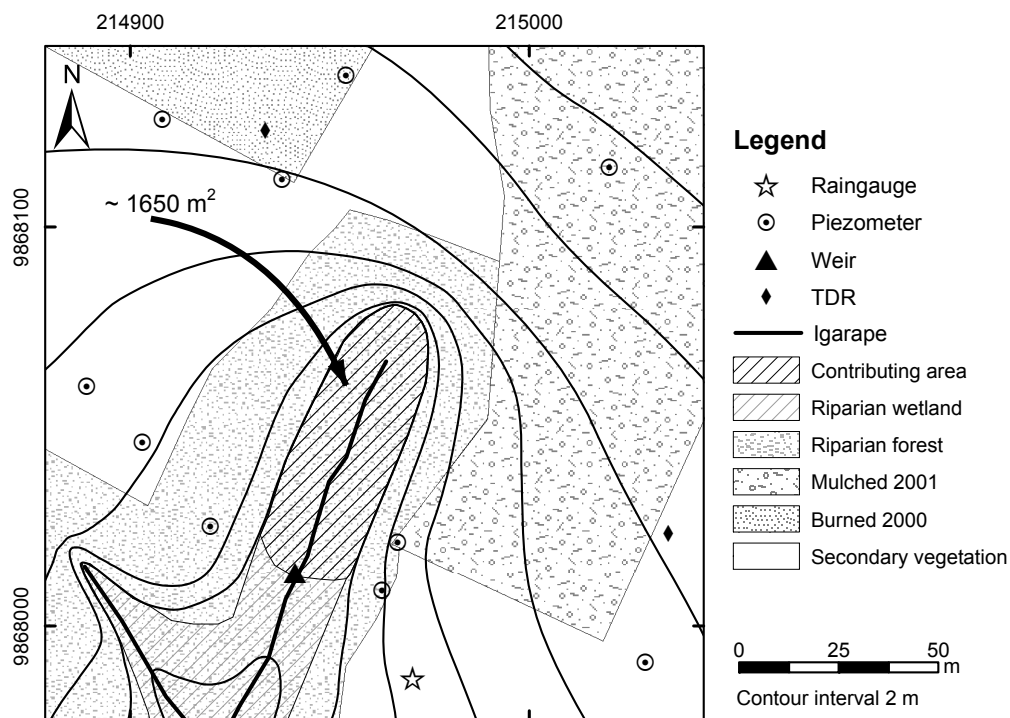


Figure 4.19 Approximate outline of the contributing area of W1 based on terrain topography, and the location of instrumentation surrounding its source

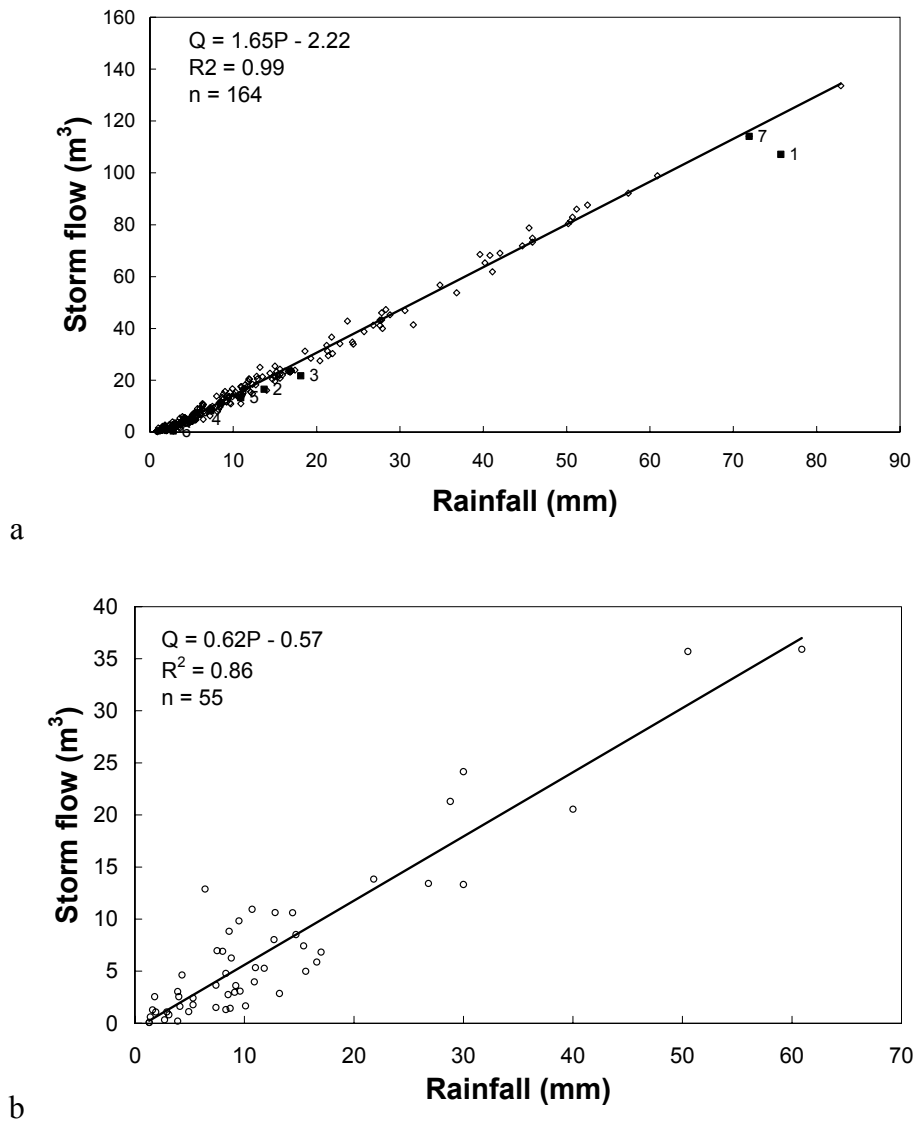


Figure 4.20 Rainfall total versus storm runoff for a) 245 storm events at W1 (The numbered dots indicated the first seven storms of the rainy season 2002) and b) 55 storm events at W3

4.5.5 Infiltration

The high infiltration rates (\approx Saturated hydraulic conductivity K_{sat}) suggested by the rainfall-runoff relationship described in the previous sections are illustrated with 14 double ring infiltrometer measurements distributed over WS1. Figure 4.21 gives an overview of the measured K_{sat} values at each point and the maximum measured rainfall rate over the study period (Jan. 2001-Jun. 2002). As can be seen in Figure 4.21a, the maximum rainfall rate observed over the study period of $11 \text{ mm } 5\text{min}^{-1}$ exceeds the infiltration rate at only four out of fourteen points in the watershed. Events with rainfall intensities greater than $10 \text{ mm } 5\text{min}^{-1}$ were only observed twice in 2001 and once in the first half of 2002. On an hourly basis the maximum observed rainfall intensity did not exceed the infiltration rates at any of the points (Figure 4.21b).

The average infiltration rate obtained from the 14 measurements amounted to 161 mm hr^{-1} (386 cm d^{-1}), and compared very well with reported high values of K_{sat} of Latosols in the Barreiras formation in central Amazonia by Medina and Leite (1985; 545 cm d^{-1} under secondary forest), and Nortcliff and Thornes (1989; $156\text{--}322 \text{ cm d}^{-1}$). Soil physical properties for Oxisols under pasture in Central Amazonia have been determined by Tomasella and Hodnett (1996) using a ring permeameter (area 314 cm^2) down to depths of 1.35 m yielding an estimated K_{sat} of the top 1 m of the profile of $17\text{--}66 \text{ mm h}^{-1}$ (max 158 cm d^{-1}). They attributed this high conductivity to the presence of macropores. Below this depth, the saturated hydraulic conductivity becomes more dominated by the particle size distribution as macro- and mesopore effects become negligible (Tomasella and Hodnett, 1996).

Sommer et al. (2003) estimated K_{sat} for the top 5 cm of an almost identical soil at a nearby site with the Rosetta Program (U.S. Salinity Lab., Riverside, CA) and optimized their estimates by an inverse model solution with HYDRUS-1D (U.S. Salinity Lab., Riverside, CA). This model simulation supports the suggestion of a relatively homogenous soil profile up to 10 meters of depth with high hydraulic conductivities. The model resulted in an estimate for K_{sat} of 254 cm d^{-1} for the top 5 cm of the profile, and 160 cm d^{-1} until a depth of 10 m .

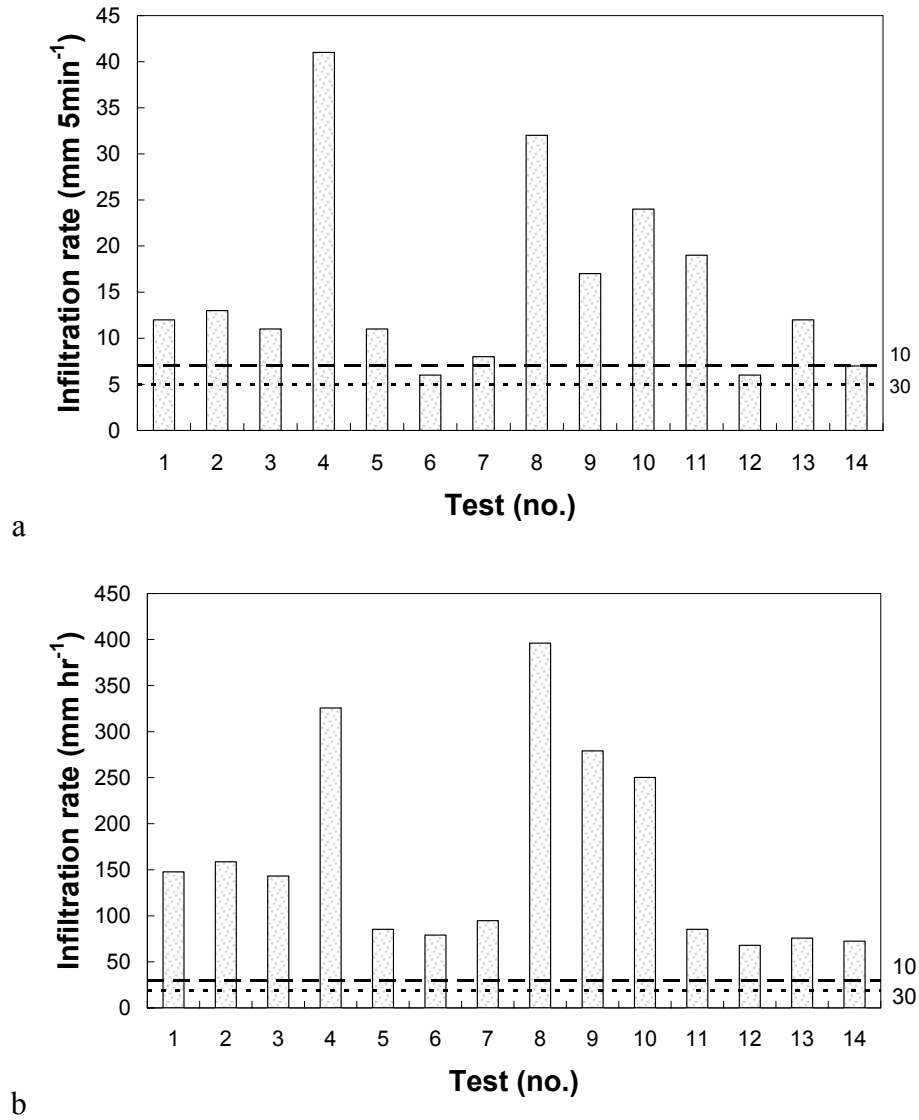


Figure 4.21 Infiltration rates as determined with a double ring infiltrometer at 14 points in WS1 in a) mm per 5 minutes and in b) mm per hour. The dashed reference lines labeled '10' and '30' indicate the rainfall intensities that have a recurrence interval of 10 and 30 times per year respectively

Three experiments were performed where water colored with blue dye was infiltrated through a ring of 25 cm in diameter. These experiments also confirmed the high infiltration rates and revealed that preferential flow occurs along the existing root system of the fallow vegetation (Figure 4.22). 20 liters of water (equaling approximately 100 mm of precipitation) infiltrated through the ring in all three tests within approximately 15 minutes. The infiltration front was exhumed immediately after the application of the water was finished and found to a depth between 1 and 1.5 meters. Previous studies by Hölscher (1995) and Sommer et al. (2003) suggested deep soil-water uptake under secondary and primary vegetation in Eastern Amazonia. The deep root networks described in these studies and others throughout the central and eastern Amazon region could provide a possible ‘secondary conductivity’, enhancing the permeability of the phreatic top soil. However, further research into this topic is needed.

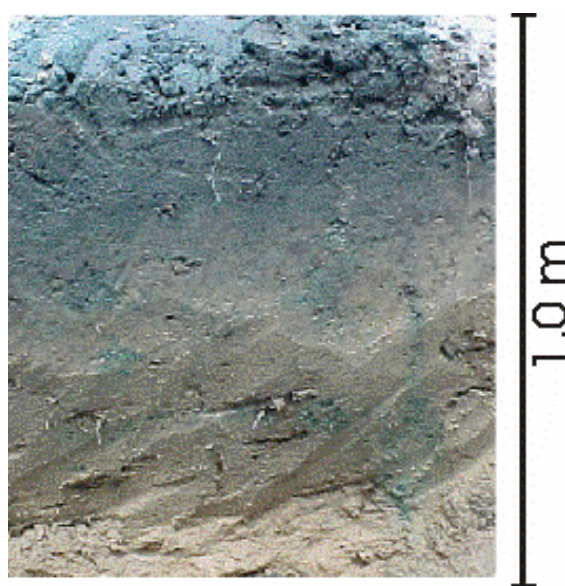


Figure 4.22 View of the top 1 m of the soil profile (Latosolo amarelo) after the infiltration of 20 liters of water colored with blue dye in approximately 15 minutes. Note the higher concentration of dye along the roots.

4.5.6 Rainfall interception estimation from stormflow measurements

As discussed in the previous section a strong correlation exists between rainfall and stormflow volume. It was deduced that the area generating stormflow in WS1 is delineated by the wetland valley bottom, which is entirely vegetated with riparian forest.

This means that when a storm event occurs, the wetland area can be viewed as a large version of a throughfall (Tf) gauge. Following this analogy, the resulting rainfall runoff plot could provide information on the storage capacity of the vegetation and an estimate of interception.

Figure 4.23a shows a plot of rainfall versus stormflow recalculated in mm by dividing by the area estimate from the DEM (1650 m^2). The Tf values for the gauges of the riparian plot which surrounded the weir were slightly lower than the stormflow because the latter also incorporated stem flow.

The 245 events used in the stormflow analysis yielded 2889.0 mm of rainfall and 2464.2 mm of stormflow (using a contributing area of 1650 m^2). This would mean that 9% of the rainwater was intercepted, a value which is in remarkable agreement with the estimate of 10% (9% Ei , 1% Sf) obtained with the Tf gauges. By adjusting the method of Jackson (1975) by including the fraction of stem flow pt in the upper envelope of the points (line of unit slope =1), the total storage value for the canopy and trunks together was estimated to be 0.9 mm (Figure 4.23b).

Using the Tf gutter measurements (section 4.4.3) this value was estimated to be 0.43, which was rather low presumably due to the influence of drip points. Furthermore, an estimate for the free throughfall coefficient (p) of 0.15 was obtained by performing a linear regression through the lower range of the stormflow points (Figure 4.23b), compared to a value of 0.18 obtained with the gutter measurements. The relative evaporation rate \bar{E}_w / \bar{R} was determined using the method of Gash (1979), by performing a linear regression of the estimated interception values against gross rainfall (P). This yielded a value of 0.08, resulting in an estimated average wet evaporation rate of \bar{E}_w 0.52.

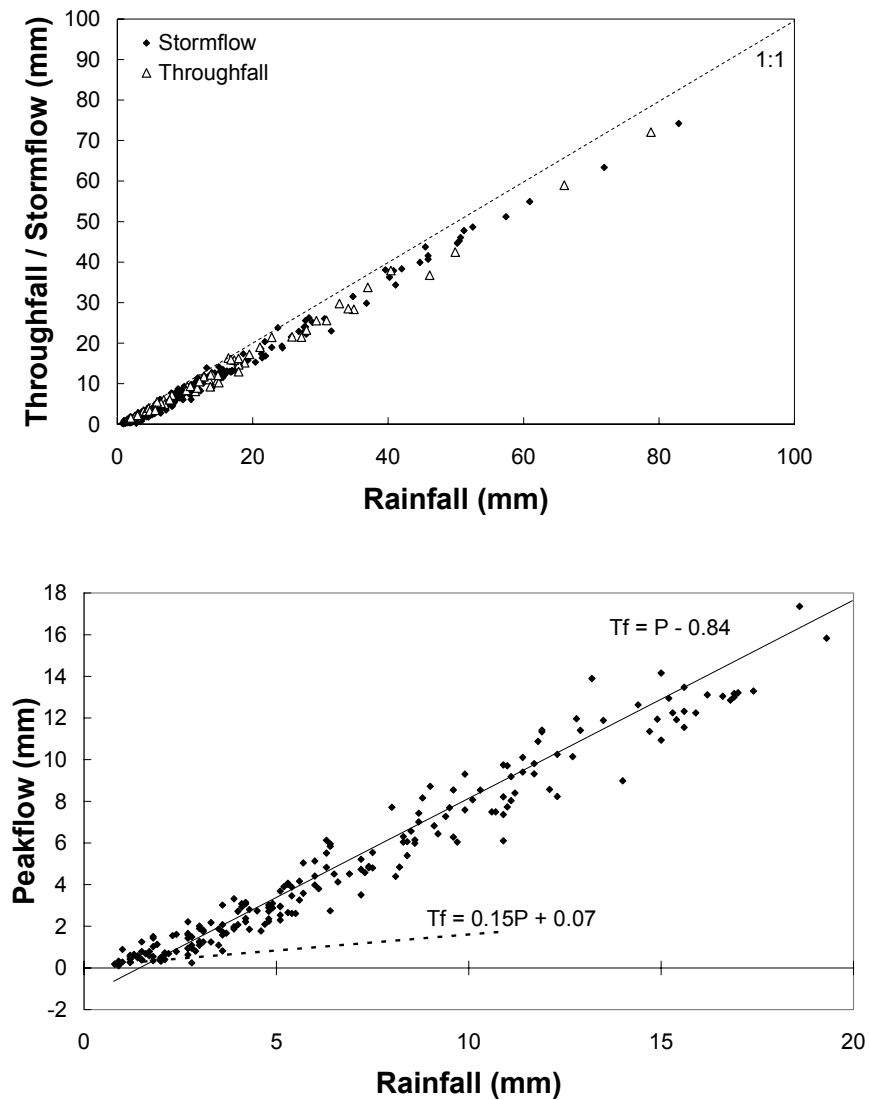


Figure 4.23 a) Rainfall versus stormflow generated by the riparian wetland area measured at weir W1 and throughfall measured with the throughfall gauges
b) Estimation of the canopy parameters S and p using an adjusted version of the method of Jackson (1975)

4.5.7 Water balance summary runoff

The analysis of 245 rainfall-runoff events over the study period at WS1 revealed a strong correlation between rainfall and stormflow volume. A similar result was obtained for the much smaller source area of WS3, although the correlation was less strong. It can be concluded that the stormflow in the streams in this region is generated entirely by the wetland area of the narrow valleys. Similar results were found for catchments with comparable topographical and soil characteristics in various studies in Central Amazonia (Coelho-Netto, 1987; Lesack, 1993b; Nortcliff and Thornes, 1984) and by for a watershed in Guyana (Jetten, 1994). Both Lesack (1993b) and Jetten (1994) concluded that the only part of their watershed generating stormflow was the saturated wetland surrounding the creek, and despite the observed high rainfall intensities the rainfall infiltrates. In none of these studies the relation between rainfall and stormflow was so strong however, that even the filling of the wetland storage with the onset of the rainy season could be observed. Furthermore, no study so far has used runoff data to estimate interception. It seems that the observed relation originates in the topography (generally gently undulating terrain with sharp incised canyons) and drainage pattern which in turn are the result of the hydraulic characteristics of the soils.

The total runoff over the year 2001 at WS1 was estimated at approximately 920 mm, of which almost all consisted of baseflow (905 mm). At WS3 the total estimated runoff over the year 2001 yielded 857 mm (843 baseflow and 14 mm peakflow). Over the first half of 2002, 338 mm of stream flow, 327 mm of baseflow and 11 mm of stormflow were measured. The first half of 2002 generated relatively higher stormflow in comparison to the same period in 2001, which was simply due to the fact that more rainfall was measured over this period. The baseflow amount over the first half of 2001 was relatively higher however, which can be explained by the later start of the rainy season in 2002.

Water balance

Table 4.10 Summary of the monthly totals of water fluxes (in mm) at WS1 in the form of baseflow (Q_b), stormflow (Q_p) and total runoff (Q_t) for 2001 and the first half of 2002

	2001				2002			
	P	Q_b	Q_p	Q_t	P	Q_b	Q_p	Q_t
January	423	46	3	49	450	46	3	49
February	439	57	3	60	238	51	2	52
March	360	106	2	108	296	60	2	62
April	239	131	2	132	335	71	2	73
May	135	119	1	120	353	100	2	102
June	187	83	1	84	182	92	1	93
July	179	75	1	77				
August	49	70	0	71				
September	142	66	1	67				
October	5	55	0	55				
November	78	51	1	51				
December	17	47	0	47				
<i>Jan.-Jun.</i>	<i>1784</i>	<i>540</i>	<i>12</i>	<i>552</i>	<i>1854</i>	<i>419</i>	<i>12</i>	<i>431</i>
Total	2253	906	15	920				

Table 4.11 Summary of the monthly totals of water fluxes (in mm) at WS3 in the form of baseflow (Q_b), stormflow (Q_p) and total runoff (Q_t) for 2001

	2001			
	P	Q_b	Q_p	Q_t
January	423	40	1	41
February	439	53	1	54
March	360	99	2	101
April	239	121	3	124
May	135	111	3	114
June	187	79	1	80
July	179	70	1	71
August	49	65	0	65
September	142	62	1	63
October	5	51	0	51
November	78	48	1	49
December	17	44	0	44
Total	2253	843	14	857

4.6 Groundwater

4.6.1 Introduction

In the previous section a strong correlation between streamflow and groundwater was demonstrated. By analyzing the observations made with the observation well network, the relation between groundwater and baseflow was determined. Although an extensive groundwater modeling effort was outside the scope of the current study, an attempt was made to use a Finite Element Model MicroFEM (Hemker and Van Elburg, 1987) to visualize the regional groundwater flow. The main purpose of the model was to provide an estimated distribution of the groundwater table under stationary conditions, and to evaluate if the modeled groundwater divides coincide with the topographical boundaries used for the catchment delineation.

4.6.2 Observations and analysis

Figure 4.24 shows the variation in groundwater levels of 38 observation wells throughout the three watersheds over the study period. Wells that were installed after the 1st of July 2001 were not included. The groundwater levels in these observation wells reveal a very similar pattern of variation over the course of a year. The groundwater levels in virtually all observation wells return to their initial levels after a quick rise during the wet season, indicating that over an entire year no water was lost or gained from groundwater storage. The well levels at each watershed are highly cross-correlated, with correlation coefficients typically higher than 0.7. This suggests, as was expected from the soil profiles, that the aquifer is unconfined and relatively homogenous. Figure 4.25 shows the maximum and minimum level of groundwater over the study period, at five selected observation wells along a NW-SE transect in WS1 (from the stream upslope). The observed variations of wells G010, G009 and G014 as well as the baseflow level are shown in Figure 4.26a. The stream (baseflow) level strongly correlates with the observed levels in these wells (Figure 4.26b). The strongest correlation ($r^2 = 0.88$) between groundwater level and baseflow volume was found for the observation wells closest to the stream, and decreased gradually with distance (Figure 4.26b). The increasing ‘looping’ of the points with distance is thought to result from a longer lag time between the observation well and the stream.

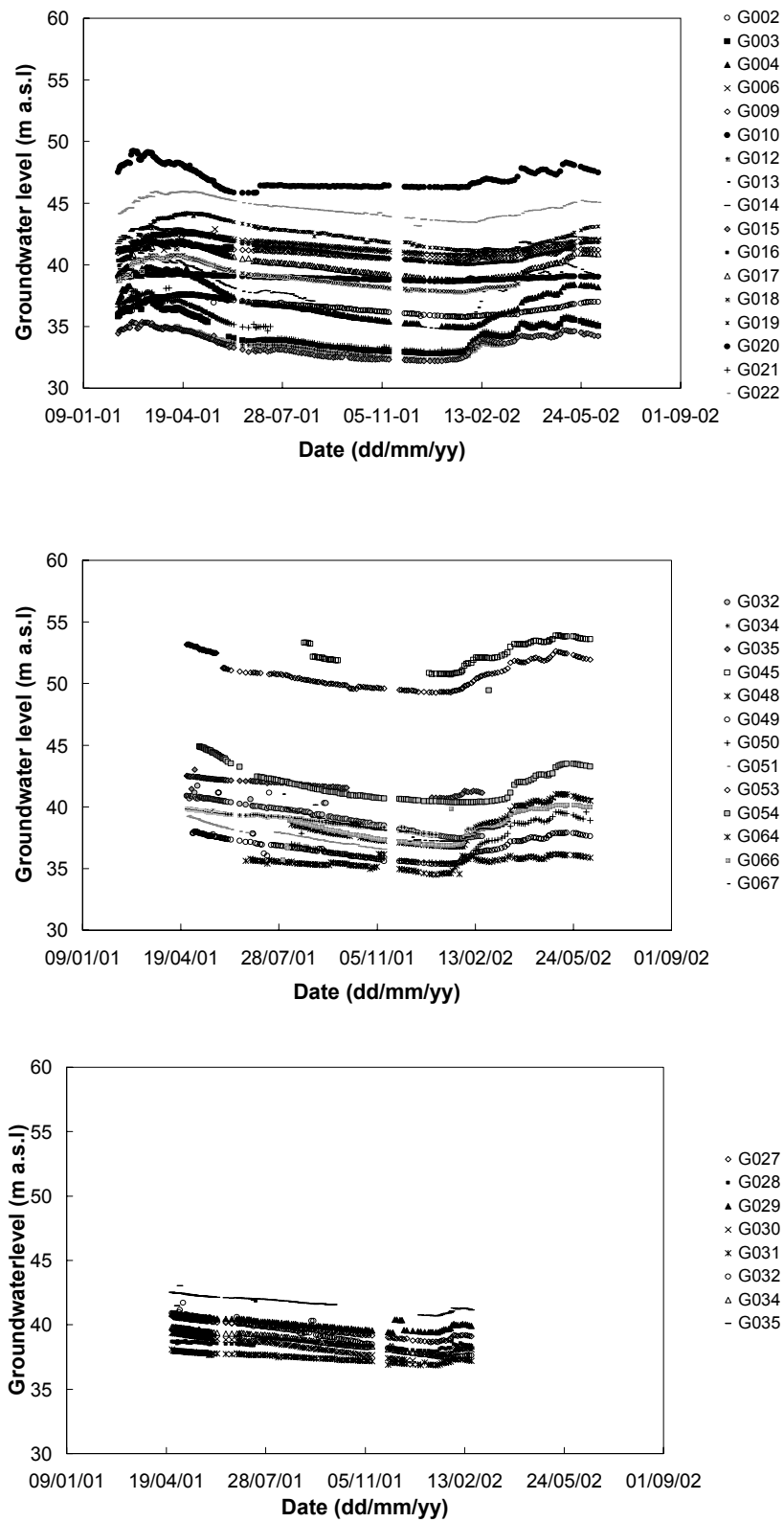


Figure 4.24 Groundwater level variations over the study period at a) WS1, b) WS2, and c) WS3

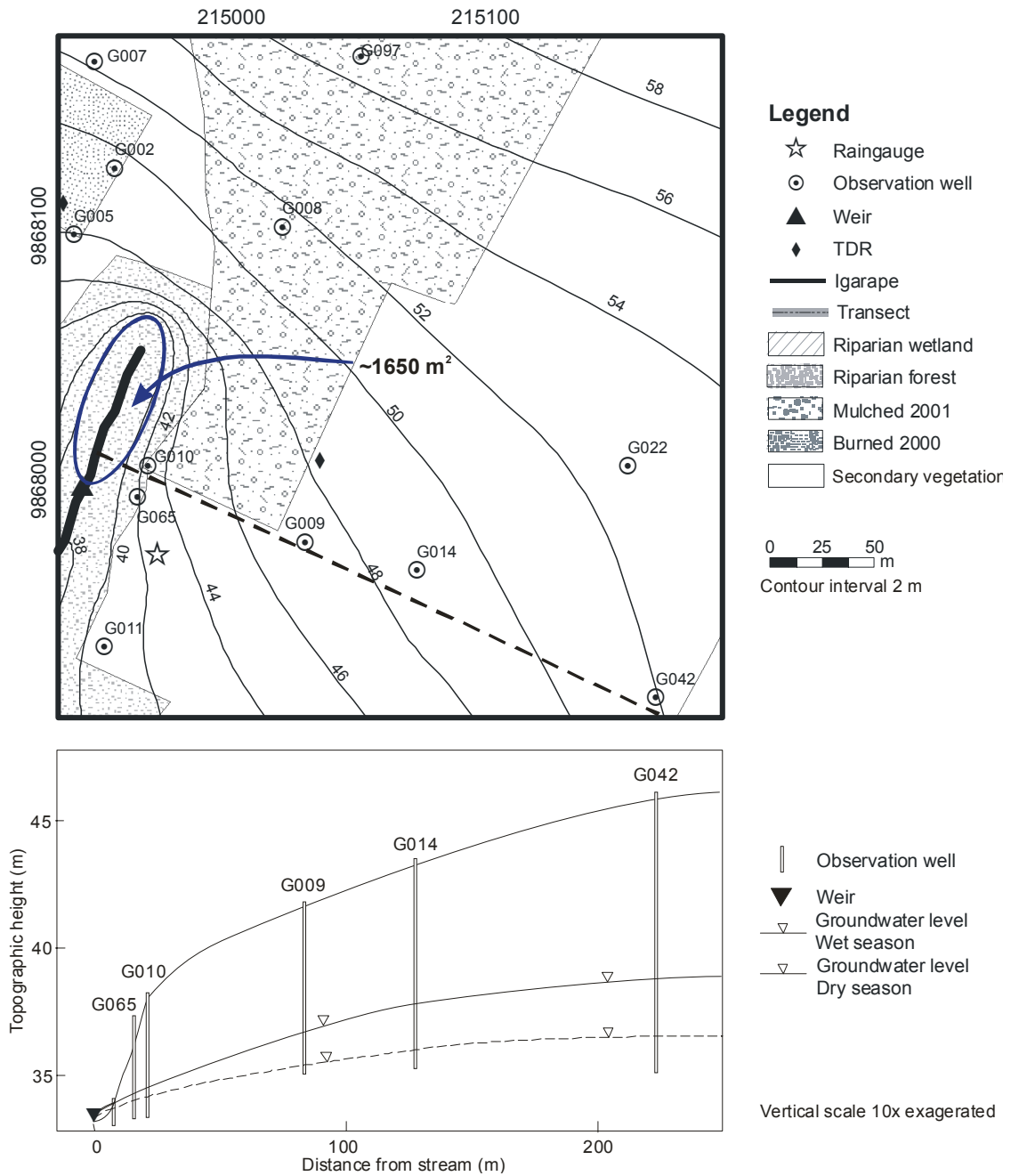


Figure 4.25 Detailed view of the topographical map and the topographical profile from the stream towards the watershed boundary,

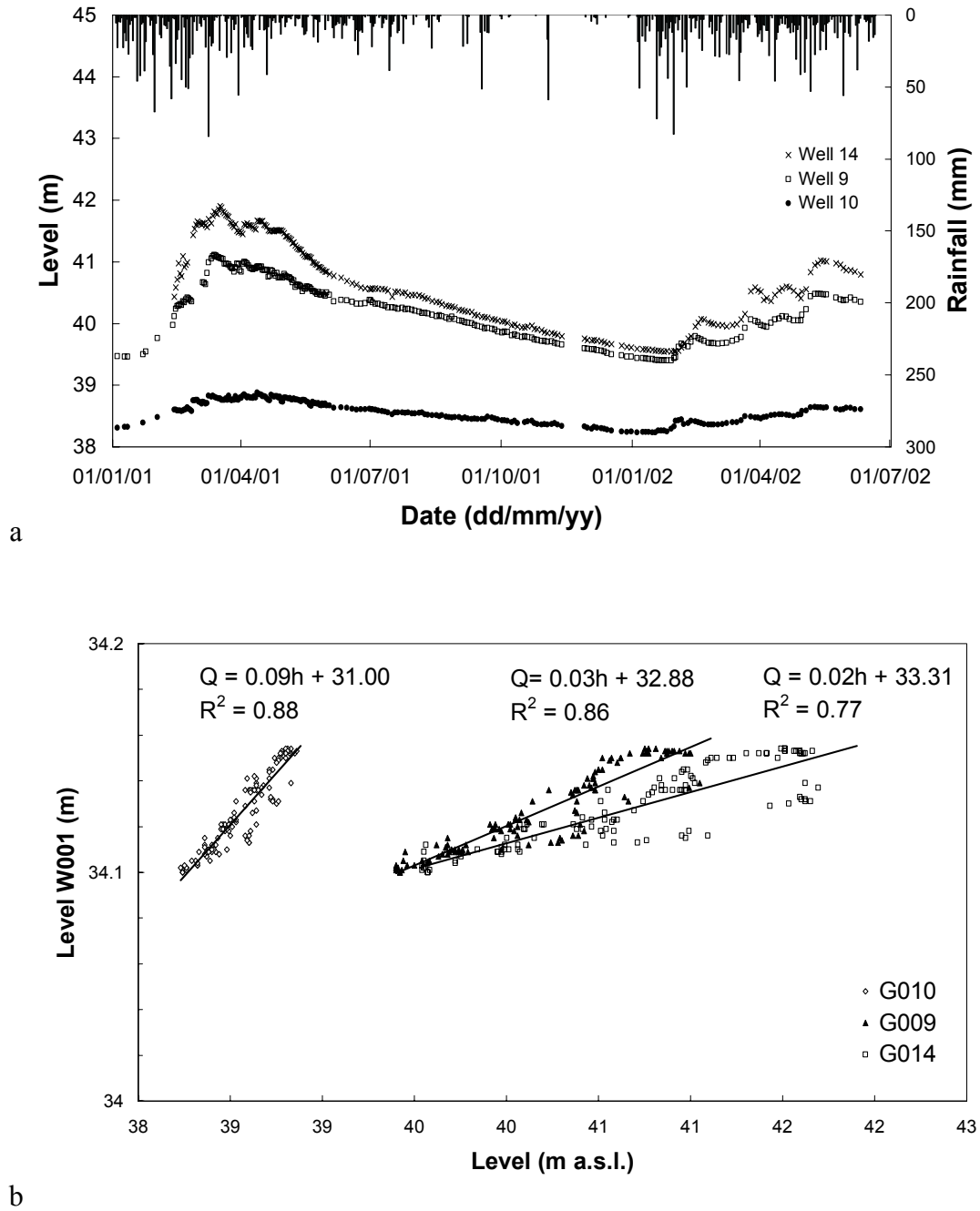


Figure 4.26 a) Groundwater level variations (points) for three selected observation wells and rainfall (bars) over the study period and b) their correlation with streamwater level at WS1

4.6.3 Storativity

The storage coefficient or storativity (S) is defined as the volume of water taken into or released from storage per unit horizontal area per unit rise or decline in head and is given by

$$(4.20) \quad S = \frac{dV}{A dh}$$

S = storativity
 dV = change in volume
 dh = change in head
 A = unit cross sectional area

The storativity under falling water table conditions is controlled by the porosity and the dewatering processes acting at the pore level, and increases with the duration of drainage. For the volume estimate, the baseflow total over the month October 2001 (54.9 mm; section 4.5.7) at W1 was taken in the middle of the groundwater recession period. In this month, recharge was minimal. The average change in groundwater for WS1 was 0.24 m ($n=23$), yielding an average storativity of the phreatic aquifer at WS1 of 0.23. Typical storativity values for sandy phreatic aquifers range between 0.2 and 0.3 (Kruseman and de Ridder, 1990).

4.6.4 Finite Element Model

For the current study the groundwater model (MicroFEM) was merely used to visualize the groundwater flow in the study area, and to verify the assumption that the subterranean groundwater divides coincide with the topographical boundaries which were used for the catchment delineation. Based on the observations of the profiles made during the installation of the observation wells, the model area was defined as a homogenous, isotropic, unconfined (phreatic) aquifer with combined boundary conditions. For the western, southern and eastern boundary condition, a constant head following the stream gradient was assumed (Dirichlet boundary condition) and for the north side a topographic zero flow boundary (Neumann boundary condition). In MicroFEM the study region was covered with a triangular network, with a node distance of 50 m at the boundaries and 10 m around the streams (Figure 4.26a). For the steady state model the following input parameters were used: recharge 2.5 mm d^{-1} , saturated conductivity $50 \text{ m}^2 \text{ d}^{-1}$, and a storativity of 0.25. The resulting groundwater level distribution (Figure 4.26b) coincides with the topographical pattern as shown in Figure 2.5.

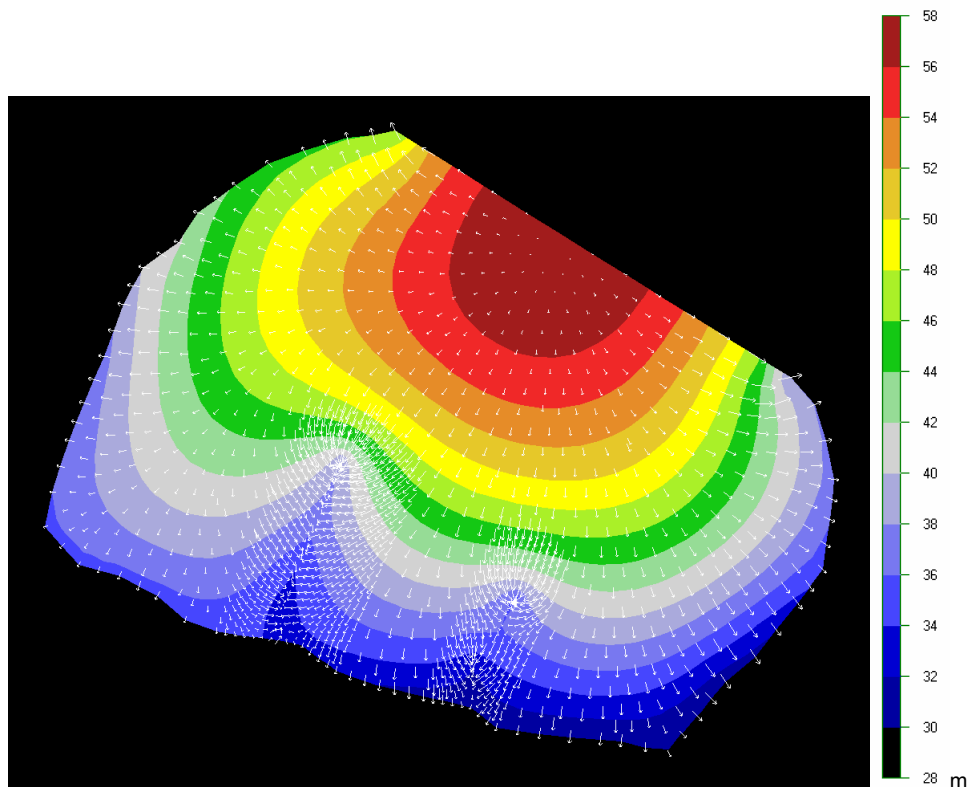
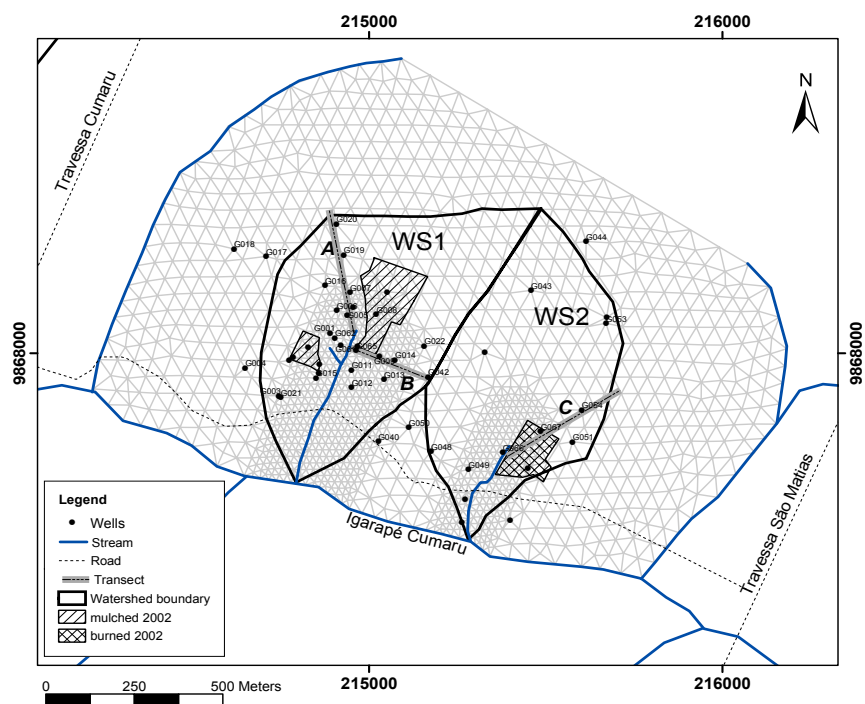


Figure 4.27 a) Monitoring network of observation wells and the FEM triangular element distribution and b) groundwater flow lines under stationary conditions

4.7 Catchment water balance

By following the water from the moment it entered the system and quantifying the losses that occur in the main hydrological compartments on its way out of the system an accurate water balance was obtained for WS1 (Table 4.11). A strong seasonal variation in rainfall amounts was observed, with a wet season in the first four months of the year and a distinct dry season between September and January (section 4.2). The main surface processes, which bring water back into the atmosphere, are transpiration and interception (section 4.3). Evapotranspiration (ET) was determined with the micro-meteorological method using the Penman-Monteith equation (ET_{pm}) and a combination of this method with interception measurements (ET_{comb}), (section 4.4).

When the catchment is watertight and the storage (S) known or negligible, ET can also be estimated by solving the catchment water balance (Eq. 4.1). Analysis of the rainfall-runoff dynamics (section 4.5) resulted in the hypothesis that only a small part of the watershed generates stormflow, and that the contribution of stormflow to the total annual water budget is minimal. Most water infiltrates due to the high hydraulic conductivity of the soils, and ends up in the stream by groundwater recharge. Quickflow processes, such as saturation overland flow, or Horton overland flow were shown to be absent. Storage (S) losses over the year were shown to be minimal from the records of the groundwater observation wells (section 4.6).

The resulting estimates for the components of the water balance of WS1 are summarized in Table 4.11. Of the approximately 2253 mm of rainfall over the year 2001, 1333 mm was evaporated back into the atmosphere, and 920 left the system as streamflow. At WS3 the total annual runoff was approximately 857 mm, yielding an estimated 1396 mm for ET . The estimate for ET obtained with the Penman-Monteith method of 1337 mm over young fallow vegetation, was very close to the result obtained with the water balance method of 1333 mm. Including interception (Ei) into the ET estimate (ET_{comb}) seems to lead to an overestimation for this value (1429.7). This could be due to an error in the spatial averaging when Ei is estimated for the entire watershed area. The values for S are given to show the effect on the catchment water balance if the ET_{comb} value is used. Their low values illustrate that storage over the year indeed is minimal. Although the water balance for this catchment is closed, one should bear in

Water balance

mind that the accuracy of determination the water balance parameters typically ranges between 5 and 20 % and that there is always a potential for errors.

Table 4.12 Water balance (in mm) for WS1 for the year 2001 and the first half of 2002

2001	P	Q	P-Q	ET_{pm}	ET_{comb}	S (1)	S (2)
January	423	49	374	100	114	274	260
February	439	60	379	94	107	285	272
March	360	108	252	94	114	158	138
April	239	132	107	105	114	2	-7
May	135	120	15	118	123	-103	-108
June	187	84	103	123	131	-20	-28
July	179	77	102	132	142	-30	-40
August	49	71	-22	126	129	-148	-151
September	142	67	75	124	135	-49	-60
October	5.0	55	-50	123	124	-173	-174
November	78	51	27	108	113	-81	-86
December	16.9	47	-30.1	90	87	-120	-117
Total	2253	920	1333	1337	1432	-5	-101

2002							
January	450	49	401	96	119	305	282
February	238	52	186	94	98	92	88
March	296	62	234	111	115	123	119
April	335	73	261	122	136	140	126
May	353	102	251	127	132	124	119
June	182	93	89	121	112	-32	-23
Total	1854	431	1423	671	712	751	711

Table 4.13 Water balance (in mm) for WS3 for the year 2001 assuming zero storage

2001	P	Q	P-Q
January	423	41	382
February	439	54	385
March	360	101	259
April	239	124	115
May	135	114	21
June	187	80	107
July	179	71	108
August	49	65	-16
September	142	63	79
October	5	51	-46
November	78	49	29
December	17	44	-27
Total	2253	857	1396

5 NUTRIENT BALANCE

5.1 Introduction

The nutrient cycling in an ecosystem involves a complex set of interactions between soil and vegetation (Proctor, 1987). Nutrient losses are usually estimated from stream nutrient concentrations or from lysimetry measurements (Jordan, 1982; Likens, 1985; Likens and Bormann, 1977; Proctor, 1987). In a literature review, Bruijnzeel (1990) elucidated large discrepancies between the results obtained using these two methods. The main cause of these discrepancies is thought to originate from scale differences, given that lysimetry is based on point measurements while catchment methods integrate losses over the entire watershed domain. Highly infertile soils represent a special case in nutrient studies in that they require different approaches depending upon whether the knowledge of nutrient losses from the biologically active portion of the ecosystem or from the system at large is desired (Bruijnzeel, 1990). Relatively few studies have utilized groundwater nutrient concentrations to estimate export fluxes (Lesack, 1993a; Williams et al., 1997).

In this chapter the nutrient balance is determined for different types of land use at various spatial levels, ranging from a point scale to the level of the entire Cumaru watershed. Nutrient inputs from rainfall and dry deposition are discussed in section 5.3, and nutrient exports to groundwater in section 5.4. The streamflow chemistry during baseflow and stormflow conditions is discussed in section 5.5. The estimated nutrient budgets at a point to plot scale as well as at a watershed level are discussed in section 5.6.

5.2 Field and laboratory procedures

The electrical conductivity (EC), acidity (pH) and temperature of every sample were measured in the field with a WTW 310 EC meter and WTW 320 pH meter. All samples were filtered with a 0.45 μm Millipore membrane filter and were preserved by adding 15 mg of Thymol (2-isopropyl-5-methyl phenol), a biocide which prevents microbial uptake in the sample bottle during storage. The samples were stored in 50 ml Polyethylene (PET) flasks with minimal inclusion of air, and refrigerated below 4°C upon arrival from the field (APHA, 1989).

Rainwater samples of large rainfall events were taken on an event basis, and smaller events were taken as an integrated sample with one sealed totalizing rain gauge in the center of a large open plot at watershed 1. The collector was continuously open, so dry deposition was included in the sample.

Groundwater sampling was initiated two months after the installation of the observation wells. The majority of the groundwater samples were taken at WS1. The well water was pumped with a low discharge peristaltic pump for about 15 minutes prior to sampling in order to avoid contamination of the sample (Appelo and Postma, 1994; Stuyfzand, 1983). The samples were taken with a steel bailer that allowed instantaneous sampling without contact with the sample.

Stream flow was sampled manually for baseflow and selected stormflow events at the four weirs and the Cumaru main channel (W1-W5; Figure 3.1). The samples taken at W003 were not used in the current analysis because of contamination from a nearby spot used by the farmers to wash their dishes and laundry etc. Stormflow was sampled at W1 with the use of an ISCO 6700C automatic sampler in 500 ml PET flasks. The sampling routine was triggered by the rise of the stream level above a pre-selected level and then continued every 10 minutes. On a daily basis, a 50 ml sub-sample was taken by the method described above.

The water samples were analyzed for their chemical composition by the Institute for Soil Science and Forest Nutrition (IBW) of the University of Göttingen, Germany. The concentrations of the elements Na, K, Mg, Ca, Mn, Fe, Al, S and P were measured with the ICP-OES-technique (Spectro Analytical Instruments, Kleve). NH_4 , NO_3 , Total-N (UV treated) and Cl were analyzed with a CFC (Continuous Flow Colorimeter, Skalar, Erkelenz). The lower detection limits of the individual elements are indicated in Table 5.1.

5.3 Rainfall chemistry

5.3.1 Introduction

The atmospheric input of nutrients into a forested ecosystem is governed by wet and dry deposition (Waterloo, 1994). Obtaining a reliable estimate of atmospheric nutrient input is notoriously difficult (Bruijnzeel, 1989a; Bruijnzeel, 1991; Galloway and Likens, 1978; Galloway et al., 1982; Lewis et al., 1987). Wet only deposition measurements are

relatively straightforward, but underestimate the total atmospheric input since dry deposition is not included (Poels, 1987). Nutrient input in rainfall is likely to be fairly variable, and may be greatly influenced by smoke from shifting cultivation (Klinge, 1998; Proctor, 1987). Other possible sources of dry deposition aerosols in the study region are sea spray, mining dust and local aerosols generated by the tropical vegetation (Appelo and Postma, 1994; Artaxo and Hansson, 1995; Brouwer, 1996; Bruijnzeel, 1989a; Proctor, 1987). In the current study the collectors were permanently open, so at least part of the dry deposition was thought to be included in the analysis.

5.3.2 Methodology

Assuming that all Chloride (Cl) in the rainwater sample originates from the ocean, the fractions of the other ions in relation to the ocean water concentration of these ions can be calculated using Eq. 5.1 (Eriksson, 1960). The concentration difference between the calculated (expected) and the observed concentration consequently be attributed to continental sources (Appelo and Postma, 1994; Eriksson, 1960).

$$(5.1) \quad [X_{expected}] = \frac{[X_{sea}]}{[Cl_{sea}]} \cdot [Cl_{rain}]$$

$[Cl_{rain}]$ = chloride concentration in rainwater

$[Cl_{sea}]$ = chloride concentration in seawater

$[X_{sea}]$ = sea water concentration of ion X

$[X_{expected}]$ = expected concentration of ion X

5.3.3 Rainwater composition

Nutrient concentrations in the rainwater were very low and often near the lower limits of detection (Table 5.1). The electrical conductivity (EC) of the samples measured in the field ranged between EC 6.6 $\mu\text{S cm}^{-1}$ and 14.5 $\mu\text{S cm}^{-1}$, and pH between 5.0 and 6.19. Table 5.1 gives an overview of the nutrient concentrations of 20 rainwater samples taken between the 19th of February 2001 and the 5th of February 2002. Comparison with values reported in previous studies by Hölscher (1995) and Klinge (1998) for sites at 5 km and 100 km distance respectively from the current study site indicated that the observed values were well within the range of their averaged reported concentrations (Table 5.3).

The dominant cation (in meq l⁻¹) in rainfall was Na followed in descending order by Ca, Mg, Al, Fe, NH₄ and Mn. The dominant anion was Cl followed by SO₄, PO₄ and NO₃. The average charge balance of the studied samples was slightly positive. A positive balance is common in tropical studies and is usually due to the lack of inclusion of HCO₃ or organic anions in the analyses (Brouwer, 1996; Galloway et al., 1982; Hölscher, 1995; Klinge, 1998; Lesack and Melack, 1991). For the dry season samples, however, the charge balance was slightly negative to neutral, indicating a possible seasonal variation. The negative charge balance in the dry season could be secondary to higher concentrations of organic anions. Unfortunately insufficient samples were available to support this apparent seasonal variation.

Table 5.1 Weighted averages of EC (μS cm⁻¹), pH and nutrient concentrations (mg l⁻¹) in rainwater with the analytical detection limits (mg l⁻¹)

n	EC	pH	Na	K	Ca	Mg	Fe	Mn	Al	NH ₄	Cl	SO ₄	PO ₄	NO ₃	N-tot	N-org
Detection limit			0.03	0.08	0.01	0.01	0.01	0.01	0.04	0.15	0.25	0.01	0.02	0.15	0.15	0.15
Sea water¹																
60850	8.34		10820	408	392	1356	0.02	0.02	0.05	0.26	20210	2754	0.39	0.05	0.05	0.11
Rainwater composition																
<i>Wet season 2001</i>																
6	9.40	5.00	0.54	0.11	0.12	0.06	0.01	0.00	0.00	0.00	0.84	0.16	0.04	0.00	0.06	0.06
<i>Dry season 2001</i>																
4	14.52	5.53	0.69	0.35	0.11	0.08	0.00	0.00	0.00	0.00	1.54	0.21	0.07	0.05	0.11	0.07
<i>Wet season 2002</i>																
9	8.10	5.02	0.40	0.18	0.14	0.05	0.01	0.00	0.01	0.00	0.80	0.15	0.02	0.00	0.07	0.07
<i>Average 2001</i>																
19	12.90	5.53	0.59	0.16	0.11	0.07	0.00	0.00	0.01	0.00	1.07	0.18	0.06	0.02	0.08	0.06

¹From Waterloo (1994)

Table 5.2 Calculated oceanic contribution (%) to rainwater composition

	Na	K	Ca	Mg	Fe	Mn	Al	NH ₄	Cl	SO ₄	PO ₄	NO ₃	N-tot	N-org
Wet season 2001	84	15	14	87	0	0	0	0	100	73	0	0	0	0
Dry season 2001	119	9	27	128	0	0	0	0	100	98	0	0	0	0
Wet season 2002	108	9	11	107	0	0	0	0	100	73	0	0	0	0
Average	96	13	18	102	0	0	0	0	100	82	0	0	0	0

The calculated oceanic contribution (Table 5.2) indicates that the Na, Mg, Cl and SO₄ in the rain originate mainly from the ocean. The observed positive correlation (>0.65) between these ions supports this indication. K, Ca and N are thought to originate mainly from local sources since their ratio to seawater ranges between 13 and 17 %. Klinge (1998) and Brouwer (1996) reported similar ratios for their sites. Lesack and Melack (1991) attributed the elevated levels of K found in a study by Lindberg et al. (1989) to

localized plumes of terrestrial particulates undergoing cyclic re-suspension into the atmosphere, and suggested that they actually originate in the local ecosystem. In the current situation it is likely that the PO₄ and N originate from the burning of biomass (Artaxo and Hansson, 1995; Hölscher, 1995; Hölscher et al., 1997; Mackensen et al., 1996).

Table 5.3 Weighted averages of pH and ion concentrations (mg l⁻¹) in rainwater at selected humid tropical forest sites. Adapted from a summary by (Brouwer, 1996)

location	pH	Na	K	Ca	Mg	Cl	SO ₄	PO ₄	NO ₃	NH ₄	N-tot
<i>Eastern Amazonia</i>											
Current study (n=20)	5.6	0.59	0.16	0.11	0.07	1.07	0.18	0.04	0.02	0.00	0.08
Hölscher (1995), Ig.-Açu (n=85)	5.0	1.03	0.13	0.23	0.15	2.18	0.25	0.03	0.00	0.00	0.16
Klinge (1998), Belém (n=119)	4.9	0.86	0.08	0.21	0.06	1.84	0.18	0.10	0.00	0.09	0.24
<i>Central Amazonia</i>											
Lesack & Melack (1991)	4.9	0.13	0.02	0.03	0.01	0.13	0.14	0.00	0.05	0.09	0.14
Franken et al. (1985)		0.40	0.12	-	-	0.66		0.00		0.25	
Forti and Moreira (1991)		0.15	0.08	0.11	0.01	0.35	0.16				
Brinkmann (1983, 1985)	4.7	0.01	0.01	0.01	0.01	0.30		0.01		0.07	0.24
<i>Other S-American sites</i>											
Brouwer, Guyana (1996)	5.3	0.48	0.11	0.10	0.05	0.81	0.10	0.00	0.05	0.05	0.10
Grimaldi, French Guyana	5.4	0.23	0.16	0.16	0.05	0.39				0.01	

The ratio of molar S/Na (Stallard and Edmond, 1981), can be used as another indicator for oceanic influence. A ratio of 0.15 is typical for precipitation of oceanic origin and 0.41 for continental precipitation. For the current study the ratio was estimated at 0.25 supporting the suggestion that the rainwater is mainly of oceanic origin. Hölscher (1995) and Klinge (1998) reported higher ratios of 0.36 and 0.44 respectively. Based on this ratio they concluded that the rainwater had a more continental origin.

5.3.4 Nutrient inputs from rainwater

The total atmospheric inputs of nutrients were calculated by multiplying the concentrations in rainwater with the total annual rainfall (Table 5.4). Although the estimates for atmospheric inputs differ from previous values reported by Hölscher

(1995), they remain within the range of inter-annual variations and analysis accuracy. The substantially higher inputs reported by Klinge (1998) are thought to originate from more intense burning in the area surrounding his study site.

Table 5.4 Rainfall totals P (mm) and associated calculated yearly atmospheric inputs of nutrients (kg ha⁻¹) for sites in the zona Bragantina, Eastern Amazonia

	P	Na	K	Ca	Mg	Cl	SO ₄	PO ₄	N-Tot
Current study, Ig Açu	2251	13.3	3.6	2.6	1.6	24.0	4.0	1.2	1.8
Hölscher (1995), Ig.-Açu	1985	19.7	2.1	5.5	2.8	37.2	4.0	0.8	2.6
Klinge (1998), Belém	2479	21.6	3.8	7.2	2.0	46.2	5.1	2.5	6.6

5.4 Groundwater chemistry

5.4.1 Introduction

As was noted in the introduction to this chapter, few previous studies have included groundwater solute concentrations in the nutrient balance. In a study of an area with mainly groundwater based runoff at Lago Calado, Lesack (1993a) concluded that groundwater exports of nutrients were minimal, and that their determination involves relatively large errors. In a study by Williams et al. (1997) in the same area it was demonstrated that the water chemistry undergoes substantial changes on its way through the system, and that groundwater can be significantly enriched in nutrients under fields that were prepared with slash-and-burn techniques. Hölscher et al. (1997) reported significant nutrient losses at a depth of 105 cm under slash-and burn fields in the current study region. The study of Sommer (2000) revealed that most of the plant available nutrients are retained in the system, mainly through the deep root system, and that deeper losses under plots prepared with slash-and-burn and mulch technology were minimal.

5.4.2 Groundwater composition

The electrical conductivity (EC) of groundwater at WS1 ranged between 25 and 60 $\mu\text{S cm}^{-1}$, and the pH between 4.1 and 4.7. The groundwater quality varied significantly throughout the watershed (Table 5.5). Figure 5.1 shows the weighted mean groundwater concentrations of solutes and land use along a NE-SW transect perpendicular to the stream at WS1. The observation wells in fields prepared with burning for traditional agriculture and perennial crops show higher amounts of both cations and anions and

therefore have higher EC values. The water in these wells is particularly enriched in Ca, Mg, K, NO₃ and NH₄ in comparison to wells in natural vegetation plots. These elements are common products of the burning of biomass. The well in the mulched plot shows a slight enrichment in Ca, K and NO₃ concentrations most likely originating from the decomposition of the mulch layer. The rightmost columns in Figure 5.1 represent the concentrations found in a well (G001) situated in a recently abandoned pepper plantation. The plantation (0.5 ha) had been in use for approximately 8 years (Sr. Pedro Carneiro, pers. comm.). Pepper plantations represent an important cash crop for the smallholder farmer and receive high amounts of fertilizer (NPK) and pesticides, which explains the high amounts of K and NO₃ observed at G001. The areas with ‘natural’ vegetation, such as the riparian forest and fallow plots, had the lowest elemental concentrations of all. No relation between land use and pH was observed.

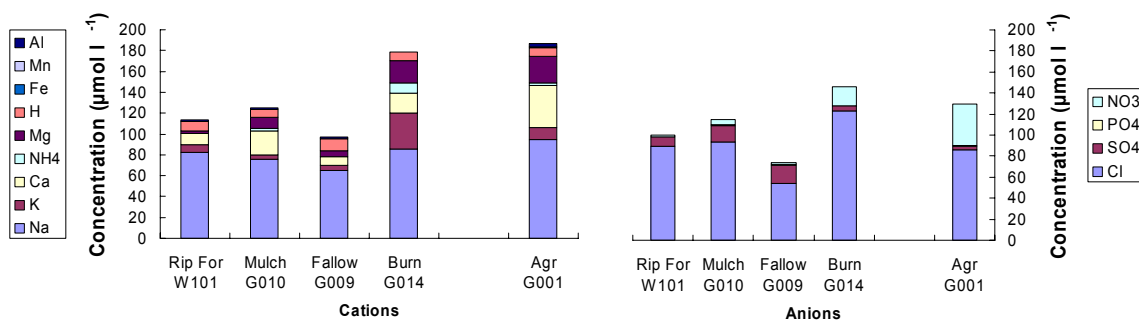


Figure 5.1 Nutrient concentrations in observation wells under various types of land use

Table 5.5 Chemical composition (mg l⁻¹) and EC (µS l⁻¹) of groundwater at selected observation wells and the spatially averaged concentration for W1 based on wells G101 to G010

Well	EC	pH	Na	K	Ca	Mg	Fe	Al	NH ₄	Cl	SO ₄	PO ₄	NO ₃	N-tot
G101	20.8	4.67	2.21	0.14	0.38	0.15	0.14	0.31	0.00	2.75	0.37	0.04	0.00	0.24
G002	25.8	4.18	1.05	0.00	0.34	0.37	0.00	0.06	0.00	2.66	0.28	0.05	0.00	0.00
G005	25.5	4.17	1.78	0.23	0.34	0.12	0.03	0.06	0.06	2.96	0.16	0.04	0.00	0.28
G006	27.4	4.32	2.33	0.27	0.21	0.28	0.00	0.05	0.07	3.80	0.19	0.04	0.20	0.26
G007	26.4	4.23	2.13	0.41	0.28	0.17	0.00	0.02	0.00	3.55	0.19	0.03	0.13	0.49
G016	28.4	4.12	1.82	0.16	0.19	0.19	0.00	0.06	0.00	3.06	0.29	0.04	0.26	0.48
G008	23.3	4.29	1.16	0.14	0.68	0.10	0.01	0.00	0.00	2.64	0.29	0.02	0.30	0.26
G009	23.9	4.22	1.50	0.18	0.35	0.14	0.00	0.06	0.00	1.91	0.57	0.05	0.09	0.39
G010	29.2	4.12	1.75	0.16	0.92	0.25	0.24	0.03	0.05	3.32	0.50	0.04	0.33	0.59
G014	58.7	4.25	1.88	0.89	0.69	0.52	0.00	0.04	0.09	3.99	0.15	0.01	1.13	3.44
G001	46.7	4.27	2.18	0.45	1.61	0.62	0.15	0.08	0.05	3.04	0.12	0.04	2.47	1.94
Avg W1 G101-10	26.2	4.21	1.69	0.19	0.41	0.20	0.03	0.04	0.02	2.99	0.31	0.04	0.16	0.34

5.4.3 Nutrient output to groundwater

As was demonstrated in the previous section, the nutrient concentrations in groundwater vary considerably between observation wells depending upon the above ground land use. In order to estimate the nutrient losses at a point level, the groundwater concentrations were multiplied with the calculated drainage water flux ($P-ET$) of 905 mm yr⁻¹. The calculation of a spatially averaged value for the entire watershed was obtained by using the average composition of the wells in the catchment area of W1. This average value did not include the well under the pepper plantation, since it was located outside of this area and did not contribute to the water measured at W1. The total area of pepper plantations in WS1, was approximately 0.3 ha. Hence it was assumed that for the calculation of the nutrient output of WS1 the average concentration measured at W1 was most representative.

The overall balance calculated for the entire watershed (WS1) and for individual fields is given in Table 5.6. From this balance it appears that between rainwater input and groundwater output at a watershed level the system is accumulating K and PO₄, while losing Ca, Al, NO₃ and total N. This apparent accumulation of mainly K is thought to be largely due to local cycling (section 5.3.3; Lesack and Melack, 1991). Inputs and outputs of Mg, Fe, NH₄ and SO₄ are balanced. When looking in detail at the estimated exports under a particular type of land use a large variation was observed (Table 5.6). Under a recently abandoned pepper plantation, large losses of NO₃, total N, Ca, Mg, and Na were observed, which were most likely due to the inputs of fertilizer by the farmer. The observation well under the burned field showed a similar pattern, though much less pronounced. The nutrient balance obtained for fallow vegetation plot showed mainly slight positive balance for K and losses of total N and SO₄. Under none of the plots losses of PO₄ were observed indicating that even under heavily fertilized plots (pepper and passion fruit) all phosphorus is fixed.

Table 5.6 Nutrient input with rainwater and output with groundwater at selected wells in WS1 and the resulting balance at a field level and watershed level in kg ha⁻¹ per year

	Na	K	Ca	Mg	Fe	Al	NH4	Cl	SO4	PO4	NO3	N
Inputs / Outputs												
Rainwater	13.34	3.60	2.58	1.58	0.07	0.15	0.00	24.00	3.99	1.24	0.37	1.74
Fallow	13.58	1.63	3.17	1.27	0.00	0.54	0.00	24.07	5.16	0.45	0.81	3.53
Mulch	11.44	1.42	5.16	1.05	0.02	0.00	0.00	24.62	4.63	0.26	1.36	2.35
Burn	18.24	2.42	2.31	1.72	0.07	0.43	0.29	30.25	1.88	0.34	1.33	3.42
Pepper	19.73	4.07	14.57	5.61	1.36	0.72	0.45	27.51	1.09	0.36	17.56	19.46
WS1	16.84	2.67	4.02	1.68	0.23	0.93	0.18	28.89	3.78	0.34	1.41	3.12
Balance												
Fallow	-0.24	1.97	-0.59	0.31	0.07	-0.39	0.00	-0.08	-1.17	0.79	-0.45	-1.79
Mulch	-1.90	2.18	-2.58	0.53	0.05	0.15	0.00	-0.62	-0.64	0.98	-0.99	-0.61
Burn	-4.90	1.18	0.27	-0.14	0.00	-0.28	-0.29	-6.25	2.11	0.90	-0.97	-1.68
Pepper	-6.39	-0.47	-11.99	-4.03	-1.29	-0.57	-0.45	-3.51	2.90	0.88	-17.19	-17.72
WS1	-3.50	0.94	-1.44	-0.10	-0.16	-0.78	-0.18	-4.89	0.21	0.91	-1.04	-1.38

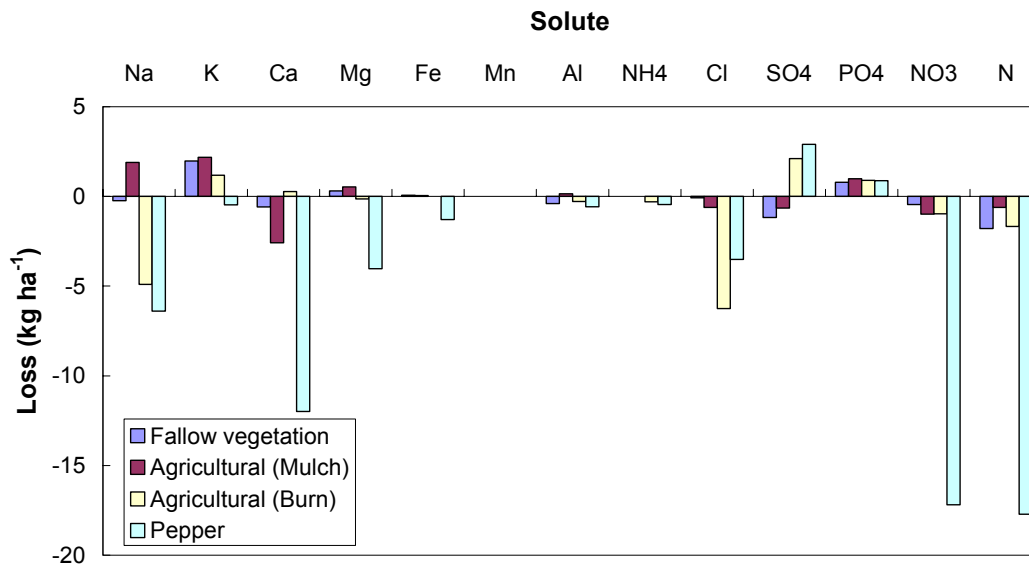


Figure 5.2 Nutrient balance based on groundwater concentrations under different land use types

5.5 Streamwater chemistry

5.5.1 Introduction

Nutrient losses at a watershed level can be estimated when streamflow volume and chemistry are monitored simultaneously. In order to evaluate land-use change effects, paired catchment studies and time-trend studies are most effective (Bosch and Hewlett, 1982). Lesack (1993a) stated that the exclusion of stormflow losses from most previous studies in tropical forest catchments could have led to serious underestimation of annual nutrient exports. He found for a catchment in Central Amazonia that 25% of the annual K exports occurred during stormflow events. McLain and Elsenbeer (2001) showed that the flowpaths of water strongly determine baseflow and stormflow chemistry, by comparing various studies at the two hydrological extremes in the Amazon basin. Markewitz et al. (2001) demonstrated that substantial Ca, Mg, K and HCO_3 losses occur with shallow quickflow through soils with an impeding layer of low permeability under pastures near Paragominas, also in the eastern Amazon region. This study also reported a strong seasonal pattern in nutrient exports.

5.5.2 Methodology

To partition the inferred flux of nutrients contributed by stormflow water from the background signal of baseflow, a two source mixing model (DeWalle et al., 1988; Pinder and Jones, 1969) was used. This model is based on the assumption that during a storm discharge can be separated into two components as:

$$(5.2) \quad Q = Q_b + Q_p$$

$Q = \text{Total discharge (l s}^{-1}\text{)}$
 $Q_b = \text{Baseflow (l s}^{-1}\text{)}$
 $Q_p = \text{Stormflow (l s}^{-1}\text{)}$

The two-source mixing model represents a simplification of the complex combination of flow paths (Lesack, 1993a; Pearce et al., 1986; Schellekens, 2000), but, based on the results of the hydrograph separation method (section 4.5) , the model is thought to provide a decent approximation for the conditions present in the current study. Lesack (1993a) gives a detailed methodology for the calculation of the total annual contribution of baseflow and stormflow to the nutrient budget. This method is based on the assumption that the transport flux for a solute / nutrient for any given interval of time is defined as (Lesack, 1993a):

$$(5.3) \quad Y = \int_{t_i}^{t_e} C(t)Q(t)dt$$

$C(t) = \text{Nutrient concentration in the streamwater as a function of time } t$
 $Q_t = \text{stream discharge}$
 $t_i, t_e = \text{starting and ending times}$

The solute fluxes separately contributed by base and stormflow water are defined by the mass balance equation (Lesack, 1993a; Pinder and Jones, 1969):

$$(5.4) \quad CQ = C_B Q_B + C_P Q_P$$

$C_B, Q_B = \text{Concentration and discharge of the baseflow component}$
 $C_P, Q_P = \text{Concentration and discharge of the stormflow component}$

Equation 5.4 was used to obtain inferred concentrations of stormflow water while the concentrations of baseflow water were known, and the component discharges derived from the Hewlett and Hibbert technique (section 4.6.2).

Hence the total annual solute flux contributed by baseflow discharge (Y_{BA}) was calculated as (Lesack, 1993a):

$$(5.5) \quad Y_{BA} = \sum_{j=1}^m Y_{Bj}$$

Y_{Bj} = solute flux contributed by
baseflow discharge in time interval j
 m = the number of intervals

And the total annual solute flux contributed by stormflow discharge (Y_{PA}) was calculated as (Lesack, 1993a):

$$(5.6) \quad Y_{BA} = \sum_{j=1}^m Y_{Pk}$$

Y_{Pk} = solute flux contributed by
stormflow discharge in time interval k
 m = the number of storms

The annual volume-weighted mean concentrations of nutrients (C) in streamwater exported from the catchment as baseflow and stormflow runoff were calculated as:

$$(5.7) \quad \begin{aligned} C_{Bvm} &= Y_{BA} / V_{BA} \\ C_{Pvm} &= Y_{PA} / V_{PA} \end{aligned}$$

V_{BA} = Annual volume of baseflow
 V_{PA} = Annual volume of stormflow

5.5.3 Baseflow composition

The nutrient concentrations, EC and pH in streamwater at WS1 were fairly constant throughout the year (Figure 5.3). Only during the dry season and at the onset of the wet season following a period of extended drought were increases in the concentration of K, NO₃ and Ca, and to a lesser extent Al, Mg and SO₄ observed (Figure 5.3). Na, Cl, and PO₄, concentrations remained relatively constant. Ca showed the strongest seasonal trend, following the general pattern of the baseflow. The baseflow composition at WS3 resembled the composition observed at WS1, but seemed more variable in the dry season (Figure 5.4). The first baseflow samples taken at WS2 in 2002, showed elevated concentrations of Cl, Na, K, Mg, and SO₄ (Figure 5.4). During the burning of the plot near the source of WS2 the fire unfortunately went out of control and entered the riparian vegetation. It is therefore more likely that this resulted in a strong nutrient input into the stream. Furthermore, in December 2001 the stream at WS2 ceased flowing and allowed the accumulation of nutrients by dry deposition. Based on these observations and results it was concluded that WS2 was not directly comparable with the other two watersheds.

The ratio of concentrations in base flow (Q) to rainfall concentrations (P) provides a good indication of how the composition of the water is altered on its way

through the ecosystem (Likens and Bormann, 1977; Waterloo, 1994). As was determined with the water balance (Section 4.8) evapotranspiration (*ET*) reduced the amount of water leaving WS1 by a factor of 2.49 and for WS3 by a factor of 2.81. If *ET* were the only process affecting the composition of the rainwater before it leaves the system as streamwater, all concentrations would increase for WS1 and WS3 by a factor of 2.49 and 2.81 respectively. For WS2, unfortunately, this value could not be determined because of a lack of runoff data.

The calculated Q/P ratios for the individual watersheds amounted 2.51, 2.46 and 2.87 for WS1, WS2 and WS3 respectively (Table 5.7). Given that the *ET* factor ratio and the Q/P ratio show such strong correspondence, it can be concluded that the Q/P ratio can be used to get a reliable estimate of the annual *ET* at a watershed level. Seemingly the average *ET* at WS2 and WS3 is lower than at WS1, which reflects the greater amounts of agricultural land in these watersheds (and therewith less *ET*).

A comparison of the Q/P ratios of the individual solutes with the calculated ratio for Cl gives an indication about their dynamics at a watershed level (Table 5.6). All watersheds had lower Q/P ratios for K (0.56 - 1.45) and PO₄ (0.51 - 0.57), suggesting that these elements were accumulating in the system, and a high Q/P ratio for Mg (3.34 – 4.83) indicating a systematic loss. Because the concentrations of Mn, Fe, Al and NH₄ in rainwater were below the detection limits, these were excluded from the table. The Q/P ratios for SO₄, NO₃ and Ca at WS2 also indicated that this watershed is losing these elements through leaching.

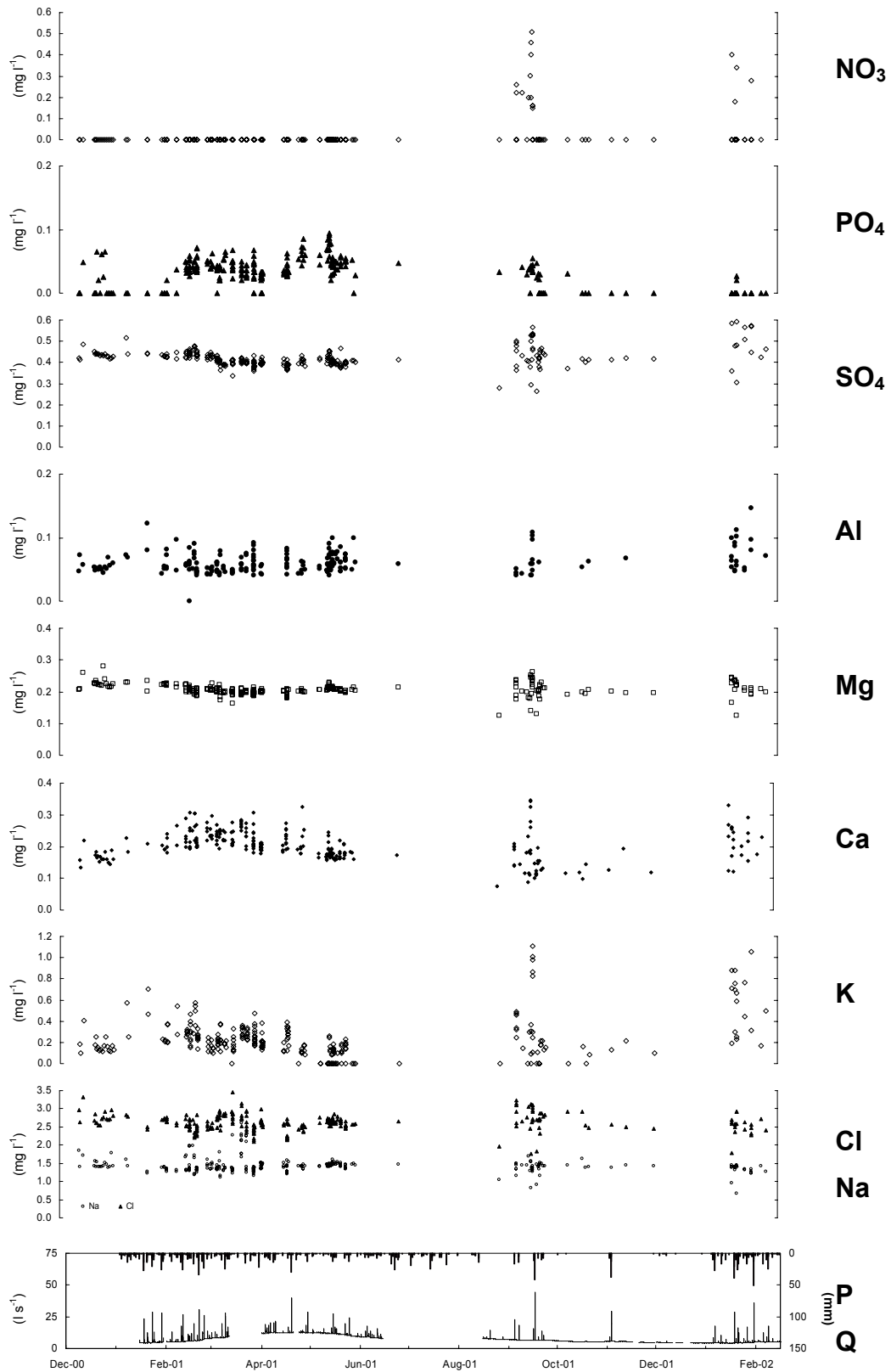


Figure 5.3 Variation in nutrient concentrations (mg l⁻¹) in streamflow (stormflow and baseflow) at W1 throughout the study period

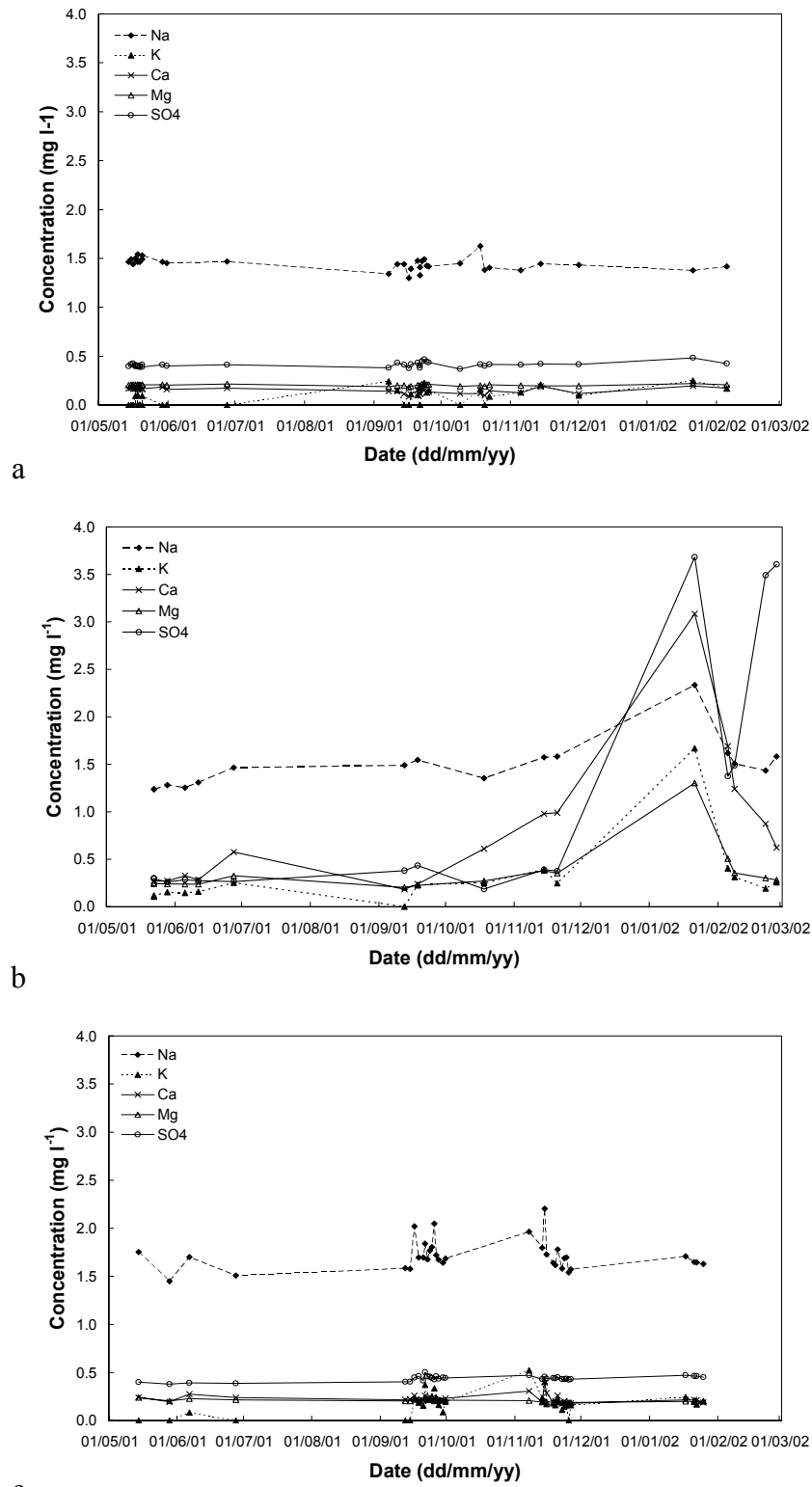


Figure 5.4 Baseflow concentrations (in mg l^{-1}) between the 14th of May 2001 and the 5th of February 2002 at a) W1, b) W2 and c) W3

Table 5.7 Mean chemical composition (in mg l⁻¹) of baseflow water of the three watersheds, (SD = standard deviation, n = number of samples) and ratio of concentrations in baseflow to the concentration in rain (Q/P ratio)

	Na	K	Ca	Mg	SO ₄	PO ₄	NO ₃	Cl
Rain								
n	20	20	20	20	20	20	20	20
Mean	0.61	0.17	0.12	0.06	0.17	0.04	0.01	1.05
SD	0.37	0.19	0.05	0.00	0.08	0.03	0.04	0.65
Watershed 1 (WS1 / weir W1)								
n	102	102	102	102	102	102	102	102
Mean	1.45	0.09	0.16	0.20	0.41	0.03	0.02	2.63
SD	0.15	0.10	0.04	0.02	0.04	0.02	0.22	0.06
Q/P ratio	2.37	0.56	1.31	3.34	2.32	0.75	1.74	2.51
Watershed 2 (WS2 / weir W004)								
n	17	17	17	17	17	17	17	17
Mean	1.40	0.20	0.61	0.29	0.81	0.02	0.04	2.58
SD	0.18	0.10	0.42	0.08	1.10	0.02	0.08	0.43
Q/P ratio	2.30	1.21	4.99	4.83	4.65	0.57	4.47	2.46
Watershed 3 (WS3 / weir W002)								
N	54	54	54	54	54	54	54	54
Mean	1.73	0.24	0.23	0.20	0.42	0.02	0.03	3.01
SD	0.37	0.30	0.05	0.03	0.05	0.02	0.09	0.63
Q/P ratio	2.84	1.45	1.86	3.34	2.42	0.51	2.92	2.87
Cumaru (weir W5)								
N	9	9	9	9	9	9	9	9
Mean	1.69	0.20	0.78	0.33	0.35	0.02	0.14	3.00
SD	0.20	0.15	0.11	0.05	0.08	0.03	0.35	0.35
Q/P ratio	2.77	1.21	6.39	5.51	1.98	0.48	14.13	2.85

5.5.4 Stormflow composition

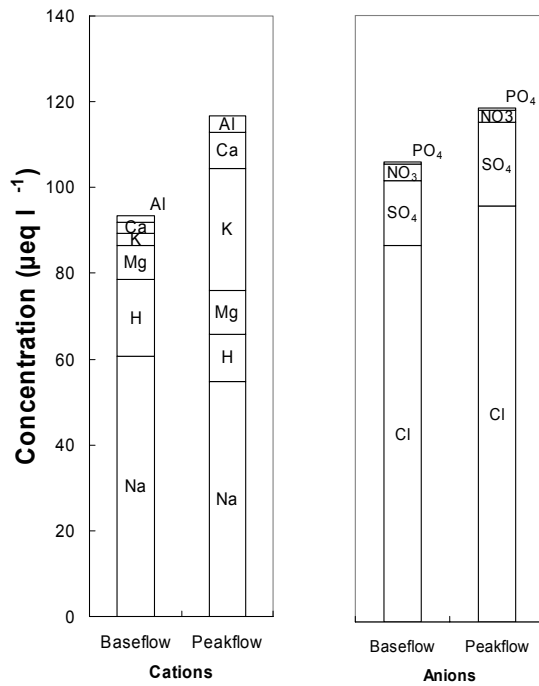
Figure 5.7 shows two selected storm events of 51.2 mm rainfall on the 17th of September 2001 (event A) and 25.6 mm of rainfall the 3rd of April 2001 (event B). It should be noted that the concentration of many of the nutrients are only just above their laboratory detection limit. Event A is thought to be representative of the stormflow chemistry after a dry period. Strong increases occur in K (6 fold increase), Ca (3 fold increase) and NO₃ (2 fold increase) concentrations while Mg, Al, SO₄ and Cl show only slight increases and Na a slight decrease (Figure 5.7). PO₄ remains constant, just above its detection limit.

Event B is representative of the stormflow conditions in the rainy season and displays a completely different reaction. The concentrations of most solutes show a decrease with stormflow, while and PO₄, NO₃ and Al become undetectably low. The explanation for this contrast is thought to originate from the dry deposition on the leaf

surface of the riparian vegetation and the accumulation of decomposition products of litter in the riparian zone during an extended dry period. After such a dry period the accumulated nutrients are flushed with the first storms. Following this flushing, the nutrient contribution from the canopy diminishes, and the nutrient concentrations in stormflow decline. After several weeks of ‘flushing’, the only signal that remains during storm events is determined by the composition of the rain. An indicator supporting this hypothesis is the concentration of H^+ , which is generally high in rainfall and low in throughfall because it compensates for the charge difference of the released elements from the canopy (mainly K and Ca). Some weeks into the wet season, the amounts of K and Ca available for leaching on the canopy surface seem to have been depleted, resulting in lower K and Ca and higher H^+ concentrations in stormflow water (Figure 5.5). Interestingly, the charge balance of baseflow water in the dry and the wet season seems to be more negative, while the charge balance of stormflow water is slightly positive. In the dry season samples a correlation between stream discharge and the concentrations of K ($r^2 = 0.77$), Ca ($r^2 = 0.67$) and Al ($r^2 = 0.59$) was observed while during the wet season events no such correlation was found (Figure 5.6).

In a study in the western Amazon, Elsenbeer et al (1994; 1995) reported a similar response of K, Ca and Mg concentrations in dry and wet season stormflow. In their study, however a double peak in the dry-season chemograph was found, leading to the conclusion that the first peak originated from canopy flushing (Elsenbeer et al., 1995), and the second peak from overlandflow / quickflow (Elsenbeer, 1996). A positive correlation peak flow and Ca was also reported (Likens, 1985).

Event A



Event B

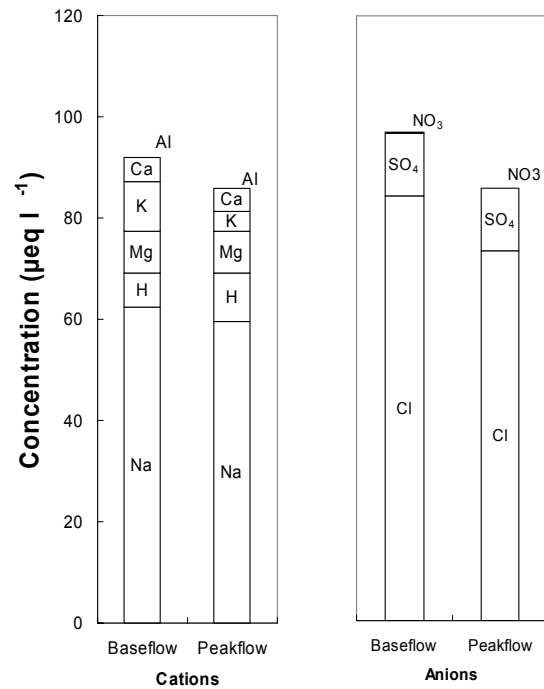


Figure 5.5 Nutrient concentrations in streamwater (in $\mu\text{eq l}^{-1}$) for storm events on 17/09/01 (event A) and 03/04/01 (event B) at W1

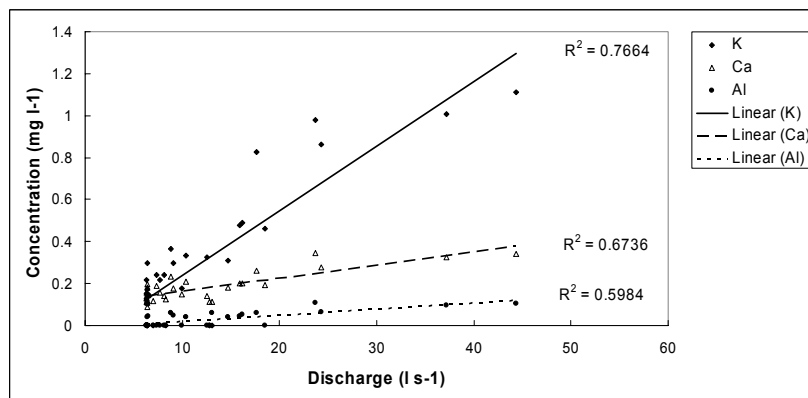


Figure 5.6 Correlation between stream discharge and concentration of K, Ca and Al during the dry season storm events at W1

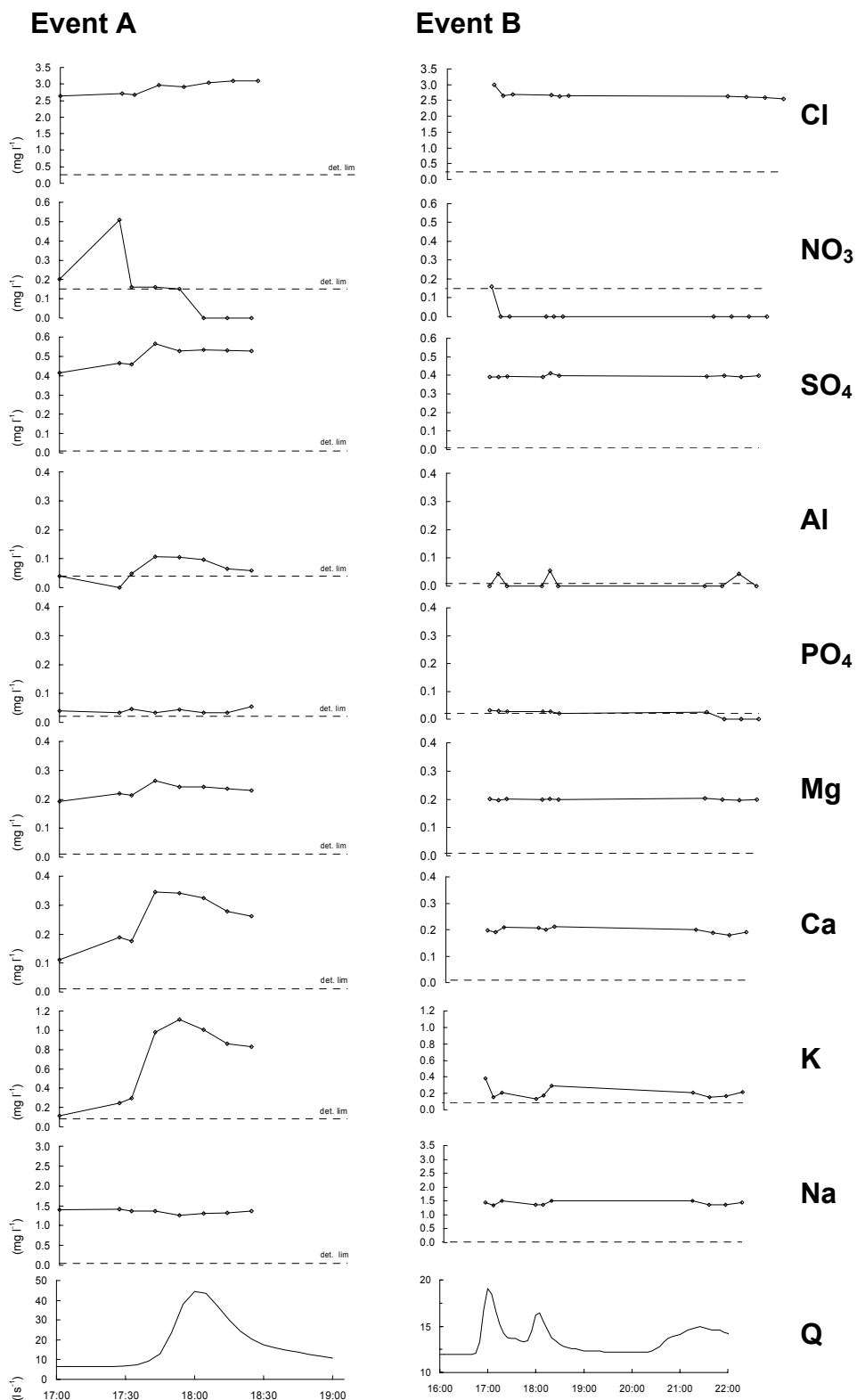


Figure 5.7 Nutrient concentrations in streamwater (in mg l^{-1}) for two storm events on 17/09/01 (event A) and 03/04/01 (event B) at W1

5.5.5 Downstream changes

With various electrical conductivity (EC) routings from the weir (W1) near the source of the stream at WS1 to the main channel of Igarapé Cumaru (W5), a systematic decrease of the EC was observed (Figure 5.9). The chemical analysis of baseflow samples close to the source of WS1 and at the outlet (W5) showed that SO_4 and K show a significant decrease while all other cations, Cl and pH show an increase (Figure 5.8). The main cause of these changes is thought to be nutrient uptake by the riparian vegetation. Van Hogezaand (1996) and Schellekens (2000) also reported downstream a decrease in EC for a tropical rain forest catchment on Puerto Rico. They attributed this to the distance of the unweathered material in respect to the soil surface. Given the deeply weathered soils in eastern Amazonia and the low topographical changes this is not thought to be of influence in the current study.

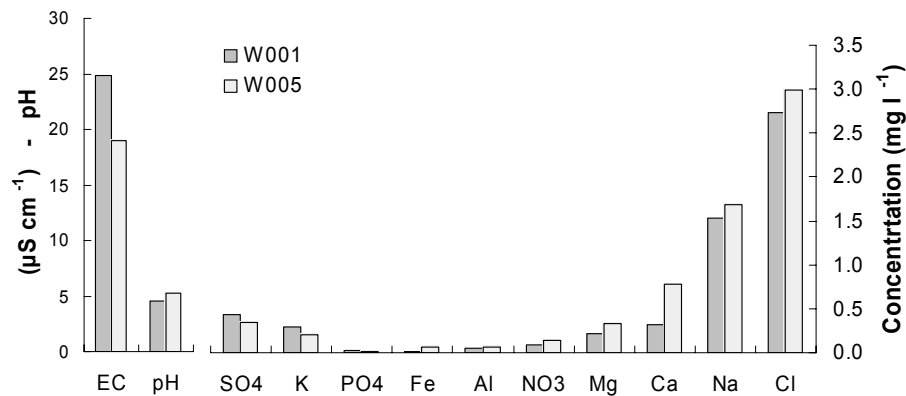


Figure 5.8 Changes in streamwater composition between W1 and W5

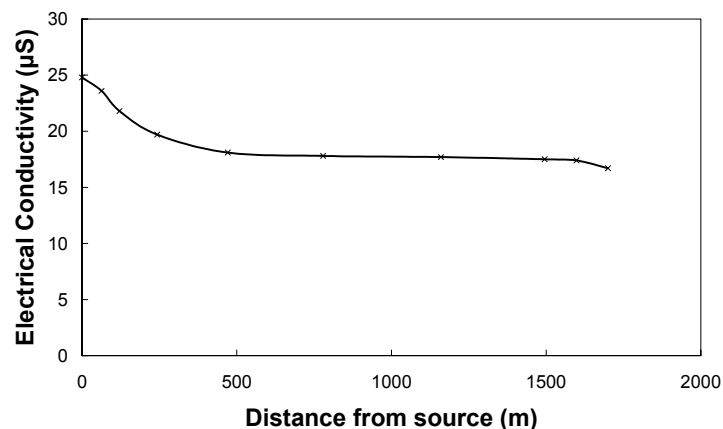


Figure 5.9 Decrease of the EC with distance from the source

5.5.6 Nutrient exports with streamflow

Given the results of section 5.5.3 and section 5.5.4, it can be concluded that the main bulk export of nutrients takes place through baseflow. The calculation of total nutrient exports requires measurement of the total annual flow volumes. At WS1 and WS3 these were accurately measured, but due to technical difficulties and theft of equipment, the volumes for WS2 and the outflow of the main stream were estimated from the chloride balance. Table 5.8 demonstrates that at a watershed level WS1 and WS3 showed a closed balance for most nutrients. All catchments seemed to be accumulating K and P and losing low amounts of Mg and Na. WS2 shows stronger losses of Ca and Mg, which are mainly attributed to the burning of an area close to its source. At a larger scale, the nutrient exports of the entire upper part of the Cumaru watershed were estimated from several samples taken throughout the year. Although the number of samples was rather low, the estimated nutrient exports at a watershed scale lay in the same range as the estimates for the first order watersheds.

5.6 Catchment nutrient balance

As concluded in section 5.3, the atmospheric nutrient inputs into the watersheds of the study area are strongly determined by the proximity of the sea. The enrichment of rainwater with K, Ca and N is thought to originate from local and regional sources. The estimated hydrochemical budgets over the study period for the three first order watersheds are given in Table 5.9. The nutrient exports to groundwater vary strongly depending on the land use at the surface (Section 5.4). Strong agricultural nutrient inputs, mainly originating from the application of fertilizers, were observed under older pepper and passion fruit plantations. The analysis of well water composition throughout the watershed also revealed a strong variation depending upon the aboveground land use. The budget for chloride at a watershed scale based on point measurements (groundwater) was similar to the budget estimated from streamflow measurements. For K, Ca, Mg, Al, SO₄ and total N, the balance based on streamflow exports differed significantly from groundwater based estimates. This is due to the greater spatial variability of these elements related to land use differences, and to processes which take place on the transition from groundwater to streamwater in the riparian forest zone.

Table 5.8 Estimated nutrient exports in kg ha⁻¹ per year for three first order watersheds (WS1, WS2 and WS3) and the entire Cumaru watershed. n = number of samples; SD = standard deviation.

	Na	K	Ca	Mg	Fe	Al	NH4	Cl	SO4	PO4	NO3	N-tot
Inputs Outputs												
Rainwater	13.34	4.52	2.58	1.58	0.11	0.15	0.00	24.00	3.99	1.24	0.17	0.98
WS1	13.26	0.91	1.48	1.85	0.06	0.29	0.00	24.17	3.74	0.26	0.15	0.73
WS2	13.61	2.10	5.95	2.75	1.30	0.46	0.00	24.53	7.56	0.22	0.40	0.70
WS3	13.78	1.92	1.81	1.60	0.06	0.20	0.00	24.00	3.38	0.15	0.22	0.91
Cumaru	13.15	2.07	6.28	2.56	0.58	0.61	0.00	23.96	3.40	0.19	1.13	1.69
Balance												
WS1	0.08	3.61	1.10	-0.26	0.05	-0.14	0.00	-0.17	0.25	0.98	0.02	0.25
WS2	-0.27	2.42	-3.37	-1.17	-1.19	-0.31	0.00	-0.53	-3.57	1.02	-0.24	0.29
WS3	-0.44	2.59	0.77	-0.02	0.05	-0.05	0.00	0.00	0.61	1.09	-0.05	0.07
Cumaru	0.19	2.45	-3.70	-0.98	-0.48	-0.46	0.00	0.04	0.59	1.05	-0.96	-0.71

The hydrochemical composition changes significantly on this transition from groundwater to streamflow (Figure 5.10). The spatial variability of groundwater composition is indicated by the much higher standard deviations in comparison with rainwater and streamwater composition. The baseflow has lower concentrations of Na, K, Ca, Al, Cl and NO_3 in comparison to groundwater. The most likely explanation is that the K, Ca and NO_3 are used by the riparian vegetation, while Al and some Ca precipitate due to the rise in pH. The enrichment of stormflow with K and Ca in respect to baseflow indicates that these elements originate from the riparian zone/throughfall (Section 5.5.4).

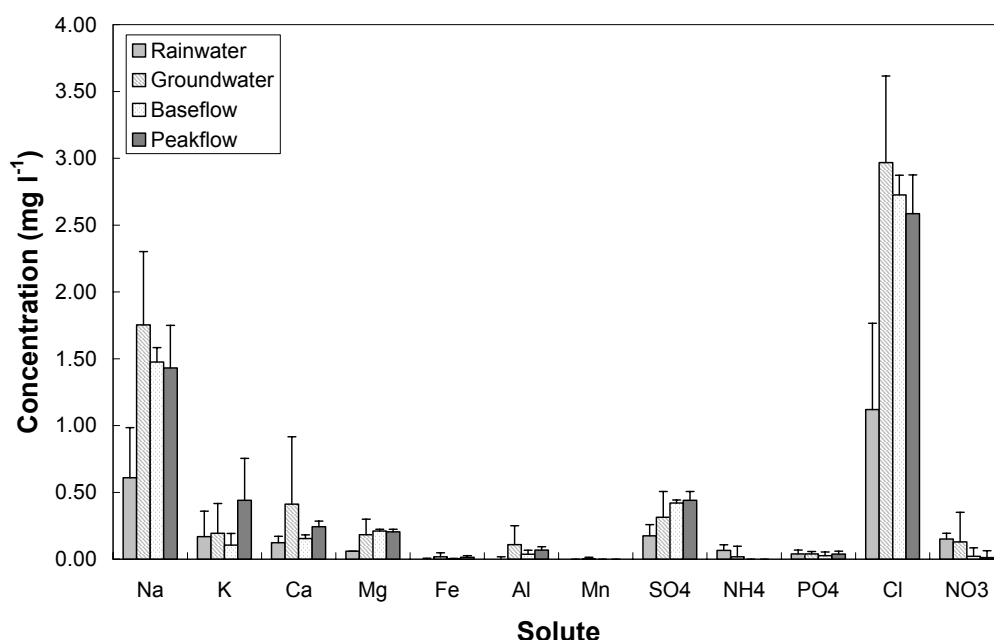


Figure 5.10 Comparison of nutrient concentrations (in mg l^{-1}) in rainwater, groundwater, baseflow and stormflow. The vertical bar indicates the observed standard deviation

The calculated nutrient fluxes in both groundwater (point measured) and in streamwater (watershed level) show that the agricultural system is generally gaining K and losing both Mg and Al. At a watershed level, the mulch watershed (WS1) and the slash-and-burn (control) watershed (WS3) had a close to balanced nutrient balance. The burned watershed (WS2) showed greater losses of most elements apart from PO_4 and K. These higher losses are mainly attributed to the burning of an area close to its source.

In section 5.5.5 it was shown that the stream EC drops and pH increases with distance from the source. In-stream processes possibly in interaction with the riparian vegetation seem to reduce K and SO₄ concentrations. The increases in Ca, Mg, NO₃ and total N (Table 5.9) are thought to originate from a tributary to the southwest of the study catchments, which drains an area with chicken farms and pepper plantations.

Table 5.9 Nutrient balance over the year 2001 in kg ha⁻¹ for WS1 based on estimates from nutrient concentrations in streamflow and groundwater

Solute	<i>Spatial level</i>							
	<i>point</i>				<i>small watershed</i>			<i>watershed</i>
	groundwater				streamwater			
	Mulch	Burn	Pepper	WS1	WS1	WS2	WS3	Cumaru
Na	1.9	-4.9	-6.4	-0.2	0.1	-0.3	-0.4	0.2
K	2.2	1.2	-0.5	2.0	3.6	2.4	2.6	2.4
Ca	-2.6	0.3	-12.0	-0.6	1.1	-3.4	0.8	-3.7
Mg	0.5	-0.1	-4.0	0.3	-0.3	-1.2	0.0	-1.0
Fe	0.0	0.0	-1.3	0.1	0.1	-1.2	0.0	-0.5
Al	0.2	-0.3	-0.6	-0.4	-0.1	-0.3	-0.1	-0.5
NH ₄	0.0	-0.3	-0.5	0.0	0.0	0.0	0.0	0.0
Cl	-0.6	-6.3	-3.5	-0.1	-0.2	-0.5	0.0	0.0
SO ₄	-0.6	2.1	2.9	-1.2	0.3	-3.6	0.6	0.6
PO ₄	1.0	0.9	0.9	0.8	1.0	1.0	1.1	1.0
NO ₃	-1.0	-1.0	-17.2	-0.4	0.0	-0.2	0.0	-1.0
N-tot	-0.6	-1.7	-17.7	-1.8	0.3	0.3	0.1	-0.7

6 CONCLUSIONS

This study was initiated as a follow up to various studies exploring the introduction of mulch technology as an alternative to the traditional slash-and-burn land preparation. In order to assess the effects of changes in land use on water and nutrient dynamics, a sound understanding of the processes that determine these pathways and fluxes is required. Therefore, the main objectives of this study were to evaluate the water and nutrient balance for a set of experimental first order watersheds with mulch and slash-and-burn land preparation.

From the results of the fieldwork conducted between July 2000 and June 2002 it was concluded that runoff dynamics are largely determined by the high permeability of the topsoil and the occurrence of deeply incised riparian wetland channels. The water balance studies at watershed 1 (WS1) and watershed 3 (WS3) revealed a strong correlation between rainfall and quick runoff (stormflow) volume. Based on this correlation, it was concluded that only the riparian wetland fringing the valley bottom contributes to stormflow in the form of saturation-overland-flow. Other forms of quickflow or overland flow were not observed. The groundwater dynamics and their strong correlation with stream baseflow also supported this conclusion. The variations in groundwater levels indicated that on an annual basis the changes in groundwater storage were minimal. The study of surface hydrological processes revealed significant differences in hydrological characteristics between fallow vegetation and riparian forest. Fallow vegetation of 4.5 years in age intercepts approximately 13.5% of rainfall, which is similar to values reported for primary rainforest, while the riparian forest intercepts approximately 9% of rainfall. The throughfall distribution and drip point occurrence under the two vegetation types seems directly related to the grade of heterogeneity of the canopy. It was also shown that the stormflow volume equaled the amount of throughfall under the riparian forest. The water balance for WS1 over 2001 showed that of the total rainfall approximately 59% is evaporated and intercepted by vegetation, 40% leaves the watershed as baseflow, and less than 1% as stormflow. This closed water balance implies that no water is lost to deep groundwater.

The nutrient balance at a watershed level is close to balanced, meaning atmospheric inputs approximately equal outputs on an annual basis. No significant differences in nutrient exports were observed between the mulched watershed and the control watershed. The nutrient budgets of all first order watersheds indicated that the system is systematically accumulating potassium and phosphorus while losing magnesium. At the main channel elevated exports of calcium and nitrogen were observed, most likely from sources such as chicken farms and extensive pepper plantations, which were not present in the headwater catchments of this study. In contrast to the observations at a watershed level, point level estimates show that depending upon the recent land use significant losses of nutrients to groundwater can occur. The observed losses to groundwater are lowest under the mulched and the burned plots, and the highest under plantations of perennial crops such as passion fruit and pepper. The transition of groundwater to the stream in the riparian zone seems to have a significant effect on nutrient loads in the water. The estimates of *ET* from the chloride balance showed a strong correlation with the water balance and micrometeorological estimates.

Based on these results the following conclusions in respect to the hydrological functioning of the agricultural first order watersheds could be drawn:

- The water balance for the study catchments W1 and W3 was closed on an annual basis
- Quick transports of water and nutrients in the form of overland flow or sub-surface stormflow were absent
- The hydrological response of both the mulched watershed and the control watershed were similar
- The riparian zone plays a vital role in stormflow generation

In respect to the nutrient dynamics the following conclusions can be drawn:

- Nutrient losses to groundwater at a point level depend strongly upon land use and are significant under intense agriculture
- With the current smallholder agricultural system the differences between land preparation with mulch technology or slash-and-burn at a watershed level are minimal

- The riparian zone exerts a strong influence on both baseflow and stormflow composition
- At a watershed level both the mulched and the control watershed showed similar nutrient budgets

7 REFERENCES

- APHA, 1989. Standard methods for the examination of water and wastewater, APHA, AWWA, WPCF, Washington D.C.
- Appelo, C.A.J. and Postma, D., 1994. Geochemistry, groundwater and pollution.
- Artaxo, P. and Hansson, H., 1995. Size distribution of biogenic aerosol particles from the Amazon basin. *Atmospheric Environment*, 29(3): 393-402.
- Asdak, C., Jarvis, P.G. and Gardingen, P.V., 1998. Modelling rainfall interception in unlogged and logged forest areas of Central Kalimantan, Indonesia. *Hydrology and Earth System Sciences*, 2(23): 211-220.
- Baar, R., 1997. Vegetationskundliche und oekologische Untersuchungen der Buschbrache in der Feldumlagewirtschaft im oestlichen Amazonasgebiet. Goettinger Beiträge zur Land- und Forstwirtschaft in den Tropen und Subtropen. PhD Thesis, Universität Göttingen, Göttingen, 202 pp.
- Bastos, T.X. and Pacheco, N.A., 1999. Características agroclimatológicas de Igarapé-Açu, PA e suas implicações para as culturas anuais: feijão, caupi, milho, arroz e mandioca. *Boletim de pesquisa no 25*: 5-30.
- Beven, K.J., Wood, E.F. and Sivapalan, M., 1988. On hydrological heterogeneity - catchment morphology and catchment response. *Journal of Hydrology*, 100: 353-357.
- Bonell, M. and Balek, J., 1993. Recent scientific developments and research needs in hydrological processes of the humid tropics. In: M. Bonell, M.M. Hufschmidt and J.S. Gladwell (Editors), *Hydrology and water management in the humid tropics. Hydrological research issues and strategies for water management*. Cambridge University Press / UNESCO, Cambridge, pp. 167-260.
- Bonell, M. and Fritsch, J.M., 1997. Combining hydrometric-hydrochemistry methods: a challenge for advancing runoff generation process research. *IAHS Publications*, 244: 165-184.
- Bonell, M., Gilmour, D.A. and Sinclair, D.F., 1981. Soil hydraulic properties and their effect on surface and subsurface water transfer in a tropical rainforest catchment. *Hydrological Sciences Bulletin*, 26: 1-18.
- Bos, M.G., 1976. Discharge measurement structures. ILRI Publication, 20, 401 pp.
- Bosch, J.M. and Hewlett, J.D., 1982. A review of catchment experiments to determine the effect of vegetation changes on water yield and evapotranspiration. *Journal of Hydrology*, 55(1-4): 3-23.
- Brienza Jr., S., 1999. Biomass dynamics of fallow vegetation enriched with leguminous trees in the Eastern Amazon of Brazil. PhD Thesis, University of Göttingen, Göttingen, 134 pp.
- Brouwer, L.C., 1996. Nutrient cycling in pristine and logged tropical rain forest. A study in Guyana. *Tropenbos Guyana Series*, 1. The Tropenbos Foundation, Wageningen, 224 pp.
- Bruijnzeel, L.A., 1983. Hydrological and biogeochemical aspects of man-made forests in South-central Java, Indonesia. PhD Thesis, Free University Amsterdam, Amsterdam, 250 pp.
- Bruijnzeel, L.A., 1989a. Nutrient content of bulk precipitation in south-central Java, Indonesia. *Journal of Tropical Ecology*, 5: 187-202.

- Bruijnzeel, L.A., 1989b. Nutrient cycling in moist tropical forests: the hydrological framework. In: J. Proctor (Editor), Mineral nutrients in tropical forests and savanna ecosystems. Blackwell Scientific Press, Oxford, pp. 383-415.
- Bruijnzeel, L.A., 1990. Hydrology of moist tropical forests and effects of conversion: A state of knowledge review. Vrije Universiteit Amsterdam, The Netherlands, UNESCO Paris, 24 pp.
- Bruijnzeel, L.A., 1991. Nutrient input-output budgets for tropical forest ecosystems: a review. *Journal of Tropical Ecology*, 7: 1-24.
- Bruijnzeel, L.A. and Wiersum, K.F., 1987. Rainfall interception by a young *Acacia Auriculiformis* A. Cunn. plantation forest in West Java, Indonesia: Application of Gash's analytical model. *Hydrological Processes*, 1: 309-319.
- Brutsaert, W., 1982. Evaporation into the atmosphere. D.Reidel Publishing Company, Dordrecht, 299 pp.
- Chapman, T.G., 1999. A comparison of algorithms for stream flow recession and baseflow separation. *Hydrological Processes*, 13: 701-714.
- Chorley, R.J., 1978. The hillslope hydrological cycle. In: M. Kirkby (Editor), Hillslope hydrology. John Wiley and Sons, Chichester, pp. 1-42.
- Clegg, A.G., 1963. Rainfall interception in a tropical rain forest. *Caribbean Forester*, 24(2): 75-79.
- Coelho-Netto, A.L., 1987. Overland flow production in a tropical rain forest catchment. *Catena*, 14: 213-231.
- Costa, J.B.S., Lea Bemerguy, R., Hasui, Y. and da Silva Borges, M., 2001. Tectonics and paleogeography along the Amazon river. *Journal of South American Earth Sciences*, 14(4): 335-347.
- Cruz, E., 1955. A Estrada de Ferro de Bragança. SPVEA, Belém, PA, 157 pp.
- De Jeu, R.A.M., 1996. Hydrology of two montane forests of contrasting stature in the Blue Mountains of Jamaica. MSc thesis Thesis, Vrije Universiteit Amsterdam.
- Denich, M., 1989. Untersuchungen zur Bedeutung junger Sekundärvegetation für die Nutzungssystemproduktivität im östlichen Amazonasgebiet, Brasilien, University of Göttingen, Göttingen, 265 pp.
- Denich, M., 1996. Ernährungssicherung in der Kleinbauernlandwirtschaft Ostamazoniens - Problem und Lösungsansätze. *Göttinger Beiträge zur Land und Forstwirtschaft in den Tropen und Subtropen*, 115: 78-88.
- Denich, M. et al., 2004. Mechanized land preparation in forest-based fallow systems: The experience from Eastern Amazonia. *Agroforestry Systems*, 61-62(1-3): 91-106.
- DeWalle, D.R., Swistock, B.R. and Sharpe, W.E., 1988. Three-component tracer model for stormflow on a small Appalachian forested catchment. *Journal of Hydrology*, 104: 301-310.
- Dickinson, W.T. and Whiteley, H., 1970. Watershed areas contributing to runoff. *IAHS Publications*, 96: 12-26.
- Diekmann, U., 1997. Vegetationskundliche und oekologische Untersuchungen der Buschbrache in der Feldumlagewirtschaft im oestlichen Amazonasgebiet. *Goettinger Beiträge zur Land- und Forstwirtschaft in*

- den Tropen und Subtropen. PhD Thesis, Universität Göttingen, Göttingen, 189 pp.
- Dingman, S.L., 1994. *Physical Hydrology*. Pearson Education Ltd., London, 646 pp.
- Dunne, T., 1978. Field studies of hillslope flow processes. In: M. Kirkby (Editor), *Hillslope hydrology*. John Wiley and Sons, Chichester, pp. 227-293.
- Dykes, A.P., 1997. Rainfall interception from a lowland tropical rainforest in Brunei. *Journal Of Hydrology*, 200(1-4): 260-279.
- Elsenbeer, H., 1996. The stormflow chemistry at la cuenca, Western Amazonia. *Interciencia*, 21(3): 133-139.
- Elsenbeer, H., 2001. Hydrologic flowpaths in tropical rainforest soilscares—a review. *Hydrological Processes*, 15(10): 1751-1759.
- Elsenbeer, H., Cassel, D.K. and Zuniga, L., 1994. Throughfall in the terra firme forest of Western Amazonia. *Journal of Hydrology (NZ)*, 32(2): 30-44.
- Elsenbeer, H. and Lack, A., 1996. Hydrometric and hydrochemical evidence for fast flowpaths at La Cuenca, Western Amazonia. *Journal Of Hydrology*, 180(1-4): 237-250.
- Elsenbeer, H., Lack, A. and Cassel, K., 1995. Chemical fingerprints of hydrological compartments and flowpaths at La Cuenca, western Amazonia. *Water Resources Research*, 31(12): 3051-3059.
- Elsenbeer, H., Newton, B.E., Dunne, T. and de Moraes, J.M., 1999. Soil hydraulic conductivities of latosols under pasture, forest and teak in Rondonia, Brazil. *Hydrological Processes*, 13(1417-1422).
- EMBRAPA, 1977-2002. *Boletim Agrometeorológico Ano 1977 - Ano 2002*, EMBRAPA - CPATU, Belém, PA.
- EMBRAPA, 1999. *Sistema Brasileiro de classificação de solos.*, EMBRAPA, Brasília.
- Eriksson, E., 1960. The yearly circulation of chlorine and sulphur in nature. Part 2. Meteorological, geochemical and pedological implications. *Tellus*, 12(1): 63-109.
- FAO, 1990. *Soil map of the world*, FAO, Rome.
- Fearnside, P.M., 1987. Causes of deforestation in the Brazilian Amazon. In: R.E. Dickinson (Editor), *The geophysics of Amazonia*. Wiley, New York, pp. 37-53.
- Fearnside, P.M., 1996. Amazonian deforestation and global warming: carbon stocks in vegetation replacing Brazil's Amazon forest. *Forest Ecology and Management*, 80(1-3): 21-34.
- Fearnside, P.M., 2000. Greenhouse gas emissions from land-use change in Brazil's Amazon region. In: R. Lal, J.M. Kimble and B.A. Stewart (Editors), *Global climate change and tropical ecosystems*. Advances in Soil Science. CRC Press, Boca Raton, FL, pp. 231-249.
- Forti, C.M. and Moreira-Nordemann, L.M., 1991. Rainwater and throughfall chemistry in a Terra Firme ran forest: Central Amazonia. *Journal of Geophysical Research*, 96: 7415-7421.
- Franken, W.K., Leopoldo, P.R. and Bergamin Filho, H., 1985. Nutrient flow through natural waters in terra firme forest in the Central Amazon, Workshop on biogeochemistry of tropical rain forests: problems for research, Piracicaba, SP, Brasil.

- Franken, W.K., Leopoldo, P.R., Matsui, E. and Ribeiro, M.d.N.G., 1992. Estudo da interceptação da água de chuva em cobertura florestal amazônica do tipo terra firme. *Acta Amazonica*, 12(2): 327-331.
- Fujieda, M., Kudoh, T., de Cicco, V. and de Calvarcho, J.L., 1997. Hydrological processes at two subtropical forest catchments: the Serra do Mar, Sao Paulo, Brazil. *Journal Of Hydrology*, 196(1-4): 26-46.
- Galloway, J.N. and Likens, G.E., 1978. The collection of precipitation for chemical analysis. *Tellus*, 30: 71-82.
- Galloway, J.N., Likens, G.E., Keene, W.C. and Miller, J.M., 1982. The composition of precipitation in remote areas of the world. *Journal of Geophysical Research*, 87(8771-8786).
- Gash, J.H.C., 1979. An analytical model of rainfall interception by forests. *Quart. J. R. Met. Soc.*(105): 43-55.
- Gash, J.H.C., Lloyd, C.R. and Lachaud, G., 1995. Estimating sparse forest rainfall interception with an analytical model. *Journal Of Hydrology*, 170(1-4): 79-86.
- Gash, J.H.C. and Morton, A.J., 1978. An application of the Rutter model to the estimation of the interception loss from Thetford forest. *Journal of Hydrology*, 38: 49-58.
- Giambelluca, T.W. et al., 1997. Observations of albedo and radiation balance over post-forest land surfaces in the Eastern Amazon Basin. *Journal of Climate*, 10: 919-928.
- Giambelluca, T.W., Nullet, M.A., Ziegler, A.D. and Tran, L.T., 2000. Latent and sensible energy flux over deforested land surfaces in the Eastern Amazon and Northern Thailand. *Singapore Journal of Tropical Geography*, 21(2): 107-130.
- Giambelluca, T.W., Ziegler, A.D., Nullet, M.A., Truong, D.M. and Tran, L.T., 2003. Transpiration in a small tropical forest patch. *Agricultural and Forest Meteorology*, 117(1-2): 1-22.
- Griesinger, B. and Gladwell, J.S., 1993. Hydrology and water resources of tropical Latin America and the Caribbean. In: M. Bonell, M.M. Hufschmidt and J.S. Gladwell (Editors), *Hydrology and water management in the humid tropics. Hydrological research issues and strategies for water management*. Cambridge University Press / UNESCO, Cambridge, pp. 84-98.
- Hedden-Dunkhorst, B. et al., 2003. *Forest-Based Fallow Systems as a Safety Net for Smallholders in the Eastern Amazon*, Center for Development Research, Bonn, Germany.
- Hemker, C.J. and Van Elburg, H., 1987. *Micro-Fem, version 2.0 user's manual*, Amsterdam, The Netherlands, pp. 152.
- Hewlett, J.D., 1982. *Principles of Forest Hydrology*. The University of Georgia Press, 183 pp.
- Hewlett, J.D. and Hibbert, A.R., 1967. Factors affecting the response of small watersheds to precipitation in humid regions. In: W.E. Sopper and H.W. Lull (Editors), *Forest Hydrology*. Pergamon Press, Oxford, pp. 275-290.
- Hewlett, J.D. and Nutter, W.L., 1970. The varying source area of streamflow from upland basins, *Symposium of Interdisciplinary Aspects of Watershed Management*. American Society of Civil Engineers, Bozeman, MT.

- Hölscher, D., 1995. Wasser- und Stoffhaushalt eines Agrarökosystems mit Waldbrache im östlichen Amazonasgebiet. PhD Thesis, Georg-August-Universität Göttingen, Göttingen, 134 pp.
- Hölscher, D., Möller, R.F., Denich, M. and Fölster, H., 1997. Nutrient input-output budget of shifting agriculture in Eastern Amazonia. *Nutrient Cycling in Agroecosystems*, 47: 49-57.
- Hölscher, D., Sá, T.D.d.A., Möller, R.F., Denich, M. and Fölster, H., 1998. Rainfall partitioning and related hydrochemical fluxes in a mono specific (*Phenakospermum guyannense*) secondary vegetation stand. *Oecologia*, 114: 251-257.
- Horton, R.E., 1933. The role of infiltration in the hydrologic cycle. *Transactions of the American Geophysical Union*, 14: 446-460.
- Hurtiene, 1998. Tropical ecology and peasant agriculture in the Eastern Amazon. A comparison of results of socio-economic research on agrarian frontiers with divers historical and agro-ecological conditions., 3rd SHIFT-Workshop March 15-19, 1998, Manaus, pp. 203-217.
- Hutjes, R.W.A., Wierda, A. and Veen, A.W.L., 1990. Rainfall interception in the Tai forest, Ivory coast: Application of two simulation models to a humid tropical system. *Journal of Hydrology*, 114: 259-275.
- IBGE, 1997. Censo Agropecuário 1995-1996 número 5 Pará, IBGE, Rio de Janeiro.
- Jackson, I.J., 1975. Relationships between rainfall parameters and interception by tropical forests. *Journal of Hydrology*(24): 215-238.
- Jackson, N.A., 2000. Measured and modelled rainfall interception loss from an agroforestry system in Kenya. *Agricultural And Forest Meteorology*, 100: 323-336.
- Jetten, V.G., 1994. Modelling the effects of logging on the water balance of a tropical rain forest. PhD thesis Thesis, University of Utrecht, Utrecht, The Netherlands, 196 pp.
- Jordan, C.F., 1982. The nutrient balance of an Amazonian rainforest. *Ecology*, 63(3): 647-654.
- Jordan, C.F. and Heuveldop, J., 1981. The water budget of an Amazonian rainforest. *Acta Amazonica*, 11: 87-92.
- Kato, M.S.A., Kato, O.R., Denich, M. and Vlek, P.L.G., 1999. Fire-free alternatives to slash-and-burn for shifting cultivation in the eastern Amazon region: the role of fertilizers. *Field Crops Research*, 62(2-3): 225-237.
- Kato, O.R., 1998. Fire-free land preparation as an alternative to Slash-and-Burn agriculture in the Bragantina region, Eastern Amazon: Crop performance and nitrogen dynamics. PhD Thesis, George-August-University Göttingen, Germany, Göttingen, 133 pp.
- Kindsvater, C.E. and Carter, R.W.C., 1957. Discharge characteristics of rectangular thin-plate weirs. *Journal of the Hydraulics Division of the ASCE*, 83(No. HY 6): Paper 1453.
- Kirkby, M. and Chorley, R.J., 1967. Throughflow, overland flow and erosion. *Bull. Intern. Assoc. Sci. Hydrology*, 12: 5-21.
- Klinge, R., 1998. Wasser- und nährstoffdynamik im boden und bestand beim aufbau einer holzplantage im östlichen Amazonasgebiet. PhD Thesis, Georg-August-Universität Göttingen, Göttingen, 260 pp.

- Köppen, W., 1936. Das Geographische System der Klimate. In: W. Köppen and I. Geiger (Editors), *Handbuch der Klimatologie*.
- Kruseman, G.P. and de Ridder, N.A., 1990. Analysis and evaluation of pumping test data. ILRI Publication, 47, 377 pp.
- Lal, R., 1975. Role of mulching techniques in tropical soil and water management. Technical bulletin no. 1, IITA.
- Lal, R., 1981. No-tillage farming in the tropics. In: R.E. Phillips, G.W. Thomas and R.L. Blevins (Editors), *No-tillage research: Research reports and reviews*. University of Kentucky, Lexington, KY.
- Leonard, R.E., 1967. Mathematical theory of interception, International Symposium on Forest Hydrology. Pergamon Press, Oxford, pp. 131-136.
- Leopoldo, P.R., Franken, W.K. and Villa Nova, N.A., 1995. Real evapotranspiration and transpiration through a tropical rain forest in central Amazonia as estimated by the water balance method. *Forest Ecology And Management*, 73(1-3): 185-195.
- Lesack, L.F.W., 1993a. Export of nutrients and major ionic solutes from a rain forest catchment in the Central Amazon Basin. *Water Resources Bulletin*, 29(3): 743-758.
- Lesack, L.F.W., 1993b. Water balance and hydrologic characteristics of a rain forest catchment in the Central Amazon Basin. *Water Resources Research*, 29(3): 759-773.
- Lesack, L.F.W. and Melack, J.M., 1991. The deposition, composition, and potential sources for major ionic solutes in rain of the central Amazon basin. *Water Resources Research*, 27(11): 2953-2977.
- Lewis, W.M., Hamilton, L.S., Jones, S.L. and Runnels, D.D., 1987. Major element chemistry, weathering and element yields for the Caura River drainage, Venezuela. *Biogeochemistry*, 4: 159-181.
- Leyton, L., Reynolds, E.R.C. and Thompson, F.B., 1967. Rainfall interception in forest and moorland. In: W.E. Sopper and H.W. Lull (Editors), *Int. Symposium on Forest Hydrology*. Pergamon Press, pp. 163-178.
- Likens, G.E., 1985. An experimental approach for the study of ecosystems. *Journal of Ecology*, 73: 381-396.
- Likens, G.E. and Bormann, F.H., 1977. *Biogeochemistry of a forested ecosystem*. Springer-Verlag, New York, 159 pp.
- Lindberg, S.E., Harriss, R.C., Hoffman, W.A., Lovett, G.M. and Turner, R.R., 1989. Atmospheric chemistry, deposition, and canopy interactions of major ions in a forest. In: D.W. Johnson and R.I. Van Hook (Editors), *Analysis of biogeochemical cycling processes in the Walker Branch Watershed*. Springer Verlag, New York, pp. 96-163.
- Lloyd, C.R., Gash, J.H.C., Shuttleworth, W.J. and Marques Filho, A.d.O., 1988. The measurement and modelling of rainfall interception by Amazonian rainforest. *Journal of Hydrology*, 43: 277-294.
- Lloyd, C.R. and Marques, A.d.O., 1988. Spatial variability of throughfall and stemflow measurements in Amazonian rain forest. *Agriculture and Forest Meteorology*, 42: 63-73.
- Mackensen, J., Holscher, D., Klinge, R. and Folster, H., 1996. Nutrient transfer to the atmosphere by burning of debris in eastern Amazonia. *Forest Ecology and Management*, 86(1-3): 121-128.

- Makloulf Carvalho, E.J., da Costa, M.P. and Costa Veloso, C.A., 1997. Caracterização físico hídrica de um Podzólico vermelho-amarelo textura arenosa/média sob diferentes usos, em Igarapé-Açu, Pará. Boletim de pesquisa no 174, EMBRAPA, Belém.
- Markewitz, D., Davidson, E.A., Figueiredo, R.d.O., Victoria, R.L. and Krusche, A.V., 2001. Control of cation concentrations in stream waters by surface soil processes in an Amazonian watershed. *Nature*, 410: 802-805.
- McClain, M.E. and Elsenbeer, H., 2001. Terrestrial inputs to Amazon streams and internal biogeochemical processing. In: M.E. McLain, R.L. Victoria and J.E. Richey (Editors), *The Biogeochemistry of the Amazon*, pp. 185-208.
- Metzger, J.P.W., 1997. Dinâmica da paisagem, tempo de pousio e estrutura espacial da vegetação secundária numa área de agricultura de corte e queima (Igarapé-Açu), Relatório de actividades, Projeto SHIFT.
- Molion, L.C.B., 1993. Amazonian rainfall and its variability. In: M. Bonell, M.M. Hufschmidt and J.S. Gladwell (Editors), *Hydrology and water management in the humid tropics. Hydrological research issues and strategies for water management*. Cambridge University Press / UNESCO, Cambridge, pp. 99-111.
- Monteith, J.L., 1965. Evaporation and environment. *Symposium of the Society of Experimental Biology*, 19: 205-234.
- Moraes, J.L. et al., 1995. Soil carbon stocks of the Brazilian Amazon. *Soil Science Society of America Journal*, 59: 244-247.
- Nepstad, D.C. et al., 1999. Large-scale impoverishment of Amazonian forests by logging and fire. *Nature*, 398: 505-508.
- Nimer, E., 1972. Climatologia da Região Norte. *Revista Brasileira de Geografia*, 34(3): 124-153.
- Nimer, E., 1991. Clima. In: IBGE (Editor), *Geografia do Brasil. Região Norte*, pp. 307.
- Nortcliff, S. and Thornes, J.B., 1981. Seasonal variations in the hydrology of a small forested catchment near Manaus, Amazonas, and the implications for its management. In: R. Lal and E.W. Russell (Editors), *Tropical Agricultural Hydrology*. John Wiley and Sons, pp. 37-57.
- Nortcliff, S. and Thornes, J.B., 1984. Floodplain response of a small tropical stream. In: T.P. Burt and D.E. Walling (Editors), *Catchment Experiments in Fluvial Hydrology*. Geo-books, Norwich, pp. 73-85.
- Nye, P.H. and Greenland, D.J., 1960. The soil under shifting cultivation. Technical communication No. 51, Commonwealth Bureau of Soils Harpenden, Reading, England.
- Paparcikova, L., Vlek, P.L.G., Langel, R. and Reineking, A., 1998. Nitrogen Cycling in a Forest Succession of the Eastern Amazon: Comparison of Two Regions with Different Geological Formations. *Isotopes in environmental health studies*, 35(4): 310.
- Pearce, A.J., Rowe, L.K. and Stewart, J.B., 1980. Nighttime, wet canopy evaporation rates and the water balance of an evergreen mixed forest. *Water Resources Research*, 16(5): 955-959.
- Pearce, A.J., Stewart, M.K. and Sklash, M.G., 1986. Storm runoff generation in humid headwater catchments. 1. Where does the water come from? *Water Resources Research*, 22: 1263-1272.

- Penteado, A.R., 1967. Problemas de Colonização de Uso da Terra na região Bragantina do Estado do Pará, UFPA, Belém, PA, 488 pp.
- Pinder, G.F. and Jones, J.F., 1969. Determination of the groundwater component of peak discharge from the chemistry of total runoff. *Water Resources Research*, 5: 438-445.
- Poels, R.H.L., 1987. Soils, water and nutrients in a forest ecosystem in Suriname. PhD Thesis, Agricultural University, Wageningen, 253 pp.
- Proctor, J., 1987. Nutrient cycling in primary and old secondary forest. *Applied Geography*, 7: 135-152.
- Puig, J., 2003. Assessment of different land covers as atmospheric carbon sinks using field and remote sensing data, eastern Amazon, Brazil. PhD project proposal Thesis.
- Rabus, B., Eineder, M., Roth, A. and Bamler, R., 2003. The shuttle radar topography mission - A new class of digital elevation models acquired by spaceborne radar. *ISPRS Journal of Photogrammetry and Remote Sensing*, 57: 241-262.
- Rego Bezera, F.H., 2001. Neotectonic movements in Northeastern Brazil : Implications for a preliminary seismic-hazard assessment. *Revista Brasileira de Geociências*, 30(3): 562-564.
- Rego, R.S., da Silva, B.N.R. and Junior, R.S.O., 1993. Detailed soil survey in an area in the municipality Igarapé- Açú, Summaries and lectures presented at the 1st SHIFT workshop. EMBRAPA-CPATU, Belém, pp. 146.
- Reis de Melo Jr., H., Wickel, A.J. and Sá, T., 2002. Caracterização hidrogeológica e mapeamento da vulnerabilidade natural do aquífero livre na bacia hidrográfica do Igarapé Cumaru, Igarapé-Açú, PA, XII Reunião Brasileiro da Água Subterreano.
- Reynolds, E.R.C. and Leyton, L., 1963. The water relations of plants. Blackwell scientific publications, Oxford, pp. 127-141.
- Roberts, J.M., Cabral, O.M.R. and Ferreira De Aguiar, L., 1990. Stomatal and boundary-layer conductances in an Amazonian terra firme rain forest. *Journal of Applied Ecology*, 27(1): 336-353.
- Rossetti, D.F., 2001. Estratigrafia da sucessão sedimentar Pósbarreiras (Zona Bragantina, Pará) com base em radar de penetração no solo. *Revista Brasileira de Geofísica*, 19(2): 113-130.
- Rossetti, D.F., 2003. Delineating shallow Neogene deformation structures in northeastern Pará State using Ground Penetrating Radar. *Anais da Academia Brasileira de Ciências*, 75(2): 235-248.
- Rowe, L.K., 1983. Rainfall interception by an evergreen beech forest, Nelson, New Zealand. *Journal of Hydrology*(66): 143-158.
- Rutter, A.J., Kershaw, K.A., Robins, P.C. and Morton, A.J., 1971. A predictive model of rainfall interception in forests. 1. Derivation of the model from observations in a plantation of Corsican pine. *Agricultural Meteorology*(9): 367-384.
- Sá, T.D.d.A., da Costa, P.R. and Roberts, J.M., 1996. Forest and pasture conductances in southern Pará, Amazonia. In: J.H.C. Gash, C.A. Nobre, R. J.M. and R.L. Victoria (Editors), *Amazonian deforestation and climate*. Wiley, Chichester, pp. 241-264.

- Sá, T.D.d.A., Oliveira, V.C.d., Auraújo, A.C.d. and Brienza Jr., S., 1999. Spectral irradiance and stomatal conductance of enriched fallows with fast-growing trees in eastern Amazonia, Brasil. *Agroforestry systems*, 47: 289-303.
- Sá, T.D.d.A., Oliveira, V.C.d., Weber Neto, O. and Carvalho, C.J.R.d., 1995a. Condutância estomática em espécies-chave de vegetação secundárias em pousio, em sistema de "derruba-e-queima", na Amazônia Oriental, Congresso Ecologia Latinoamericana, Los Andes, Mérida, Venezuela, pp. 9-11.
- Sá, T.D.d.A., Weber Neto, O., Oliveira, V.C.d. and Carvalho, C.J.R.d., 1995b. Ökophysiologische Untersuchungen an ausgewählten Arten der Sekundärvegetation de nordöstlichen Pará. In: P.L.G. Vlek, M. Denich and H. Fölster (Editors), *Sekundärwald und Brachevegetation in der Kulturlandschaft des östlichen Amazonasgebietes - Funktion und Manipulierbarkeit*, pp. 139 pp.
- Sanchez, P.A., 1976. *Properties and management of soils in the tropics*. Wiley and Sons, New York, 618 pp.
- Schellekens, J., 2000. *Hydrological processes in a humid tropical rain forest: a combined experimental and modelling approach*. PhD Thesis, Vrije Universiteit Amsterdam, Amsterdam, 158 pp.
- Schellekens, J., Scatena, F.N., Bruijnzeel, L.A. and Wickel, A.J., 1999. Modelling rainfall interception by a lowland tropical rain forest in northeastern Puerto Rico. *Journal Of Hydrology*, 225(3-4): 168-184.
- Schroth, G., Ferreira da Silva, L., Wolf, M.-A., Teixeira, W.G. and Zech, W., 1999. Distribution of throughfall and stemflow in multi-strata agroforestry, perennial monoculture, fallow and primary forest in central Amazonia, Brazil. *Hydrological Processes*, 13(10): 1423-1436.
- Schuler, A.E., 2003. *Fluxos hidrológicos em microbacias com floresta e pastagem na Amazônia Oriental, Paragominas, Pará*. PhD Thesis, Universidade de São Paulo, São Paulo, Brazil, 133 pp.
- Schultz Jr., A., 2000. *Kaolin Exploration in the Capim River Region, state of Pará, CPRM, Rio de Janeiro*.
- Schuster, B., 2001. *Vegetationsstruktur einer Sekundärvegetation in der Wald-Feld-Wechselwirtschaft im östlichen Amazonasgebiet. Brasilien*. Diploma Thesis, University of Göttingen, Göttingen, 136 pp.
- Shuttleworth, W.J., 1988. Evaporation from Amazonian rain forest. *Proc. R. Soc. Lond.*, B233: 321-346.
- Shuttleworth, W.J., 1989. Micrometeorology of temperate and tropical forest. *Phil. Trans. R. Soc. Lond.*, B324: 299-334.
- Sombroek, W.G., 1966. *Amazon soils. A reconnaissance of the soil of the Brazilian Amazon region*. PhD thesis Thesis, 303 pp.
- Sombroek, W.G., 1984. Soils of the Amazon region. In: H. Sioli (Editor), *The Amazon: Limnology and Landscape Ecology of a Mighty Tropical River and Its Basin*. W. Junk Publishers, Dordrecht, pp. 521-535.
- Sommer, R., 2000. *Water and nutrient balance in deep soils under shifting cultivation with and without burning in the Eastern Amazon*. PhD Thesis, Georg-August-University, Göttingen, Germany, 226 pp.

- Sommer, R., Fölster, H., Vielhauer, K., Maklouf Carvalho, E.J. and Vlek, P.L.G., 2003. Deep Soil Water Dynamics and Depletion by Secondary Vegetation in the Eastern Amazon. *Soil Science Society of America Journal*, 67: 1672-1686.
- Sommer, R. et al., 2002. Transpiration and canopy conductance of secondary vegetation in the eastern Amazon. *Agricultural And Forest Meteorology*, 112: 103-121.
- Souza-Filho, F.R.d., 2004. Family agriculture: The historical dynamics of their reproduction in the Amazon region., University of Bonn, Bonn, in press pp.
- Stallard, R.F. and Edmond, J.M., 1981. Geochemistry of the Amazon. 1. Precipitation chemistry and the marine contribution to the dissolved load at the time of peak discharge. *Journal of Geophysical Research*, 86: 9844-9858.
- Stuyfzand, P.J., 1983. Important sources of errors in sampling groundwater from multilevel samplers (in Dutch). *H2O*, 22: 141-146.
- Teixeira, W.G., 2001. Land use effects on soil physical and hydraulic properties of a clayey ferralsol in the Central Amazon. PhD Thesis, Universität Bayreuth, Bayreuth, 255 pp.
- Thielen-Klinge, A., 1997. Rolle der biologischen N₂ Fixierung von Baumleguminosen im oestlichen Amazonasgebiet, Brasilien - Anwendung der 15 N natural abundance Methode, University of Goettingen, Göttingen, 202 pp.
- Thom, A.S., 1975. Momentum, mass and heat exchange of plant communities. In: J.L. Monteith (Editor), *Vegetation and the atmosphere*. Vol. 1 Principles. Academic Press, London, pp. 57-109.
- Thurston, H.D., 1997. Slash/Mulch systems: sustainable methods for tropical agriculture. IT Publications, London, UK, 196 pp.
- Tobón Marin, C., Bouten, W. and Sevink, J., 2000. Gross rainfall and its partitioning into throughfall, stemflow and evaporation of intercepted water into four forest ecosystems in Western Amazonia. *Journal of Hydrology*, 237: 40-57.
- Tomasella, J. and Hodnett, M.G., 1996. Soil hydraulic properties and van Genuchten parameters for an oxisol under pasture in central Amazonia. In: J.H.C. Gash, C.A. Nobre, R. J.M. and R.L. Victoria (Editors), *Amazonian deforestation and climate*. Wiley, Chichester, pp. 101-124.
- Ubarana, V.N., 1996. Observations and modelling of rainfall interception at two experimental sites in Amazonia. In: J.H.C. Gash, C.A. Nobre, R. J.M. and R.L. Victoria (Editors), *Amazonian deforestation and climate*. Wiley, Chichester, pp. 152-162.
- Uhl, C., 1987. Factors controlling succession following slash-and-burn agriculture in Amazonia. *Journal of Ecology*, 75: 377-407.
- Uhl, C. and Jordan, C.F., 1984. Succession and nutrient dynamics following forest cutting and burning in Amazonia. *Ecology*, 65(5): 1476-1490.
- USDA, 1999. Soil Taxonomy: A basic system of Soil Classification for Making and Interpreting Soil Surveys. Agriculture Handbook No. 436. U.S. Dept. of Agriculture, Natural Resources Conservation Service, 869 pp.
- Van Dijk, A.I.J.M., 2002. Water and sediment dynamics in bench-terraced agricultural steepplands in West-Java, Indonesia. PhD Thesis, Free University, Amsterdam, 363 pp.

- Van Hogezaand, R.J.P., 1996. The use of chemical tracers in identifying stormflow generating processes in a small catchment in the Luquillo Mountains, Puerto Rico. Working Paper no. 1 Thesis, Vrije Universiteit, Amsterdam.
- Vieira, L.S., Dos Santos, W.H., Falesi, I.C. and Filho, J.P.S.O., 1967. Levantamento do reconhecimento dos solos da região Bragantina, Pesquisa Agropecuária Brasileira, Belém.
- Vosti, S.A., Witcover, J. and Carpentier, C.L., 2002. Agricultural intensification by smallholders in the Western Brazilian Amazon. Research Report 130, IFPRI, Washington DC, USA.
- Vrugt, J.A., Dekker, S.C. and Bouten, W., 2003. Identification of rainfall interception model parameters from measurements of throughfall and forest canopy storage. *Water Resources Research*, 39(9): 1251.
- Walsh, R.P.D., 1980. Runoff processes and models in the humid tropics. *Zeitschrift für Geomorphologie, Supplement*, 36: 176-202.
- Ward, R.C. and Robinson, M., 2000. *Principles of Hydrology*. McGraw-Hill, Maidenhead, 450 pp.
- Waterloo, M.J., 1994. Water and nutrient dynamics of *Pinus Caribea* plantation forests on former grassland soils in Southwest Viti Levu, Fiji, Vrije Universiteit, Amsterdam, 478 pp.
- Watrin, O.d.S., 1994. Estudo da dinâmica na paisagem da amazônia oriental através de técnicas de geoprocessamento. MSc Thesis, 153 pp.
- Whitmore, 1998. *An introduction to tropical rain forests*. Oxford University Press, Oxford, 282 pp.
- Wickel, A.J., 1997. Rainfall interception modelling in lowland and montane rain forests in the Luquillo Mountains, Eastern Puerto Rico. Working Paper no. 2., Vrije Universiteit, Amsterdam, 60 pp.
- Wiesenmüller, J., 1999. Einfluß landwirtschaftlicher Flächenvorbereitung auf die Dynamik de Wurzelsystems und die oberirdische Regeneration der Sekundärvegetation Ostamazoniens, Pará, Brasilien. PhD Thesis, Universität Göttingen, Göttingen, 228 pp.
- Williams, M.R., Fisher, T.R. and Melack, J.M., 1997. Solute dynamics in soil water and groundwater in a central Amazon catchment undergoing deforestation. *Biogeochemistry*, 38: 303-335.
- Zinke, P.J., 1967. Forest interception studies in the United States. In: W.E. Sopper and H.W. Lull (Editors), *Int. Symposium on Forest Hydrology*. Pergamon Press, pp. 137-161.

ACKNOWLEDGEMENTS

Ever since my first hydrological fieldwork in the rain forest of Puerto Rico in 1996 with Dr. Sampurno Bruijnzeel and Dr. Jaap Schellekens of the Vrije Universiteit (VU) Amsterdam, I have had the wish to perform a similar project on my own. In December of 1999 this opportunity was granted through a proposal for a hydrological study for the SHIFT project. During the years I spent in Brazil and in Germany I had the privilege to meet and work with many magnificent people.

The fieldwork in Brazil started with the back breaking but also enjoyable job of constructing dams and installing equipment at the experimental watersheds with the help of EMBRAPA technician Reginaldo Frazão. With his ingenuity and experience, Reginaldo was an indispensable force behind this work. After a few months Homero Reis de Melo Jr. (at the time an MSc student with the Federal University of Pará) completed the team with added experience and extra energy. Field workers Osvaldo ('Val'), Piau, Bedilson and others provided the work force and showed remarkable interest even when they did not see why this 'Holandes loco' wanted to dam streams and perforate the area with wells. Without their help and friendship, the realization of this work would have been very difficult, if not impossible. I sincerely thank the families Carneiro and Gomes of the Cumarú community for their hospitality and friendship, and for allowing me to use their land and water for this research. I furthermore thank the EMBRAPA drivers (Malá, Gonzaga and Bigode) for their friendship and logistical support.

A workable environment in Belém was created by the project coordinators Dr. Konrad Vielhauer, Dra. Tatiana Sá, Dr. Osvaldo Kato, the project administration and the students of the SHIFT project. In the final stage of my stay in Brazil it was a pleasure to get to know Dr. Ricardo Figueirido, who is continuing the hydrological studies at the Cumarú watershed for EMBRAPA, and to have a scientific exchange with Dra. 'Marysol' Azeneth Eufrausino Schuler, who performed a similar study near Paragominas.

On the German side of the project I thank Prof. Dr. Paul Vlek, director of ZEF, for being my first supervisor and for giving me the opportunity to perform this study with ZEF, and Prof. Dr. Bernd Dieckkrüger for being second supervisor on the exam committee and for his constructive contributions to my dissertation. It was a pleasure to work with Dr. Nick van de Giesen, who as my direct coordinator was always available for questions and discussions. Dr. Christopher Martius and Dr. Jan Hendrickx provided a great deal of help in the final stages of my dissertation and defense, for which I am very grateful. I also thank Dr. Manfred Denich for coordinating the SHIFT project at the ZEF office in Bonn. I thank Prof. Dr. Horst Fölster from the University Göttingen for his suggestions for this study and the scientific discussions during the elaboration of this dissertation. I would also like to thank Dr. Günther Manske, the secretaries Sabine, Andrea and Hannah and assistants Inga, Georg and Sandra who helped in innumerable ways. I thank my office mates Francisco 'Parahyba', Kirsten and Akmal, and all the students of the doctoral program from all over the world for being great colleagues and for making ZEF an enjoyable place to work.

From my former professor at the VU in Amsterdam, Dr. Sampurno Bruijnzeel, I received not only a great deal of scientific support, but also the inspiration to pursue a hydrological study in the tropics. I would like to acknowledge Dr. Jaap Schellekens and

Dr. Maarten Waterloo for their interesting suggestions and feedback in various stages of this study, and Dr. Kick Hemker for providing me with the MicroFEM software and many suggestions on groundwater modeling.

I cannot fully express my gratitude to my parents Joop and Elly for their constant love and support. My gratitude also to my sister Ilse and her husband Dick, and my mother-in-law Anne Wheeler for their support. I thank all of our dear friends: Miroslav and Cara Honzak, Victor and Sylvia Bense, Remko de Lange, Natali Hellberger, Jurgen and Valentina Foeken, Frantisek Brabec, Nanny, Sarah and Christopher Martius, Jan Friesen, Jens Liebe, Marc Andreini and Jim and Judy Dougherty for their support and friendship.

I thank my wonderful wife Beth for always being there for me, for giving her unconditional love and support and for proofreading this dissertation.